

ADVANCED MASTERS IN STRUCTURAL ANALYSIS
OF MONUMENTS AND HISTORICAL CONSTRUCTIONS

Master's Thesis

Safa'a Burhan Joudeh

Static Assessment of Judit
Tower in Prague.



University of Minho

Czech Republic | 2023



DIPLOMA THESIS ASSIGNMENT FORM

I. PERSONAL AND STUDY DATA

Surname: <u>Joudeh</u>	Name: <u>Safaa</u>	Personal number: <u>520835</u>
Assigning Department: <u>Department of Mechanics or Department of Architecture or Department of Hydraulic Structures (select one, for ITAM use Dept. of Mech.)</u>		
Study programme: <u>Civil Engineering</u>		
Study branch/spec.: <u>Advanced Masters in Structural Analysis of Monuments and Historical Constructions</u>		

II. DIPLOMA THESIS DATA

Diploma Thesis (DT) title: <u>Statické analýza Juditina věž v Praze</u>	
Diploma Thesis title in English: <u>Static assessment of Judit tower in Prague</u>	
Instructions for writing the thesis: - Research the history of the tower. - Find out the dimensions, geometry, material properties, crack patterns. - Statical model. - Identification of the models parameters according to dynamics measurements. - FEM analysis - model with solid and shells elements. - Results and discussion. - Conclusions.	
List of recommended literature: Manual of Dlubal Software, Ing. Vesely - the little tower of charles bridge, 2011.	
Name of Diploma Thesis Supervisor: <u>Petr Fajman</u>	
DT assignment date: <u>14.3.2023</u>	DT submission date in IS KOS: <u>6.7.2023</u> <i>see the schedule of the current acad. year</i>
DT Supervisor's signature	Head of Department's signature

III. ASSIGNMENT RECEIPT

I declare that I am obliged to write the Diploma Thesis on my own, without anyone's assistance, except for provided consultations. The list of references, other sources and consultants' names must be stated in the Diploma Thesis and in referencing I must abide by the CTU methodological manual "How to Write University Final Theses" and the CTU methodological instruction "On the Observation of Ethical Principles in the Preparation of University Final Theses".

<u>21.3.2023</u>	<u>Safa'a Joudeh</u>
Assignment receipt date	Student's name

DECLARATION

Name: Safa'a Joudeh

Email: 95joudeh@gmail.com

Title of the Msc Dissertation: Static Assessment of Judit Tower in Prague

Supervisor(s): Petr Fajman

Year: 2023

I hereby declare that all information in this document has been obtained and presented in accordance with academic rules and ethical conduct. I also declare that, as required by these rules and conduct, I have fully cited and referenced all material and results that are not original to this work.

I hereby declare that the MSc Consortium responsible for the Advanced Masters in Structural Analysis of Monuments and Historical Constructions is allowed to store and make available electronically the present MSc Dissertation.

University: Czech Technical University in Prague

Date: 06/07/2023

Signature:

_____*Safa' Joudeh*_____

This page is left blank on purpose.

DEDICATION

This thesis is dedicated to my mother and father – May his soul rest in peace.

To my best friend Leen Mahasneh and all people who supported me throughout this year.

Thanks for making me see this adventure through to the end.

This page is left blank on purpose.

ACKNOWLEDGEMENTS

I would first like to thank my thesis advisor Professor Petr Fajman of the faculty of engineering at the Technical University of Prague. The door to Prof. Fajman office was always open whenever I ran into a trouble spot or had a question about my research or writing. He consistently allowed this thesis to be my own work but steered me in the right direction whenever he thought I needed it.

I want to express my gratitude to SAHC Managing Board for the generous Consortium Scholarship. With this financial support, I got to live and experience this amazing opportunity.

I would also like to thank the experts who were involved in the in-situ activities for this research project: prof. Ing. Michal Polak, CSc. and Ing. Tomas Plachy, CSc. Without their passionate participation and input, the dynamic identification tests could not have been successfully conducted. I would like to acknowledge the Technical University of Prague for providing the resources for the project, including the testing equipment and computing resources,

Finally, I must express my very profound gratitude to my mother, sisters and my best friends for providing me with unfailing support and continuous encouragement throughout my years of study and through the process of researching and writing this thesis. This accomplishment would not have been possible without them. Thank you.

Safa' Joudeh

This page is left blank on purpose.

ABSTRACT

The Judit Tower (Juditina věž) in Prague is a national cultural monument of great importance. It is one of the Charles Bridge's towers, located upriver Vltav in the southeast corner of the oldest core of Malá Strana, Prague. The construction consists of masonry, stone vaulting, half-timbered partitions, and a wooden ceiling. The Romanesque tower is in a state of disrepair and exhibits several deficiencies, primarily shear cracks on the external masonry walls and internal half-timbered partition walls. This study focuses on carrying out in-situ inspection and diagnosis of the monument, namely, identifying the primary mechanical or material pathologies, assessing the bearing capacity and the influence and causes of cracks in the masonry, and, eventually, offering recommendations for additional research and interventions. Therefore, the aim of this study is to perform a thorough static analysis of the structure, taking into account its development over time and examining the state of its structural system in its current condition.

This study also utilized the integration of dynamic identification results with 3D Finite element Model assessments. Henceforth, Operational Modal Analysis (OMA) was performed, providing the natural frequencies and mode shapes of the main regions of the building, reducing the uncertainties associated with the tower's structure, and characterizing its system. Moreover, the test results were used to calibrate the numerical models. The information obtained in the previous studies was also integrated into the numerical model of the building for conducting the linear analysis. The results of the analysis provided insight into the behavior of the building and set the direction for future work to investigate the building's safety.

This page is left blank on purpose.

ABSTRAKTNÍ

Juditina věž v Praze je národní kulturní památka velkého významu. Je jednou z věží Karlova mostu na Malé straně proti proudu Vltavy. Materiálové a konstrukční řešení je velmi rozmanité – kamenné zdivo, cihelné klenby a dřevěné stropy a krovy. Románská věž vykazuje několik trhlin, jedná se zejména o smykové v obvodových zdech a v hrázděné příčce. Práce se nejdříve soustředila na historii konstrukce, pak na pasportizaci trhlin a na kontrolu rozměrů konstrukce in situ. Poté byly získány materiálové charakteristiky a další potřebné prvky pro zjištění možné příčiny vzniku trhlin. Ke splnění cíle byl udělán statický model konstrukce, kde bylo využito i výsledků z dynamického experimentu provedeného na konstrukci.

Model pro analýzu konstrukce byl sestaven z 3D objemových prvků. Z něho pak byly získány potřebné statické a dynamické veličiny. V prvním kroku byly hledány materiálové charakteristiky a okrajové podmínky. Hledané veličiny byly odvozeny porovnáním vypočtených výsledků vlastní frekvence a tvarů kmitání věže s naměřenými hodnotami z experimentu. Získané hodnoty pak byly použity ve statické analýze, jejíž výsledky jsou v souladu s chováním konstrukce a jejími poruchami. Důležitým poznatkem je, že daný postup je možné použít i pro statickou analýzu podobných objektů.

This page is left blank on purpose.

المخلص

برج جودت نصب ثقافي تشيكي وطني ذو أهمية كبيرة. إنه أحد أبراج جسر تشارلز المشهور، ويقع في الزاوية الجنوبية الشرقية في قلب الحي الاثري مارلا سترانا، في مدينة براغ. تهدف هذه الدراسة إلى إجراء تحليل انشائي شامل للبنية الاثرية للبرج، مع مراعاة تطوره عبر الزمن وتقييم الوضع الحالي لنظامه الهيكلي.

البرج يعود بناءه الى عصر النهضة، وقد تم بناءه بالطريقة التقليدية، حيث استخدم ببناء جدرانه الخارجية العريضة حجارة رسوبية وطوب محروق. وغير ذلك، فقد بنيت أرضياته من الأقبية الحجرية، وحوائطه الداخلية من العوارض الخشبية المدموجة مع الطوب المحروق، وسقفه بني من خشب الصنوبر. يعاني حالياً من حالة تدهور ويظهر في نظامه الانشائي عدة مشاكل، يتمثل أبرزها في تشققات وتصدعات تظهر على الواجهات الخارجية والحوائط الداخلية. تركز هذه الدراسة على إجراء تشخيص شامل لهذا النصب التذكاري، بهدف تحديد المسببات الأساسية للعلات الميكانيكية أو الفيزيائية للجدران، وتقييم القدرة التحملية لها.

تبنت هذه الدراسة دمج نتائج القياسات الديناميكية للصرح الاثرية مع تقييم باستخدام نماذج العناصر ثلاثية الأبعاد. لذلك تم تنفيذ تحليل النمط النموذجي (**Operational Modal Analysis**) بحيث يوفر مثل هذا النوع من التجارب الترددات الطبيعية وأشكال الانماط الرئيسية في المبنى. وبهذا يتم تكوين صورة أوضح للنظام الهيكلي الخاص بالبرج ويقدم وصف ادق لتحركاته والتغيرات التي يوجهها. تم أيضا استخدام نتائج هذا الاختبار لمعايرة النماذج الرقمية. علاوة على ذلك، تم دمج ما تم دراسته بالأبحاث السابقة لإغناء هذه النماذج، مما يجعلها توصف الواقع بطريقة دقيقة. ساعد ذلك في الحصول على نتائج ادق عند إجراء التحليل الخطي، وتحديد أسباب التصدعات في الجدران الخراجية وأثارها على القدرة البرج التحملية. وبناءً على ما ذكر أعلاه، قدمت هذه الدراسة تفسيرات للمشاكل التي تواجه المبنى، وتوصيات وتوجيهات للأبحاث المستقبلية وأعمال الترميم التي ستقام على البرج في المستقبل القريب والبعيد.

This page is left blank on purpose.

TABLE OF CONTENTS

Table of Contents	xiii
List of Tables	xv
Table of Figures	xv
1 INTRODUCTION	1
1.1 Judit Tower	1
1.2 Thesis Outline	1
1.3 Aim and scope.....	2
1.4 Motivation and Context	2
1.5 Methodology	3
2 Judit Tower	6
2.1 Description of the tower.....	6
2.2 Location and its urban sitting.....	6
2.3 The Tower layout.....	9
2.4 Facades.....	11
2.5 Building materials.....	14
2.5.1 Masonry walls:.....	14
2.5.2 Decay mechanism of Opuka stone masonry	16
2.5.3 The roof and floors.....	16
3 HISTORICAL DEVELOPMENT OF JUTIT TOWER	19
3.1 Beginnings of the tower's history, the 12 th and 13 th centuries:.....	19
3.2 Emperor Charles IV – 14 th Century.	20
3.3 Restoration of the Tower after the fire during the 16 th century.....	22
3.4 From the 17 th century Until today	27
4 VISUAL INSPECTION AND DAMAGE SURVEY.....	30
4.1 Geometrical Survey	30
4.2 Visual inspection.....	30
4.2.1 Masonry behavior and failure moods.....	31
4.2.2 Limitations of the visual inspection.....	33

4.3	Damage Survey	33
4.3.1	North facades	33
4.3.2	Eastern Façade	36
4.3.3	Southern and western façades	39
4.3.4	The Interior of The Tower	39
4.3.5	Attic, Truss, and Roof	43
5	Geometry Idealization and System Characterization	45
5.1	Idealization Of Building Geometry And Structural System	45
5.1.1	FE Model 1 (M1)	45
5.1.2	FE Model 2 (M2)	52
5.2	System Characterization Based On Dynamic Identification Test	57
5.2.1	Experimental campaign	57
5.2.2	Test results and system characteristics	59
5.3	Model calibration	61
6	Linear analysis	67
6.1.1	Displacement	67
6.1.2	Stresses	68
6.1.3	Vault	73
7	Conclusion and Recommendations	75
7.1	Conclusions	75
7.1.1	Historical survey	75
7.1.2	Visual inspection and damage survey	75
7.1.3	Material and system characterization	76
7.1.4	Structure idealization and numerical model creation	76
7.1.5	Preliminary static analysis	76
7.2	Recommendations:	77
7.2.1	Material damages and pathologies	77
7.2.2	Future inspection and diagnosis	78
7.2.3	Recommendations for future numerical analysis	79
8	References	81
9	Annex A	85
10	Annex B	97
11	Annex c	103

LIST OF TABLES

Table 1 Geometry of the Masonry walls.....	47
Table 2 Model Element and Mesh Parameters	51
Table 3 Model Element and Mesh Parameters (M2)	56
Table 4 Experimental frequencies.....	60
Table 5 Calibrated Young’s Modulus.....	62
Table 6 Input Parameters of The Boundary Conditions.....	63
Table 7 Model 1 Updating - Eigenvalues analysis.....	64
Table 8 Model 2 calibration – Eigenvalues analysis.....	65

TABLE OF FIGURES

Figure 1.1 Methodology.....	4
Figure 2.1 Judit Tower – Eastern Façade facing Charles Bridge.....	6
Figure 2.2 Location and urban sitting: Prague, Czechia.	7
Figure 2.3 Aerial photo of the tower showing its roof and urban setting with the bridge.	8
Figure 2.4 Reconstruction of the probable original height of Judit Tower (Veselý, 2017)	8
Figure 2.5 Plans; CAD Documentation of the building, created by (Veselý, 2017), validated and redrawn by the Author.	9
Figure 2.6 Eastern Façade – The accessible to the via a gallery in the northern wing of the house.....	10
Figure 2.7 Sections; CAD Documentation of the building, created by (Veselý, 2017), validated and redrawn by the Author.	11
Figure 2.8 Photographic documentation – (a) Northern façade, (b) Eastern façade.....	12
Figure 2.9 Southwest corner of the tower – The Building attached to the residential house and the Renaissance Gate.	12
Figure 2.10 The tower’s Elevation; CAD Documentation of the building, created by (Veselý, 2017), validated and redrawn by the Author. (a) Northern Elevations, (b) Eastern Elevations, (c) Southern Elevations.....	13
Figure 2.12. Map showing position of Predni' Kopanina quarry within the Bohemian Cretaceous Basin (Prikryl, Lokajcekb, Svobodov, & Weishauptovab, 2003).....	15
Figure 2.13 Model half-timbered partitions with different types of infill, (Ruzicka) Centrum stavitelského dědictví NTM, 2023.....	15

Figure 3.1 Historical drawings of Judith Tower, Muzeum hl. m. Prahy; (a) F. X. Sandmann akvarel, kolem 1840, (b) Vincenc Morstadt sepiová kresba, 1874.....	20
Figure 3.2 The atmosphere of the immediate surroundings of the Malostranské Mostecké věže (Malostranská Bridge Towers), as seen in her childhood by Marie Popelková, the future collector of Prague legends and writer Popelka Bilianová. Sepia drawing by Vincenc Morstadt from 1874, Prague City Museum.....	21
Figure 3.3 The connection between the Tower and the gate – North Façade	22
Figure 3.4 Vincenc Morstadt: Dvůr pod Juditinou věží.....	24
Figure 3.5 Tzv. Juditina věž, Prague - Malá Strana; Scheme of the reconstruction of the development of the floors and roofing of the tower: Drawing: Jan Veselý, 2007.	25
Figure 3.6 Detailed survey and documentation of the ground floor walls, with an evaluation of findings processed by Jan Veselý, 2005-07.	26
Figure 4.1 Methodology – damage sheet: (a) general information, (b) localization of the damage, c) damage mapping, d) photographic documentation, and e) definition of each damage.....	32
Figure 4.2 Northren Façade – The conecction between the tower and the piers of Mostecká Gate	34
Figure 4.3 The lower part of the Northern façade, the dashed line highlighted the vertical groove.....	35
Figure 4.4 North Façade – (a) Topographic diagram by J. Veselý, (b) 3D diagram showing the street level of the north and level of the courtyard on the south.	36
Figure 4.5 Eastern façade – (a) orthoimage documentation of the damaged part of the facades, (b) sketch showing the façade deficiencies and damages.	37
Figure 4.6 cracks mapping – Southeast corner of the Tower.....	38
Figure 4.7 Crack mapping – the interior of the intersection between the tower and structure of the house 56.	41
Figure 4.8 Localization of the crack on the plans – (a) First floor, (b) second floor, (c) third floor.	41
Figure 4.9 Third floor – Wall partition	41
Figure 4.10 Localization of the crack on the sections.....	42
Figure 5.1 Creation of the Finite Elements Model – Methodology	45
Figure 5.2 Numerical models – (a) Shells model (M1), (b) Detailed solid model (M2)	46
Figure 5.3 Geometry of the Masonry walls adapted in the first model (M1)	47
Figure 5.4 Vaults – (a) ground floor vault, (b) basement vault.....	48
Figure 5.5 Beams elements (a) The roof, (b) Second and third floors.....	48
Figure 5.6 Active Earth (Ground) pressure – (a) shape of slope, (b) Types of ground pressures acting on the support wall. (Euro Code 4).....	50
Figure 5.7 Boundary conditions – (a) Finite elements model, (b) sketch demonstrating the reality.	50
Figure 5.8 Fist numerical model – the Mesh.	51
Figure 5.9 Details of Solid numerical model of the tower – (a) Geometry of the walls, (b) Geometry of the windows on the first floor, (c) Niches on the ground floor, (d) Simplified roof, (e) simplified vault on the ground floor, (f) simplified vault of the basement.	54
Figure 5.10 Boundary condition – Northeast corner (a) Numerical model, (b) 3D sketch of the tower.....	55
Figure 5.11 Boundary condition – Southeast corner (a) Numerical model, (b) 3D sketch of the tower.....	55
Figure 5.12 Mesh of the M2	56
Figure 5.13 The considered reference system with respect to the geographical tower location.....	58
Figure 5.14 Accelerometer placement: (a) First setup at the Roof level, (b) second setup at the Third level	58

Figure 5.15 First Setup - accelerometer placement.....	59
Figure 5.16 Second setup - accelerometer placement.....	59
Figure 5.17: Equipment used in the dynamic identification tests: (a) force balance accelerometer; and (b) communication centric multichannel recorder.....	60
Figure 5.18: Shape modes identified from the dynamic measurement.....	60
Figure 5.19: Layout of the tower	61
Figure 5.20 Model 1 Updating - Eigenvalues	64
Figure 5.21 Model 2 calibration – Eigenvalues analysis	65
Figure 6.1 Displacement – Southeastern Corner of the Tower.....	67
Figure 6.2 Global Displacement – X direction U_x (mm).....	68
Figure 6.3 Eastern Façade – M1, (a) compressive [basic] stress σ_x , (b) Tension stress τ_{xy}	69
Figure 6.4 Eastern Façade – M2, (a) compressive stress σ_x , (b) Tension stress τ_{xy} , (c) Shear stress τ_{max}	69
Figure 6.5 Eastern Façade: Comparison between (a) the Visual inspection, and (b) the shear stress distribution in M2	70
Figure 6.6 Eastern Façade: Comparison between (a) the photogrammetric documentation, and (b) the compressive stress distribution in M2.....	70
Figure 6.7 East windows on the second floor – (a) photographic documentation, (b) numerical model showing τ_{xz}	71
Figure 6.8 Interior wall partition, (a) Compressive stress σ_y , (b) Shear stress τ_{xz}	71
Figure 6.9 Interior wall partition on the third floor; (a) Compressive stress σ_y , (b) Shear stress τ_{xz} , (c) photographic documentation with crack mapping	72
Figure 6.10 Local deformation of the cross vaults; (a) Displacement on the x-direction, (b) Displacement on the y-direction	73
Figure 6.11 Stresses on the cross vaults: (a) Shear stress τ_{xz} , (b) Compressive stress σ_y	73

1 INTRODUCTION

1.1 JUDIT TOWER

The Judit Tower (*Juditina věž*) is one of the Charles Bridge's towers, located in the southeast of Malá Strana, Prague, Czechia. Due to its historical importance and status of Prague city as the only remaining part of the original Prague crossing (Za Satarou Praha, 2018), Judit Tower is considered a national cultural monument. It continues to be a living organism, a continuously inhabited and utilized structure, with fully plastered interiors from the first floor upward. The current use of the tower as used for social and cultural activities by the Club Za Starou Prahu (For Old Prague), corresponds to its cultural significance. Its advantage lies primarily in its non-expansiveness and non-commercial nature, which allow for adaptation of all activities to the possibilities of the structure.

The Romanesque monument is in a state of disrepair. The construction consists of masonry, stone vaulting, half-timbered partitions, and wooden ceiling. The tower exhibits several deficiencies, primarily shear cracks on the external masonry walls and internal half-timbered partitions walls.

1.2 THESIS OUTLINE

This thesis is divided into seven chapters. It starts with an introduction, stating the main aim, objectives, and scope of the research, discussing its motivation and context. Then it moves to a detailed description of the Judit Tower in Chapter 2, including its layout, construction material and urban setting. Furthermore, chapter 2 discusses the tower and its facades in both architectural and structural terms. Chapter 3 goes through the historical development of the tower, the major construction stages, and restoration activities with the objective of understanding the constructive sequence and current morphology of the building.

Chapter 4 covers the in-situ activities, including the geometrical survey, visual inspection, and damage survey, after then, it describes the methodology used for the damage mapping. Subsequently, the idealization and system characterization of the tower, along with the creation of the Finite Element Model process, are discussed in Chapter 5. Moreover, this chapter goes through the Operational modal analysis, the experimental campaign, and then draws a comparison of the experimental tests with the results of numerical calculation, eventually presenting calibrated material properties of the numerical models.

The static assessment of the tower is covered in Chapter 6, which focuses on the global deformation and local displacement of the tower's elements, the basic and principal stresses, and shear stresses. Then, it

illustrates the comparison between the numerical and visual inspection results. Finally, Chapter 7 provides the main conclusions of the thesis, followed by a few recommendations and a description of the possibilities for the continuation of the future research of the Judit Tower.

1.3 AIM AND SCOPE

The aim of this study is to provide a clear insight of the cause and impacts of structural deficiencies through visual inspections and computational methods. The objective is to perform a thorough static analysis of the structure, taking into account its development over time and examining the state of its structural system in its current condition. This study focuses on carrying out an inspection and diagnosis of the Judit Tower, namely, identifying the primary mechanical or material pathologies, assessing the bearing capacity and the influence and causes of cracks in the masonry, and, eventually, offering recommendations for additional research and interventions.

Due to the limited duration of the project, only two different analyses were performed. Firstly, eigenvalue analysis, which is used to calibrate the building stiffness to obtain agreement between the building's experimental and numerical natural frequencies. This analysis uses both material and geometric linearity. Then a linear Static analysis is performed. Through these calculations, the verification process of the load-bearing capacity of the vault was carried out, along with the sufficient rigidity of this monumental structure; moreover, the formation of disorders in the eastern wall in relation to changes during the construction process was investigated.

1.4 MOTIVATION AND CONTEXT

The work is informed and motivated by the comprehensive restoration of Judith Tower, a decision of the Department of Monument Care, City of Prague. According to the report and recommendation presented by the architect (Veselý, 2011), the following issues were discussed:

- The previous assessment of the tower failed to recognize the authentic structural system of the building and incorrectly interpreted the identified disorders.
- Recommendation for performing scientific studies of buildings for detailed diagnosis and intervention planning, adapting the following objectives:
 - a) Improving knowledge of building materials and construction techniques.

- b) Better characterizing existing masonry pathologies, including staining, biological colonization, black crust, salt efflorescence, inadequate mortar materials, degraded mortar, and cracked elements.
- c) The assessment of the statics of the tower should adapt to the use of a spatial mathematical model that includes the weakened masonry of the tower, openings, vaults, partitions, and ceilings.

Consequently, the information and conclusions achieved in the inspection and diagnosis activities of this project can assist in accomplishing the intervention goals and help facilitate the informed design and execution of the update investigations of the tower.

1.5 METHODOLOGY

The methodology and main tasks for the case study are summarized in Figure 1.1. The first step in the assessment of the tower is to identify and prepare a general description of tower's geometry, facades, and construction material. Then conducting full historical research in which literature sources, photographic resources, archival records, etc. were scoured to obtain as much knowledge of the building's significance, construction, history, and current condition and arrangement as possible. The historical survey helped reveal missing information about the building, and its results provided the starting point for planning the in-situ campaign.

One of the most important aspects of this research is the acquisition of detailed information to improve the knowledge level of the structure which affects the accuracy of the subsequent analysis (Diaferio, Foti, La Scala, & Sabbà, 2021). Generally, in order to assess historical structures with numerical models, adequate material models describing the behaviour of structural elements, as well as the mechanical characteristics of the materials and/or structural elements, need to be available (Kržan & Bosiljkov, 2023). Therefore, the in-situ activities focused on investigating unknown characteristics of the building and verifying information obtained in the historical survey. A geometrical survey was performed to assess the building's global layout and dimensions and also to determine the geometry or morphology of structural systems and elements.

Subsequently, the main pathologies affecting the masonry were assessed through visual inspection, and the results were used to create damage maps for the exterior of the building and the interior wall partitions. The data sheets for the damages survey were organized using Excel sheets and each deficiency was given a code based on its categories and types. The visual assessment focuses on the mechanical and physical damage.

To reduce the uncertainties associated with the tower's structure and characterize its system, this study utilized the integration of dynamic identification results with 3D FE model assessments. Furthermore, the dynamic measurements of the structure benefited in understanding many aspects of historical construction behaviour, such as the role of soil-structure interaction (SSI). The natural frequencies and mode shapes of the building were determined using Operational Modal Analysis (OMA). However, before conducting the field experimental test, a finite element model (FEM) was developed. The model geometry was idealized based on the available drawings and the results of the geometrical and historical survey. Material properties were based on literature recommendations for the observed masonry typologies and on the linear material properties obtained by model updating using the OMA results.

As the final step in the building inspection and diagnosis, the information obtained in the previous studies was integrated into a numerical model of the building for conducting linear analysis. The results of the linear analysis provide insight into the behaviour of the building and set the direction for future work to investigate the building's safety.

Stage	Object Identification	System Characterization	Data Analysis	Structural Assessment	Deliverables
Activities	<ul style="list-style-type: none"> • Tower Significance • Historical Development • Geometry • Past Intervention • Past Issues 	<ul style="list-style-type: none"> • Geometrical Survey • Visual Inspection • Material Identification • Structural Characterization 	<ul style="list-style-type: none"> • Material Properties • Damage Mapping • Geometric model 	<ul style="list-style-type: none"> • FEA Modeling and Validation • Modal Analysis (Eigenvalues Analysis) • Linear Analysis 	<ul style="list-style-type: none"> • Validated As-built Auto-CAD Drawings. • Damage Survey. • Tower Assessment Report. • Recommendations
Tools	<ul style="list-style-type: none"> • Literature Review • Review Of Past Reports • In Situ Investigations 	<ul style="list-style-type: none"> • Tower Significance • Historical Development • Geometry • Past Intervention • Past Issues 	<ul style="list-style-type: none"> • Literature Review • Excel Sheets • Auto-CAD Validated Drawings 	<ul style="list-style-type: none"> • Literature Review • Dlubal Software • Model Updating (Calculating the Stiffness of the Building) 	

Figure 1.1 Methodology

This page is left blank on purpose.

2 JUDIT TOWER

2.1 DESCRIPTION OF THE TOWER

The "*Juditina věž*" (Judit Tower) in Prague is a national cultural monument of great importance. The interiors of the tower are well preserved and are used regularly (Figure 2.1). Since 1927, the second and third floors have been used for social and cultural activities by the Club *Za Starou Prahu* (For Old Prague), which is responsible for its maintenance. Since 2007, the club has been renovating and operating the room on the second floor called "*Juditin's Hall*" and the adjacent bookstore (*Za Starou Prahu*, 2018).

Externally, the building has various weather-related defects that have caused wear and deterioration of the plaster and masonry in certain areas. Minor problems can be observed in the roofing, gutters and downspouts. Despite these external defects, it remains an exceptionally well-preserved and authentic monument. Its unique atmosphere is the result of continuous daily use and life (Veselý, 2011).

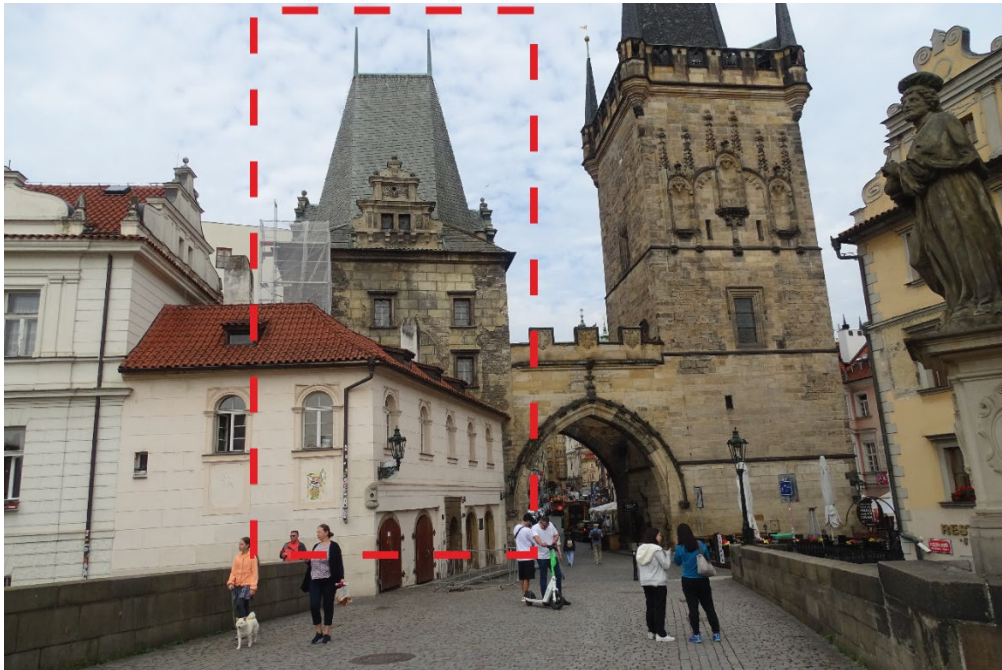


Figure 2.1 Judit Tower – Eastern Façade facing Charles Bridge.

2.2 LOCATION AND ITS URBAN SETTING

Judit Tower stands at the ends of Charles Bridges, along the connecting line of the ancient Vltava crossing and the road leading to Prague Castle and further west (Figure 2.2). It is in the southeast corner of the oldest core of the Malá Strana residential area. At the western base of the tower, there was the so-called

Walhenhof, a Malá Strana equivalent of the right-bank Ungelt, dating back to the 13th century. South of the tower, along Saska Street, the original Malá Strana stream used to flow.

Today, the tower is part of a closed residential block, with houses number 55/III and 56/III, enclosed by Mostecká, Saská, Lázeňská Streets, and Charles Bridge. The tower is also part of the structure of the Mostecká Gate, with its arches extending from the pillars connected to its northern facade. Judit Tower's floor plan is slightly rotated towards the southeast compared to the gate and the Northern Tower.

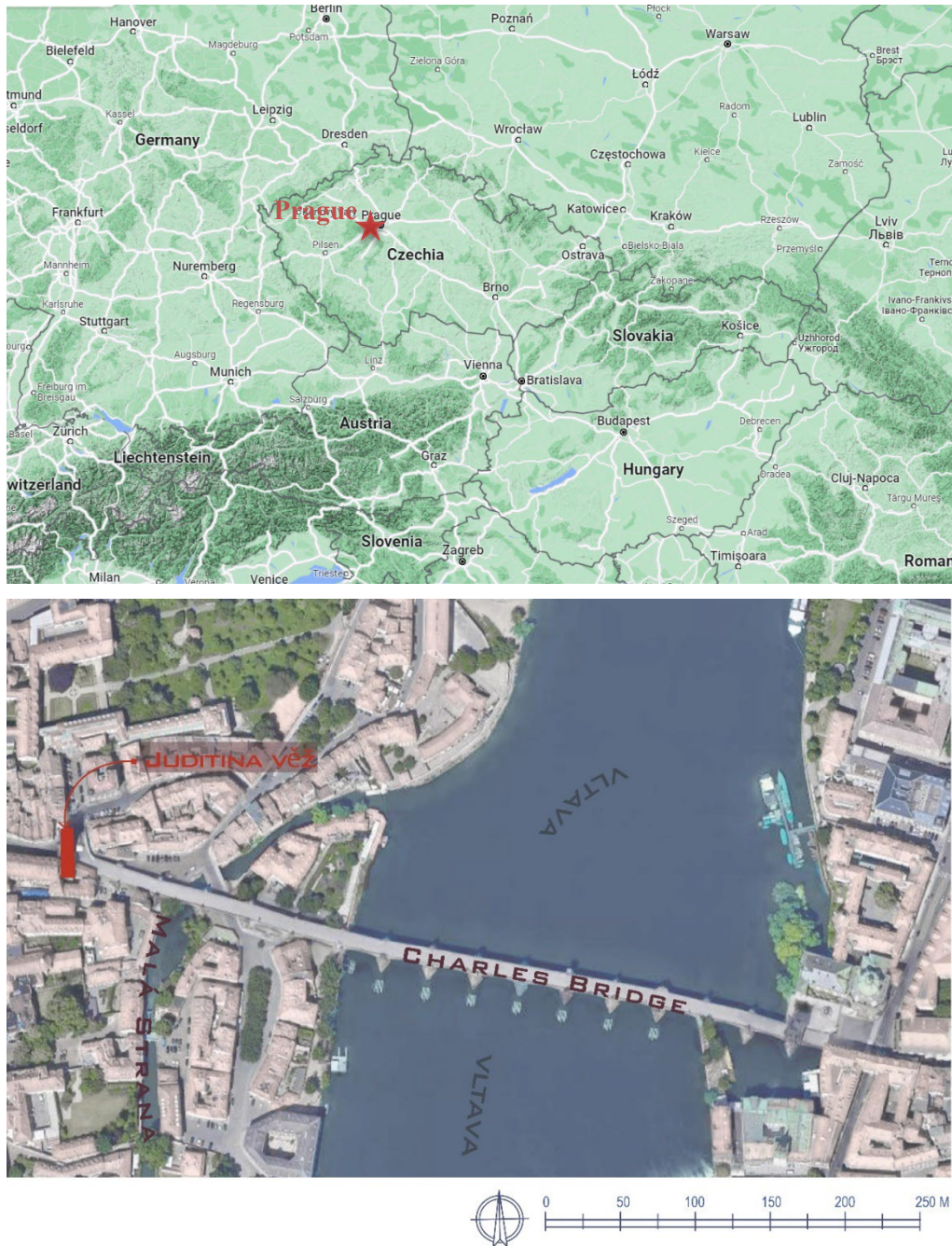


Figure 2.2 Location and urban sitting: Prague, Czechia.



Figure 2.3 Aerial photo of the tower showing its roof and urban setting with the bridge.

The end of Charles Bridge is significantly elevated compared to its surrounding, which is noticeable in the first section of Mostecká Street, between the gate and the mouth of Lázeňská Street. The probable original height of Judita's Tower (highlighted in yellow) is demonstrated in Figure 2.4, in comparison to its height relationship to the cobblestone paving. The red color represents the current surface. Architectural redrawing based on the documentation by the Czech Institute for the Care of Historical Monuments, height measurements, and depiction of height increments and proportions by Martin Müller and Jarmila Čiháková.

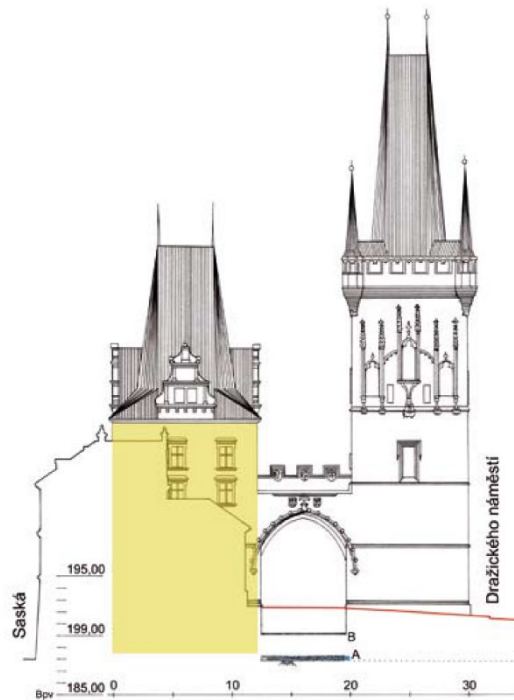


Figure 2.4 Reconstruction of the probable original height of Judit Tower (Veselý, 2011)

2.3 THE TOWER LAYOUT

The tower has a slightly rectangular footprint with clear sides measuring 9.90 x 11.10 meters, with a height of 17.50 meters (Figure 2.5) – relative to the level of Mostecká Street (Figure 2.4). The tower is divided into five unevenly high floors and its roof is steep diamond-shaped, featuring prominent gables and two pinnacles. At the base of the roof, there are large false-windows on each of the four sides, with three-tiered ornamental gables.



Figure 2.5 Plans; CAD Documentation of the building, created by (Veselý, 2011), validated and redrawn by the Author.

The massive walls of the tower were built with bearing masonry walls with thickness of 170-180 cm on the first four floors decreasing to 140-150 cm on the last floor. The spaces of the tower are accessible independently from the house's courtyard. The first floor is accessible via a gallery in the northern wing of the house, and the upper floors are connected by internal staircases within the tower. From the third floor, there is a door leading to the walkway of the Mostecká Gate (Figure 2.6).



Figure 2.6 Eastern Façade – The accessible to the via a gallery in the northern wing of the house.

The cellar (Basement) and Ground floor have barrel vaults with a segmental-arch profile, and in the northwest part of the first-floor layout, there is a barrel-vaulted kitchen and a semi-circular vaulted space under the staircase to the second floor. The other rooms of the tower have flat ceilings. All ceilings are finished with new plastered. All three upper floors of the tower have a similar layout, with a narrower northern service passage containing the staircase adjacent to the northern perimeter wall and a wider "residential" passage facing south – See Figures 2.5 and 2.7.

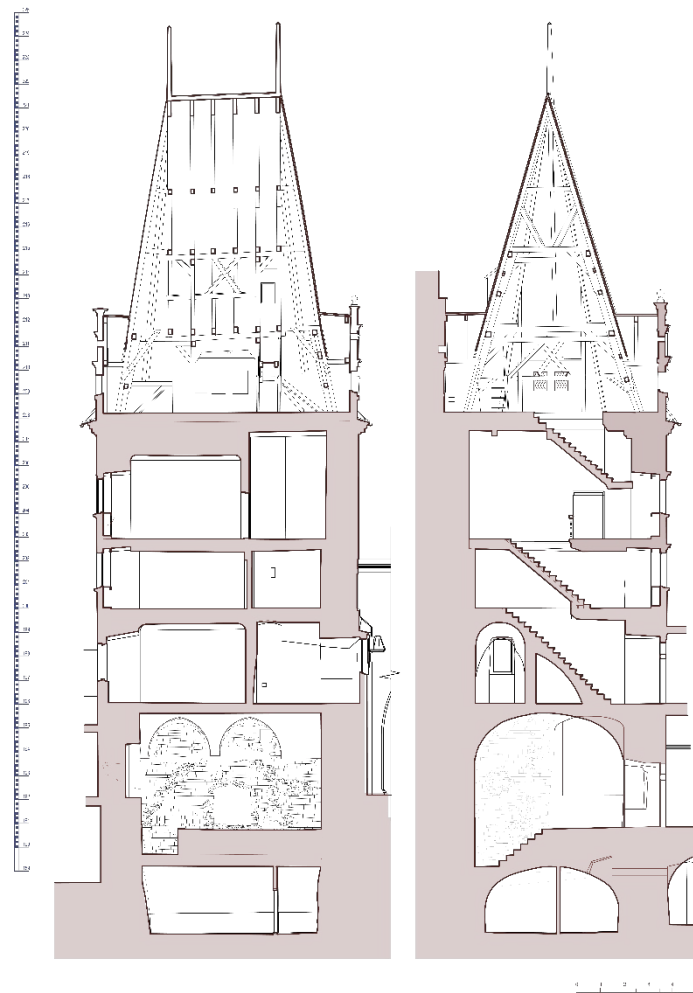


Figure 2.7 Sections; CAD Documentation of the building, created by (Veselý, 2011), validated and redrawn by the Author.

2.4 FACADES

Judit Tower is surrounded by neighboring buildings, and its facades are adjacent to these structures. The eastern elevation is blocked by the northern wing of the former customs building from the basement to the first floor, and the entire western facade is covered by the adjacent Saxon House (Figure 2.8). The northern facade faces the passage of Charles Bridge and is connected to the piers of Mostecká Gate and pedestrian bridges. The eastern façade, facing the bridge, has openings as single windows on the second and third floors and double windows blocked by house no. 56, only visible from the courtyard. The western facade of the tower is completely covered by the adjacent Saxon House, No. 55/III. Despite the apparent Renaissance symmetrical tendency represented by centrally placed gables of the oriels, the division of the facades is irregular. The southern and especially the eastern facades have a more pronounced architectural

treatment (Jan Veselý, 2007). The openings have a consistent size and architectural embellishments and are arranged on axes.

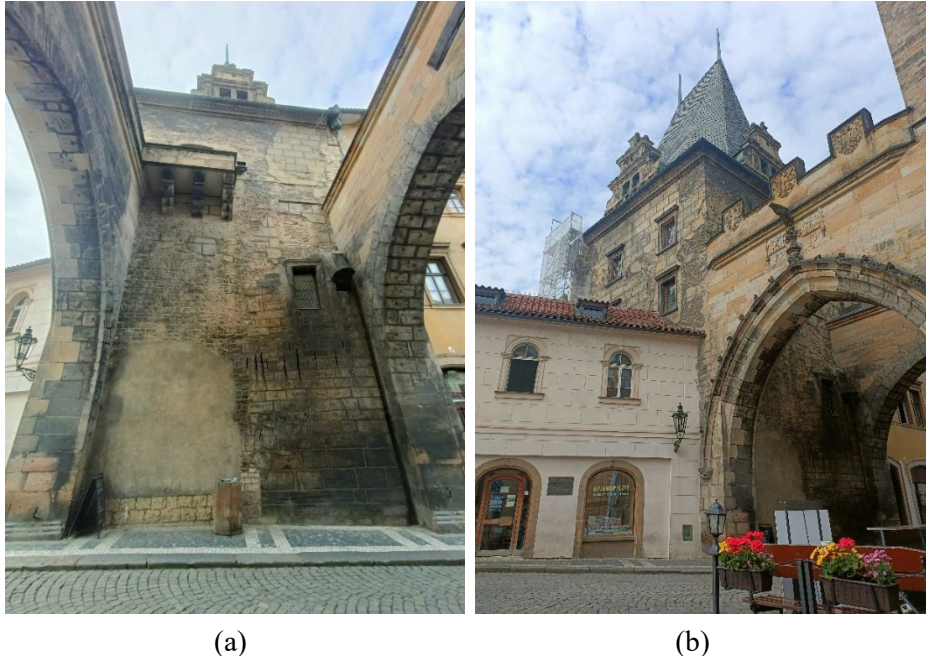


Figure 2.8 Photographic documentation – (a) Northern façade, (b) Eastern façade.



Figure 2.9 Southwest corner of the tower – The Building attached to the residential house and the Renaissance Gate.

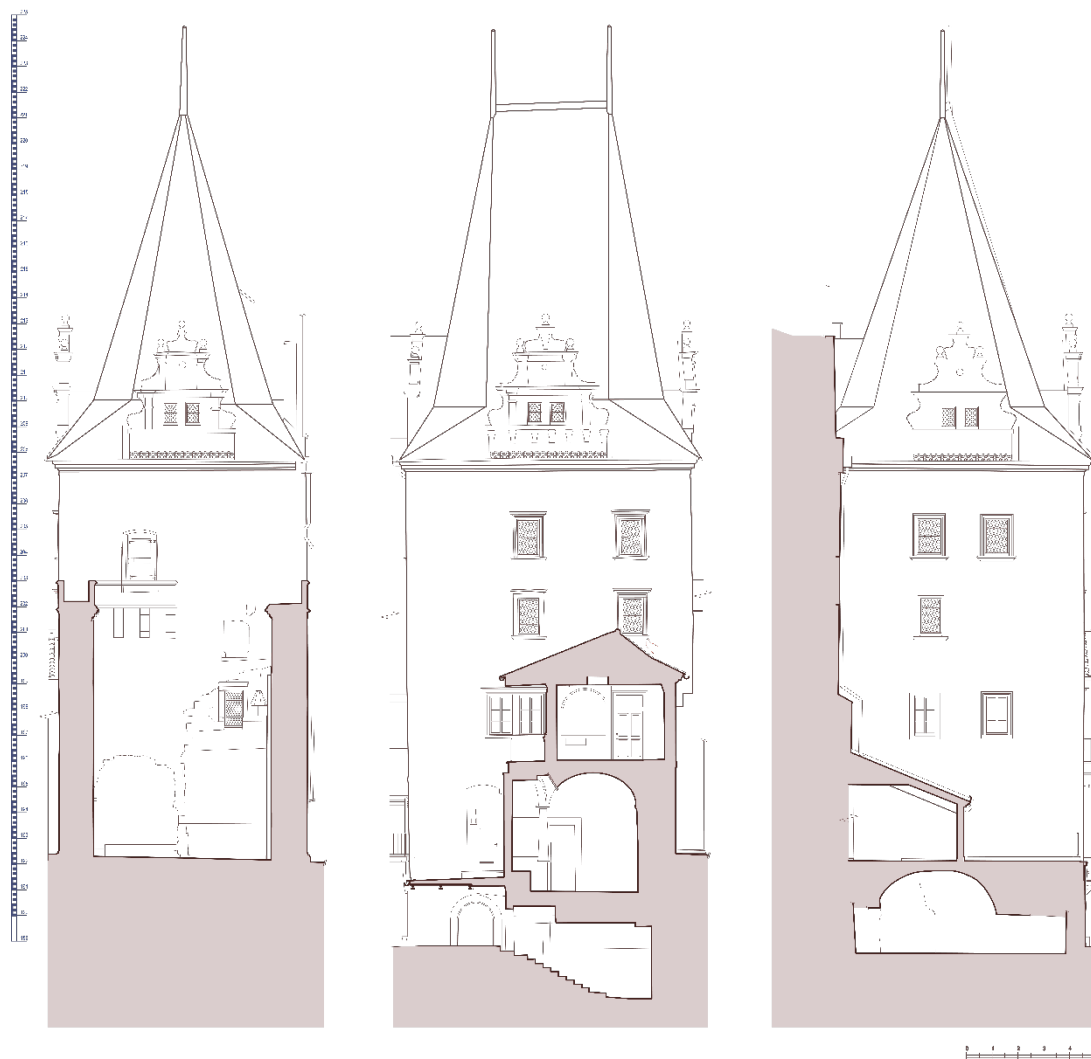


Figure 2.10 The tower's Elevation; CAD Documentation of the building, created by (Vesely, 2017), validated and redrawn by the Author. (a) Northern Elevations, (b) Eastern Elevations, (c) Southern Elevations.

2.5 BUILDING MATERIALS

2.5.1 Masonry walls:

The massive ancient masonry walls of the tower were constructed using marlstone for the outer face and brick for the inner face. Conversely, the inner core is made of heterogenous masonry with red clay bricks, natural stone conglomerate and medium-sized pebbles.

The most ancient building stone used in Prague is Cretaceous sandy marlstone called in Czech and eastern countries "Opuka", which was a common building stone in Bohemia from the beginning of stone architecture in the early mediaeval epoch (Figure 2.11). Its use for historical monumental edifices of the church, fortresses, castles, fortifications as well as burghers' houses dates back as far as the 9th century, and it continued until the beginning of the 14th century when more durable Cretaceous sandstone became the almost sole building stone (Schiitznerovd-Havclkow, 1979). Marlstone is a widespread rock type has been extensively used either as building or as dimension (sculptural) stone in the past (Prikryl, Lokajcekb, Svobodov, & Weishauptovab, 2003). The massive masonry walls of the

Marlstone from Prague, Czech Republic is, macroscopically, characterized by a pale yellow to golden yellow color and extremely fine-grain, and belonged to the Upper Cretaceous (Lower Turonian) sediments of Bohemian Cretaceous Basin (Prikryl, Lokajcekb, Svobodov, & Weishauptovab, 2003). It can be classified as clayey siliceous micritic limestone, with composition of micritic calcite, clay minerals – mainly kaolinite and illite, calcite in a form of recrystallized particle cement and calcified bioclast, where the golden yellow color occurs due to dispersed opaque minerals—limonite, goethite and anatose (Prikryl, Lokajcekb, Svobodov, & Weishauptovab, 2003).

Regarding its physical properties, they are as follows according to (Prikryl, Lokajcekb, Svobodov, & Weishauptovab, 2003): the mineralogical density 2:65 g/cm³, bulk density 2:0 g/cm³, open porosity 21:1 vol%, P-wave velocity 2:95 km/s, S-wave velocity 1:97 km/s, and the uniaxial compressive strength of Marlstone approximately equal to 65:2 MPa.

The interior walls were constructed of Half-timbered and infill. There are different types of these kinds of structure systems, one of which might be the system used for building the partition (Figure 2.12). For example: (a) wattle made from split laths, (b) wooden splitter laths with wattle made with twigs and clay and straw daub, (c) adobe bricks, (d) fired bricks or stoned joined with clay mortar – which most likely the used system for the tower. The plaster of the timber partition is single-layered, coarse-grained, and has considerable thickness, with a red coating in the lower layers (Vesely, 2011).

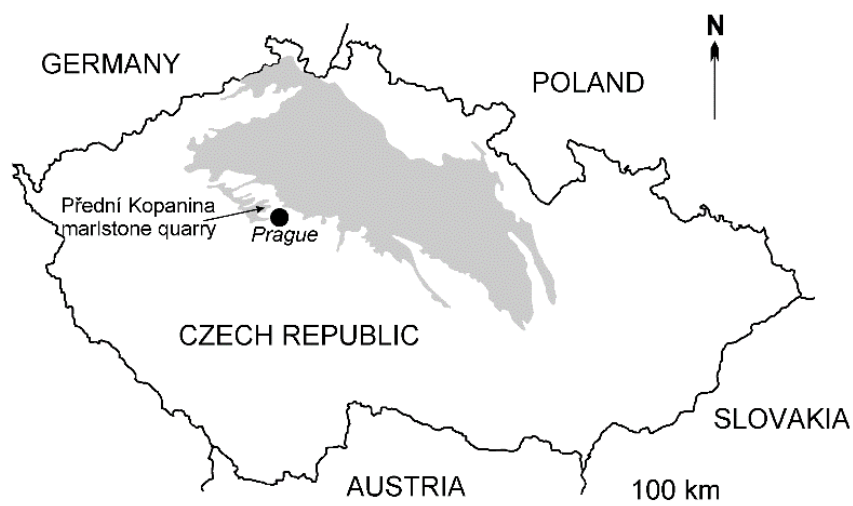


Figure 2.11. Map showing position of Predni' Kopanina quarry within the Bohemian Cretaceous Basin (Prikryl, Lokajcekb, Svobodov, & Weishauptovab, 2003)



Figure 2.12 Model half-timbered partitions with different types of infill, (Ruzicka) Centrum stavitelského dědictví NTM, 2023

2.5.2 Decay mechanism of Opuka stone masonry

The towers masonry walls constructed using Opuka stone, which is a very fine-grained sedimentary rock, accompanied by variable amounts of carbonates (mostly micritic calcite, common calcitic bioclasts—Foraminifera) and by less common clay minerals (kaolinite, poorly crystalline illite, glauconite) (Príkryl, Príkrylova, Racek, Weishauptova, & Kreislova', 2017). The masonry walls, unprotected by plaster, in the course of centuries underwent long-term weathering in the town (Prague) atmosphere (Schiitznerovd-Havclkow, 1979), most probably would exhibit deficiencies and damages related to weathering and other environmental factors. Consequently, the original light yellow or ochre color of the Opuka rock types had disappeared under a cover of dust and soot, so that its appearance changed, where the original sharp edges of the masonry become rounded and the surface layers peel off irregularly or disintegrate into flakers to depth of several centimeters (Schiitznerovd-Havclkow, 1979).

The experimental weathering of marlstone conducted by (Príkryl, Lokajcekb, Svobodov, & Weishauptovab, 2003), proved its higher sensitivity to crystallizing salt than to freeze/thaw action. Periodical cycles repeated during centuries, freezing water in pores with associated volume changes are further causes of disintegration of Opuka rock types (Schiitznerovd-Havclkow, 1979). Moreover, with the effect of the temperature changes, such as the freezing of water or condensation of water vapor increases the volume of the rock, causes the stresses caused on internal walls and capillaries of the rock can break it and can cause exfoliations. The different processes of deterioration of the rock are manifested as physical, chemical, biological, anthropogenic and even by their intrinsic properties. On the surface of uneven weathering crusts appear, consisting of mixture of calcium carbonate, calcium sulphate and fly ash, and it is affected by sack and efflorescence, mostly gypsum, under the secondary crust (Schiitznerovd-Havclkow, 1979). The different alterations found in the rock cause damage to each other, that one damage could lead to another of greater severity and depth. Eventually, the progression of these damages could lead to compromise the integrity of the structure.

2.5.3 The roof and floors

Although only four species (fir, spruce, pine, and oak) dominate in historical constructions (~99%) in the Czech lands, the use of Spruce in the historical constructions gradually increased from the beginning of the 16th century and started to dominate in the second half of the 19th century, mainly at the expense of fir and oak (Kolar, et al., 2021). According to (Veselý, 2011) the roof and the ceiling beams were constructed using Spruce during the restoration in the 16th century.

Spruce is less prone to wood warping and cracking (Kolar, et al., 2021), in comparison with pine wood, which contains a much higher amount of resin than spruce and fir (Klein & Grabner, 2015) Grabner, 2015), while Fir is heavy when freshly felled, which implies certain advantages and disadvantages in the use and processing of wood (Kolar, et al., 2021). In spite of these facts, differences in the proportions of individual conifers in historical constructions are not based on carpenters' preferences but primarily on the local availability of the species (Kolar, et al., 2021).

This page is left blank on purpose.

3 HISTORICAL DEVELOPMENT OF JUTIT TOWER

This section presents a historical survey that was carried out with several intentions: (i) the explanation of the steps that led to the current building and that are, in our opinion, necessary to understand its complexity; (ii) the presentation of the political and cultural context that influenced the construction of and interventions on the building at various periods; (iii) the production of an analysis of the value and authenticity of the building; (iv) the gathering of clues regarding the constructive details and systems necessary to understand the structure. The material analyzed to construct this study consists in various books, pamphlets, articles and reports written recently by the architect (Veselý, 2011) cross-referenced with photographs, drawings, paintings and engravings gathered from various archives. The most important documents are shown with the text, but the remaining ones may be found annexed.

3.1 BEGINNINGS OF THE TOWER'S HISTORY, THE 12TH AND 13TH CENTURIES:

The Judith Bridge, which precedes the Charles Bridge, was built during the 12th century. It's believed it was constructed between 1158 and 1172 during the reign of Vladislav II. The tower on the bridge is mentioned in several documents, including the Second Continuation of Kosmas from 1249 in connection with a battle between King Wenceslas I and his son Pemysl (Za Satarou Praha, 2018). It is also linked to the major restoration of the princely residence initiated by Soběslav I in 1135 (Dragoun, 2002). Although there is no conclusive evidence, it could be assumed the tower was first constructed as part of the fortification of the sub-castle settlement. Based on an analogy from Prague Castle and its black tower, it can be concluded that the height of the structure's ceiling was approximately 60 cm lower (Jan Veselý, 2007).

During the first third of the 13th century, the tower went through significant changes. The two flat wooden floors at the lowest levels were replaced with large, vaulted hall; a ribbed Gothic cross-vaults of pointed arch shape vaults. The ground floor was lowered by 55 cm and spiral staircase was inserted in connection with the original entrance on the second floor (Veselý, 2011). The vault occupied half the height of the former first floor and the entire height of the second floor, the last was divided by a new ceiling into two floors with a height about 3.8 m high (Jan Veselý, 2007).

The tower was used as a prison during the battle between 1250 and 1252 (Václav Vladivoj Tomek, 1974). The Second Continuation of Kosmas also briefly mentions the fortification of the towers of Prague Castle and the tower at the end of the bridge - Judith Bridge in 1252. This is the first known written mention of the tower. On December 3, 1281, a strong storm tore off the roof and timbered gallery of the tower, but not further reports on the on the subsequent repair (Veselý, 2011).

The Zbraslav Chronicle reports a battle with the Carinthians on the Lesser Town in 1310, when the tower was fortified by Henry of Lipá, the king's chamberlain, in preparation for the battle. The Carinthians made several attempts to capture the tower, but the defenders put up a brave resistance and eventually thwarted their efforts (Za Satarou Praha, 2018).

3.2 EMPEROR CHARLES IV – 14TH CENTURY.

The Judith Bridge was destroyed by a flood in 1342, and Emperor Charles IV decided to build a new stone bridge after 15 years in 1357. The new bridge was significantly higher than the old Judit bridge, which led to a significant increase in the Mostecká street that connects the bridge to the Mala Strana side (Veselý, 2011). Therefore, the relative height of the Judit Tower gradually started to decrease over time (Figure 3.1).

In 1413, the tower is explicitly referred to as a town tower, which indicates a change in its status from the earlier possession of the Saxon dukes in the first decade of the 15th century (Palacký, 1941). During the Hussite Wars, the bridge gate was most likely damaged, especially in November 1419 during heavy fighting in Lesser Town (Veselý, 2011). However, there is no exact information about the extent of the damage.



Figure 3.1 Historical drawings of Judith Tower, Muzeum hl. m. Prahy; (a) F. X. Sandmann akvarel, kolem 1840, (b) Vincenc Morstadt sepiová kresba, 1874.

After 1464 a new northern bridge tower was built, and the smaller tower was changed. The chronicles mention the foundation of the new tower and repairs to the bridge by George of Poděbrady. The smaller tower was connected with the new tower by a pair of gates and footbridges. The new tower exceeded Judit Tower by more than 9 meters, referred to here as the "Northern Tower." Then the Mostecká Gothic Gate (Figures 3.2 and 3.3) was constructed between the two towers, creating the Lesser Town Bridge Tower image that is preserved until today (Brně, 2008).



Figure 3.2 The atmosphere of the immediate surroundings of the Malostranské Mostecké věže (Malostranská Bridge Towers), as seen in her childhood by Marie Popelková, the future collector of Prague legends and writer Popelka Bilianová. Sepia drawing by Vincenc Morstadt from 1874, Prague City Museum.



Figure 3.3 The connection between the Tower and the gate – North Façade

3.3 RESTORATION OF THE TOWER AFTER THE FIRE DURING THE 16TH CENTURY

In 1503, a fire broke out in Malostranské náměstí (Lesser Town), as a result of which the southeastern part of Lesser Town burned including both towers (Jan Veselý, 2007). The Old Bohemian Chronicle explicitly mentions that in the description of the fire the "roofs of the defense towers, one with wooden shingles, very noble, and the other with tiles" were burned (Za Satarou Praha, 2018). The restoration of the smaller tower dragged on practically throughout the rest of the 16th century, while the northern tower was restored by 1527 (Veselý, 2011).

After the failed uprising against the Habsburgs in 1547, the Lesser Town Tower, together with the adjacent Customs House, was confiscated by the authorities of Prague's Old Town (Jan Veselý, 2007). However, in 1549 it was returned to them, along with the right to collect customs duties. A much clearer depiction of the smaller bridge tower is found in the well-known woodcut prospectus by Kozel and Peterle from 1562. The tower is described as crowned by a projecting walkway with battlements, and on the top floor appears the front of a vaulted half-timbered chamber with openings on the south side. On the west side, facing the Saxon House, there is a single window belonging to the attic (Za Satarou Praha, 2018).

During 1562, the absence of a visible roof was noticeable according to aforementioned Vratislavsky woodcut. The fire caused complete destruction of the interior structure of the tower, including the vaulted hall on the ground floor (Veselý, 2011). However, the masonry wall was preserved, including the walkway at the crown (Brně, 2008).

During the first phase of the tower's restoration, the high Gothic ground floor and part of the first floor were replaced by a low vaulted basement and a higher vaulted space on the ground floor (Za Satarou Praha, 2018). The basement floor was lowered by 145 cm from the original level of the lowest floor, probably even below the foundation joints (Veselý, 2011). The new two vaults were probably constructed from the destroyed Gothic vault, which is a mixture of fragments of sandstone ribs and bricks (Veselý, 2011). The low vault of the basement was built on a wall narrowing the interior space from the east and west, with an entrance on the east side at the southeast corner of the tower (Za Satarou Praha, 2018). At that time, the level of the ground floor was the same level as the pavement of the Mostecká gate, which was accessible from the east through a portal that likely led into the old customs building and was probably lit by a window in the eastern wall located below the southern vaulting rib (Veselý, 2011).

The second phase of the tower's restoration followed at the end of the 1570s. At that time the tower was still capped with walkway and battlements hiding low (Zahradník, 2005.). The portal on the ground floor, between the customs office and the vaulted space of the tower, was likely installed during this phase (Veselý, 2011). Moreover, wooden structures with new stairs were inserted into the ceilings above the first to third floors (Dragoun, 2002).



**Figure 3.4 Vincenc Morstadt: Dvůr pod Juditinou věží
sepiová kresba, 1874, Národní galerie v Praze**

Only in the third phase did the building acquire its current form. During the construction works after 1588, directed by Giovanni Bussi de Campione, the former Saxon house was apparently extended by two bays of windows to the east and connected to the smaller bridge tower. The tower, which had previously stood free, was partially integrated into the development of Mostecká Street (Veselý, 2011). The tower was still a separate structure on the west side from the Saxon House by a narrow alley, which disappeared shortly after 1600 (Figure 3.4). By 1590, the tower facades were covered with plaster and sgraffito rustication (Brně, 2008). Its western facade was also modified in the same way as the other facades, whether there were any openings in this facade, we do not know (Za Satarou Praha, 2018). The Gothic gallery with a

provisional roof was removed and, in its place, a high truss roof with four dormers was created (Veselý, 2011). Finally, The entrance on the first floor, the layout and the window frames on all three floors, and the current form of the entrance to the gallery gate on the third floor all date from the same time (Jan Veselý, 2007).

The following scheme (Figure 3.5) created by (Veselý, 2011) summaries of the reconstruction and main events of the development of the floors and roofing of tower.

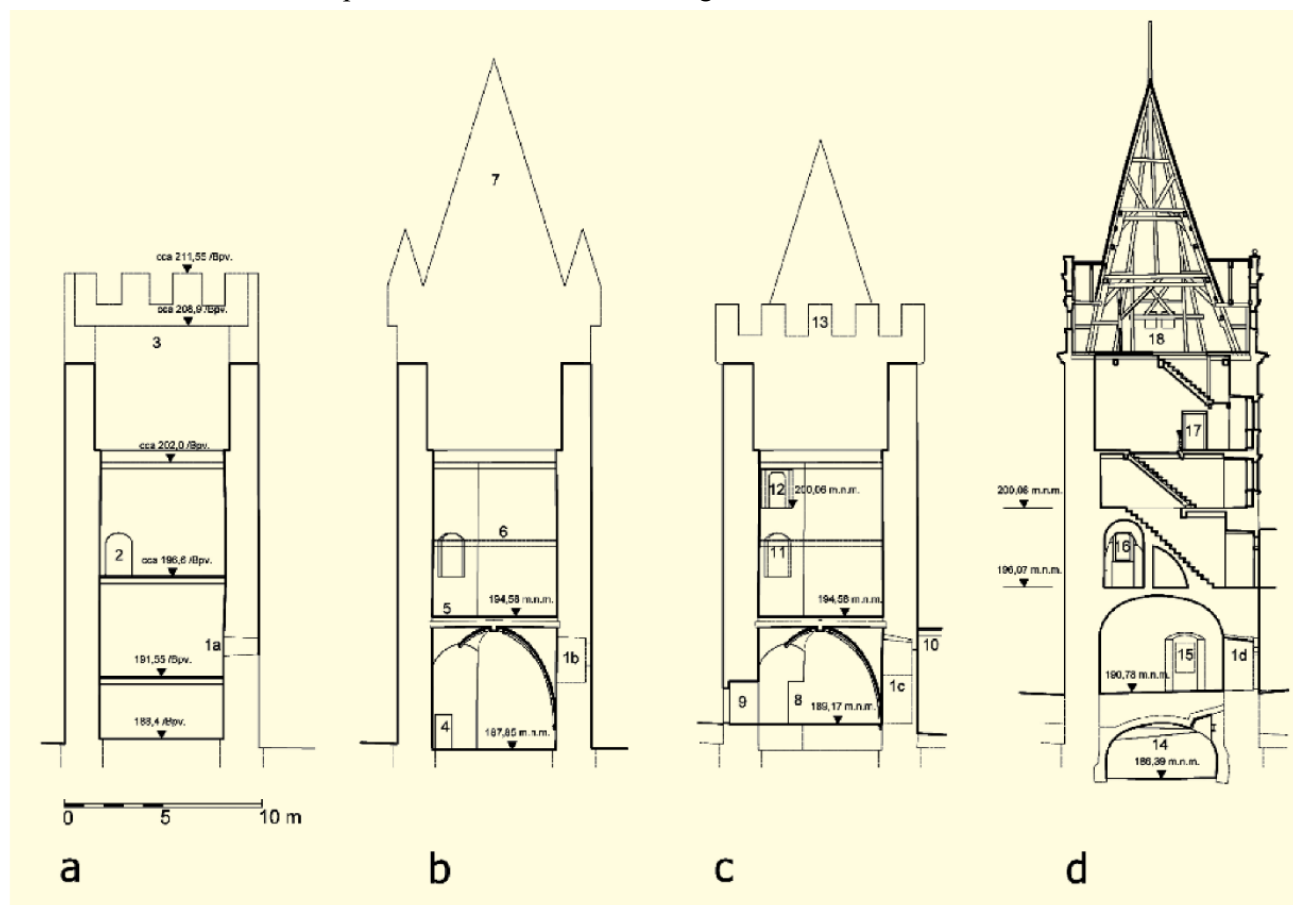


Figure 3.5 Tzv. Juditina věž, Prague - Malá Strana; Scheme of the reconstruction of the development of the floors and roofing of the tower: Drawing: Jan Veselý, 2007.

Figure 3.5 illustrates a scheme of the reconstruction of the development of the floors and roofing of the tower: Drawing: Jan Veselý, 2007, where: a - assumed form at the time of its creation, around the mid-12th century: 1a - assumed eastern Romanesque window, 2 - assumed entrance to the tower, 3 - form of the tower's masonry termination analogous to the Černá Tower at Prague Castle; b - form after reconstruction in the first half of the 13th century: 1b - expanded eastern window, 4 - entrance to the spiral staircase, 5 - level of the first-floor floor according to traces on the walls of the current ground floor, 6 - assumed new position of the second-floor floor, 7 - new roof of the tower documented by a report of a storm in 1281; c - form at the end of the 15th century: 1c - second expansion of the window opening into the door to the customs office, 8 - shifted entrance to the staircase, 9 - new western entrance, 10 - bridge customs office, 11 - original entrance to the tower, 12 - entrance to the walkway of the initial gate of Charles Bridge, 13 - protruding walkway and roofing with battlements, which was created after 1281; d - form after Renaissance reconstruction at the turn of the 16th and 17th centuries: 14 - newly deepened cellar, 15 - opening leading to the passage of the bridge, 1d - entrance from the arcade loggia of the customs office, 16 - window at the location of the oldest entrance, 17 - new entrance to the walkway of the bridge gate, 18 - new roof from 1590. (Za Satarou Praha, 2018)



Figure 3.6 Detailed survey and documentation of the ground floor walls, with an evaluation of findings processed by Jan Veselý, 2005-07.

Notable here are the scars of a vanished early Gothic vault and the angular body of the staircase (Figure 3.6). (1) revealed Romanesque arrow slit window; (2) preserved reveal of an opening, likely of Romanesque origin - assumed position of the second Romanesque window; (3) regular rectangular pockets in the Romanesque masonry at a level of 191.5 /Bpv. on the southern wall and 191.34/Bpv. on the western wall, interpreted as remnants of a ceiling structure between the first and second Romanesque floors; (4) damaged limestone polygonal corbel and a remaining projection of a diagonal vaulting rib; (5) Renaissance infill of a Gothic door opening with reveals constructed from large, finely dressed blocks of limestone or fine-grained sandstone; (6) two small areas with distinct soot deposits above a blocked Gothic opening, probably indicating the placement of torch holders; (7) Renaissance infills of scars from the vanished Gothic vault are not affected by fire; (8) scars on the walls of the angular staircase. Surveyed and processed by Jan Veselý, 2005-07.

3.4 FROM THE 17TH CENTURY UNTIL TODAY

During the 17th century and most of the 18th century there are no reports informing people about changes in the tower. It was only after the damage caused to the bridge by the flood of 1784 that repairs and renovations were carried out, including to the towers of Lesser Town. Between 1826 and 1828, the former Saxon House was extensively rebuilt in neoclassical style according to the plans of engineer Jedlička and builder Švestka (Veselý, 2011). A regular third floor and a new roof were built, partially blocking the view of the tower from Mostecká Street and closing the previously open western gable dormer (Brně, 2008).

Between 1874 and 1882, a relatively extensive restoration and reconstruction of the north tower took place (Jan Veselý, 2007). The smaller tower - the Judith Tower, which at that time was used for residential purposes and was privately owned. The renovation works on the smaller tower were much less and easier at that time (Za Satarou Praha, 2018). On August 22, 1888, the then owner received permission to install a toilet "on the second floor in the corridor adjacent to the tower." On November 28, 1888, František Bárt applied for permission to divide a large room on the second floor into two smaller living rooms by installing a partition 16 cm thick, closing the existing door and installing new doors in the same partition (Veselý, 2011). This adaptation was to be carried out according to the plan of the contractor F. Kindl. The requested permission was granted to František Bárt.

In 1893, the Prague municipality purchased the tower, along with the house numbered 56/III, from František Bárta and became the owner of all three bridge towers (Václav Vladivoj Tomek, 1974). On July 18, 1927, the club was granted permission to make structural changes on the 2nd and 3rd floors of the smaller Mostecká Tower at house No. 56 in Prague III, involving the removal of two load-bearing partitions, the installation of interior windows, and a dark chamber (Za Satarou Praha, 2018). In 1938, thanks to the

efforts of the Club for Old Prague, the toilet on the first floor of the house in front of the Romanesque relief was removed, re-exposed, and preserved (Veselý, 2011).

In 1969, a complete restoration activity took a place of the tower's facade, including the stabilization work and reconstruction of fragments of Renaissance sgraffito plaster (Za Satarou Praha, 2018). However, the newly renovated ground floor was not made widely accessible, likely due to the climatic conditions affecting the sgraffito artworks. The entrance from the passage of the Mostecká Gate was sealed, and the ground floor was only accessible through the courtyard of the house (Za Satarou Praha, 2018). In 1984-1985, the sandstone relief on the eastern facade of the tower was restored, where the northern side of the relief recess was modified, and remnants of Renaissance plaster on the upper part of its niche were removed (Veselý, 2011).

Between 2005 and 2007, under the guidance of Ing. V. Jandáček and according to the project by Ing. Arch. Martin Kris, the restoration of the tower's ground floor, together with the adjacent space in the former customs office, was finally carried out at the expense of the Club for Old Prague. Extensive monument documentation was conducted as part of the restoration (Veselý, 2011). The restored spaces became an information center and a bookstore for the Club for Old Prague (Za Satarou Praha, 2018).

This page is left blank on purpose.

4 VISUAL INSPECTION AND DAMAGE SURVEY

A vital aspect when modelling the mechanical behavior of existing masonry structures is the accuracy in which the geometry of the real structure is transferred in the numerical model (Loverdos, Sarhosis, Adamopoulos, & Drougkas, 2021). The first, and simplest, approaches for the assessment of any masonry structure should include the visual identification of irregularities, discontinuities, out-of-plumb elements, cracks and damages, settlements and a detailed geometric, material and technological survey (Pallarés, Betti, Bartoli, & Pallarés, 2022). This chapter is devoted to briefly explaining the methodology used for the visual inspection, then going through how the geometry and photographic documentation of the tower was obtained. At the end, the damage mapping was demonstrated thoroughly and in detailed.

4.1 GEOMETRICAL SURVEY

Full documentation of the tower was created in 2011 within the course of the tower's architectural study done by the architect Jan Veselý. He employed Geodetické Zaměřeníby/stávajícího stavu to conduct the detailed survey and prepare the AutoCAD drawings of the building. In this study, a validation of these drawings was performed, by taking onsite measurements using laser meters. All of the document and the drawings are shown in Annex A.

Mainly, photographic documentation of the building was done using SONY Alpha A7 II + FE 28-70 mm. Each camera was localized on CAD drawings. For the purposes of the damage survey, 2D photogrammetric documentation for specific damaged areas in the buildings was generated. These were prepared by taking photographs onsite, then processed using Agisoft Metashape Pro, which is a stand-alone software product that performs photogrammetric processing of digital images and generates 3D spatial data to be used in GIS applications, cultural heritage documentation, and visual effects production as well as for indirect measurements of objects of various scales (Agisoft, 2023). This software also allows the generation and export of detailed orthophotos to be processed later.

4.2 VISUAL INSPECTION

Following the historical and geometrical survey, the visual inspection revealed the tower suffers from several biological, mechanical, chemical, and anthropogenic damages. This study aims to map these structural deficiencies and provides a clear insight into the causes and impacts of them on the building. Before carrying out the damage inspection, the layout of the tower was divided into 5 zones, where each zone represents one floor and the roof.

The identification of these damages was localized on CAD drawings then authenticated with photographic documentation. Using Excel sheets, the data sheets for the damages survey were organized by families, that is, to the classification within pathologies of chemical, mechanical, or anthropogenic type according to the Broto Encyclopaedia of Construction Pathologies and the ICOMOS Glossary (ICCOMOS Monuments and sites XV, 2008). Each damage given a code based on its categories and types. For example, the mechanical damages – the focus of the study, are 4 types: Cracks, deformation mechanical damages and missing parts, and each were divided into subcategories – under the type “crack”, there are fracture (MD-01-1), hair crack (MD-01-2), and splitting (MD-01-3) – See Annex c.

Annex B was prepared for the visual inscription, containing 6 pages of the damages survey, one for each zone. Each data sheets were divided into four main sections showing in Figure 4.1: (a) general information, (b) localization, which contain a plan and section of the floor, (c) damage mapping, on the available resources, such as: CAD drawings, photogrammetric documentation, 3D sketch etc., (d) photographic documentation, and (e) definition of each damage with its code, photo number, and intervention strategies.

4.2.1 Masonry behavior and failure moods

Masonry structures are challenging to assess due to the heterogeneity of materials and their mechanical behavior, therefore, the damage causes, crack patterns, deficiencies, and material characteristics should be identified and addressed before performing repairs (Latifi, Hadzima-Nyarko, Radu, & Rouhi, 2023). A possible cause of the structural cracks may be the stress concentration through the regions of the structure (Bilgin & Ramadani, 2021). In 1966, Jacques Heyman formulated constitutive assumptions in determining the admissibility domain of the no-tension, rigid in compression masonry models (Latifi, Hadzima-Nyarko, Radu, & Rouhi, 2023):

- (a) masonry is incapable of withstanding tensions, or the masonry has no tensile strength.
- (b) the infinite compressive strength of masonry.
- (c) negligible elastic strains.
- (d) sliding cannot happen since masonry has infinite shear strength and the only possible deformation is detachments or cracks (Heyman, 1997).

DAMAGE SURVEY - DATA SHEET

PROJECT NAME: Static Assessment of Judit Tower in Prague
ADDRESS/COORDINATES: Muzikova 101, Praha 1, 110 00
PLANNED TO BE REALIZED: Real Project
REASON: Repair and upgrade - Wall Bands
PART OF MEASURE: Other

ORIGINALITY: (a) **FORMER DAMAGE:** [Color scale legend]

DATE/COORDINATES: 2023/01/20
REFERENCE PLACE: 50.071120N

LOCALIZATION: Part Second Floor

DAMAGE LOCALIZATION: Crack Mapping East facade - second floor level

RELEVANT IMAGES: Image number: 0-1 Image number: 0-2
 Image number: 0-3 Image number: 0-4, 0-5, 0-6
 Image number: 0-7 Image number: 0-8
 Image number: 0-9 Image number: 1-0

(b) (c) (d)

Image	Code	Damage	Description	REPAIR/RECOMMENDATION
0-1	BD-01-0	Crack status	Minor vertical crack in the masonry wall.	Monitor the crack development and repair if it widens.
0-2	BD-01-0	Spalling	Small area of mortar loss and brick surface damage.	Repair the damaged area with compatible mortar and bricks.
0-3	BD-01-0	Fracture	Vertical crack in the masonry wall.	Monitor the crack development and repair if it widens.
0-4	BD-01-0	Deterioration due to groundwater	Water staining and efflorescence on the masonry wall.	Identify the source of groundwater and implement waterproofing measures.
0-5	BD-01-0	Impact damage	Local damage to the masonry wall caused by impact.	Repair the damaged area with compatible mortar and bricks.
0-6	BD-01-0	Deterioration due to groundwater	Water staining and efflorescence on the masonry wall.	Identify the source of groundwater and implement waterproofing measures.
0-7	BD-01-0	Fracture	Crack in the masonry wall.	Monitor the crack development and repair if it widens.
0-8	BD-01-0	Spalling	Small area of mortar loss and brick surface damage.	Repair the damaged area with compatible mortar and bricks.

(e)

Figure 4.1 Methodology – damage sheet: (a) general information, (b) localization of the damage, (c) damage mapping, (d) photographic documentation, and (e) definition of each damage.

The stress evaluation within masonry vertical wall bands is significantly related to blocks (brick or stone) and mortar bed characteristics (Latifi, Hadzima-Nyarko, Radu, & Rouhi, 2023), where phase of the evaluation of the stress is without crack, then the ultimate cracked phase where tensile stress vanished.

According to (Angelillo, Lourenco, & Milani, 2014), there are basically three failure modes that are visible locally in masonry structures:

- (a) the one associated to the brittleness of the material and that manifests itself with detachment fractures,
- (b) mixed mode in which fractures of detachment alternate to lines of sliding, such as those appearing in the examples of in-plane shear shown,
- (c) the so-called crushing of the material and occurs essentially under compression.

Judit Tower exhibits the common crack locations and patterns that usually observed in masonry buildings, involving: (1) in-plane diagonal or shear cracks, (2) cracking near openings, (4) separation between roof and walls or wall intersections, and (5) cracking in the arch and vault (Latifi, Hadzima-Nyarko, Radu, & Rouhi, 2023). These deficient are mapped and discussed thoroughly in the following section.

4.2.2 Limitations of the visual inspection

There may be lesions that were not uncovered during the pathological study, since during the intervention work itself there are usually problems with the appearance of materials that were not studied and identified because they were hidden. In addition, stone is a heterogeneous material and therefore there is always the possibility of different textures and porosities within the same area of the building. Any intervention in a building of great architectural value should include the history of the monument, its pathologies, causes, intervention proposals and additional control and registration sheets of the interventions carried out. These must consider the further testing on the materials to be used in the element to be intervened, since the compatibility of the commercial materials must be verified according to the characteristics of the material that makes up the structure and the environmental characteristics.

4.3 DAMAGE SURVEY

4.3.1 North facades

The northern façade, which faces the passage of Charles Bridge, is connected to the piers of Mostecká Gate and the pedestrian footbridges. Some parts of the Renaissance plastered with sgraffito are lost, revealing the regularly patterned sandstone. A wedge-shaped wall was built to even out the difference between the southwest pillar of the gate and the northern facade of the tower, extending part of the wall to a width of 3.6 meters from the western pier (Figure 4.2). It was built using larger blocks of the same marlstone that used the rest of the original facades. The joint bed of the masonry wall was restored and repointed using lime-based mortar. On the western pillar of the gateway there is a vertical groove for a roof

ridge, which is 15-18 cm wide and 19 cm deep (Figure 4.3). The former stone window opening on the first floor was recently filled in with ashlar masonry and smoothly plastered but is still visible.

The Northern facade exhibit mechanical damage and Loss of material due to the action of an edge tool. The stone blocks of the wedged addition the appearance of an excavated cavity with an incision and missing edges. The propagation of these deficiencies happened because of weather conditions and the nature decay mechanism of the types of stones with the high porosity punctuated by water.

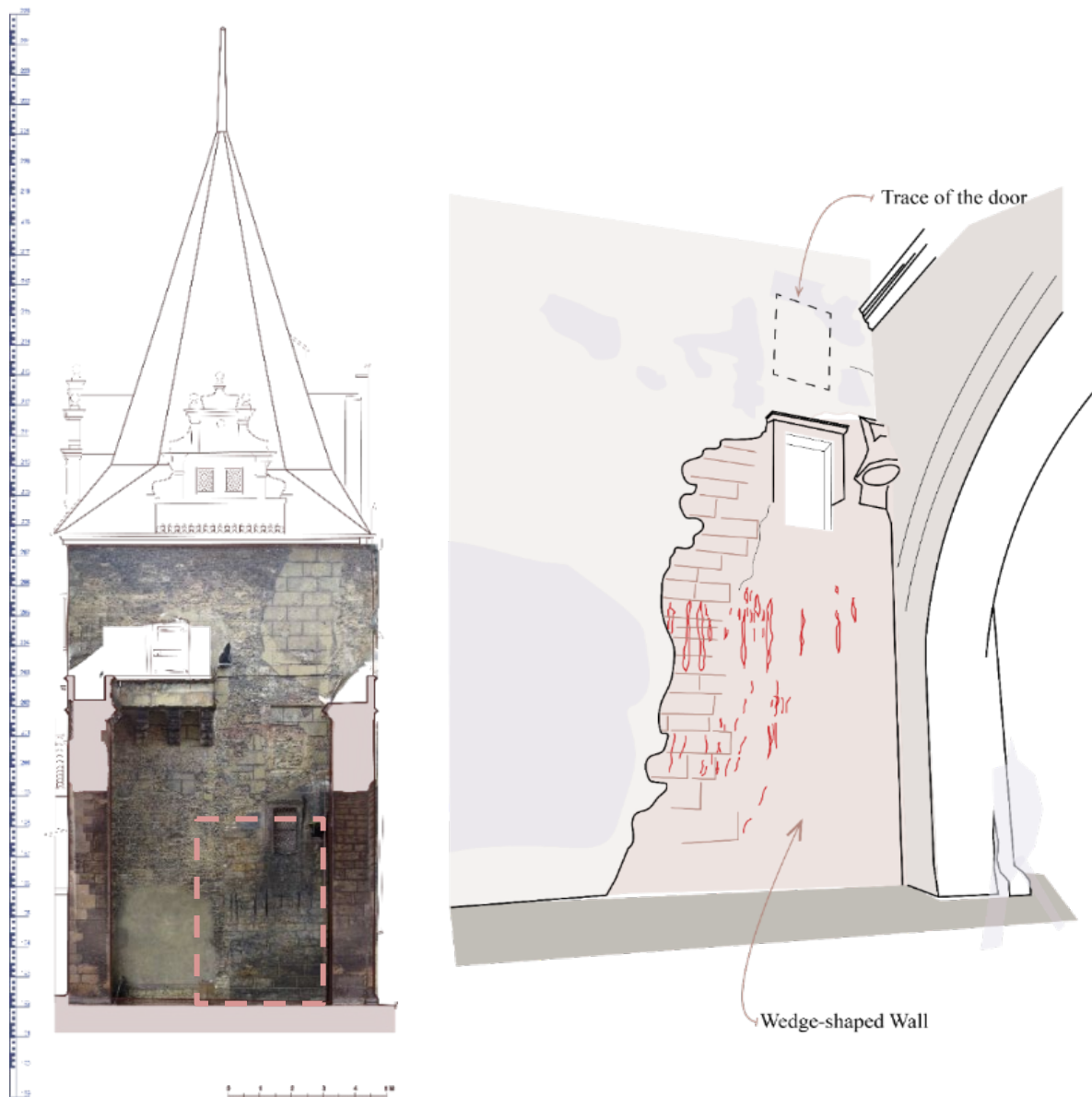


Figure 4.2 Northren Façade – The conection between the tower and the piers of Mostecká Gate



Figure 4.3 The lower part of the Northern façade, the dashed line highlighted the vertical groove.

Most of the north and south facades of the ground floor, along with the basement's walls, are hidden under the street's current level. (Figure 4.4, a) is a topographical diagram illustrating a vertical section of the tower and terrain below. (1) and (2) levels captured by J. Čiháková on Mostecká Street in 1997; (3) and (4) levels exposed of diabase paving of Judita Bridge on the ground floor of house No. 77/III; (5) level of older paving of Charles Bridge captured by Z. Dragoun in 2007; (6) assumed level of the floor of the Romanesque ground floor of Judita Tower; the current ground level is shown by a solid thick line (Survey and drawing by J. Veselý, topography of remnants of Judita Bridge taken from the book by V. Hlavsa and J. Vančura, Lesser Town, Prague 1983).

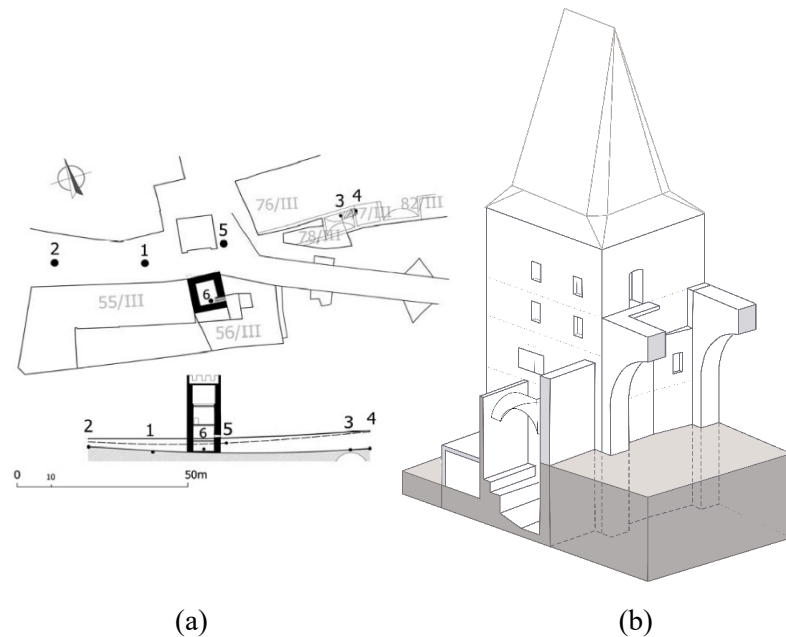


Figure 4.4 North Façade – (a) Topographic diagram by J. Veselý, (b) 3D diagram showing the street level of the north and level of the courtyard on the south.

4.3.2 Eastern Façade

The eastern façade, facing the bridge, is blocked by the two-level house no. 56, with a height of 8.70 meters and a width of approximately 6.60 meters, covering 28% of the façade. Moreover, the south corner of the tower is only accessible nowadays from the courtyard (Figure 4.5). Similar to the northern façade, some parts of the Renaissance plastered with sgraffito are lost, revealing the stone blocks (Figure 4.5). Several types of cracks were observed on this façade in the eastern wall, particularly in the lintels, sills, and window ledges, which extended as shear cracks through the wall through the window's pediment then spread into the interior of the structure. It appears as minor cracks with a width dimension of 0.1 mm on the Renaissance plaster.

The stress prerogative on these elements had caused fractures at their edges, as strongly observed in the double window on the first floor, which suffers from multiple fractures where the crack that crosses completely its decorative stone. In the middle of the window's lintel, the stone exhibits some splitting and fracturing caused by microcracks or clay/silt layers. The shear crack under the window extends to the top of the door on the ground floor level (Figure 4.6 – a).



Figure 4.5 Eastern façade – (a) orthoimage documentation of the damaged part of the facades, (b) sketch showing the façade deficiencies and damages.

To the left of the door on the ground floor (The toilet), cracks have developed diagonally, causing a fracture and detachment that alternate with lines of sliding between the joint of the masonry wall. The stress release causes cracks with detachment fractures in the stones observed at the end bottom of the wall (Figure 4.6 – a). This type of crack is usually associated with the brittleness of the material (Angelillo, Lourenco, & Milani, 2014)), but the sliding between the stones is associated with the in-plane shear (Figure 4.7 – b and c). The loss of some of the stones on the southeast corner of the tower is caused by the installation of the railing in the courtyard.



Figure 4.6 cracks mapping – Southeast corner of the Tower.

The impetus that caused the formation of cracks could have been the Baroque renovation, including the reconstruction of the cross vault on the ground floor and, more likely, the installation of a large opening on the ground floor (the current toilet). By examining the crack pattern on the drawing of the eastern façade, it can be traced that the directions of the cracks correspond to shear stresses resulting from the redistribution

of loads in the wall during the creation of openings and also the associated path of the stress of the vault's abutments – its reconstructing after it collapsed.

4.3.3 Southern and western façades

The west façade is completely blocked by the Saxon House, which is used for commercial purposes; therefore, the original outer wall is remodeled using modern and contemporary materials. The southern façade is exhibiting decay in its stone blocks and has also lost part of the Renaissance plaster. At the level of the ground floor, some cracks related to the brittleness of the material appear. A slight buckling in the wall could be noticed, but its cause can be bad workmanship or resistance to the overturning out-of-plane behavior of the wall. Also, some damage to the stone was caused by the installation of the railing in the courtyard.

4.3.4 The Interior of The Tower

The hall space on the ground floor of the tower is in good technical condition and functions, despite the fact that it is loaded by two floors of partitions with Baroque doors and a timber partition on the top floor, which was constructed in a single building phase. It is now a unit with the adjacent space in the ground floor arcade loggia of the neighboring building with house number 56 (Figure 4.7– b).

The ground level of the house is currently used as a bookshop, exhibits some deficiencies on its intersected vaults, indicating a separation of them (the older and newer structure), which were properly constructed at different times (Figure 4.7– c).

On the east face of the eastern wall, diagonal hair cracks have appeared, connected to the crack in the cross vault. Also, it appears on the lintel of the doors in three locations. In the northern wing of the house, it appears that the crack extended into the first floor (Figure 4.7– c), causing a complete fracture of the lintels of the door (Figure 4.7– e). The path of these cracks seems to be associated with the continuation of the shear crack under the windows of the first and second floors.

A secondary crack appears longitudinally in the intersection between the tower's eastern façade and the north wall of the house on the first floor. It continues to the middle of the segmental pediment of the door, drawing a wide diagonal crack. This kind of cracks usually a result of deformation due to generalized movement and appears due to differential settlement, where the presence of cracks at 45° with an emphasis on spans—weak points (ICCOMOS Monuments and Sites XV, 2008). Usually, it is recommended to study the soil and settlement to understand their behavior and effect on the building. Similarly, the east-facing windows on the second and third floors exhibit similar deficiencies, where the shear cracks that appear on

the eastern façade extend to the segmental pediment of the four windows, and the same is true for the two windows to the north on the third floor – See Figures 4.9 and 4.10.

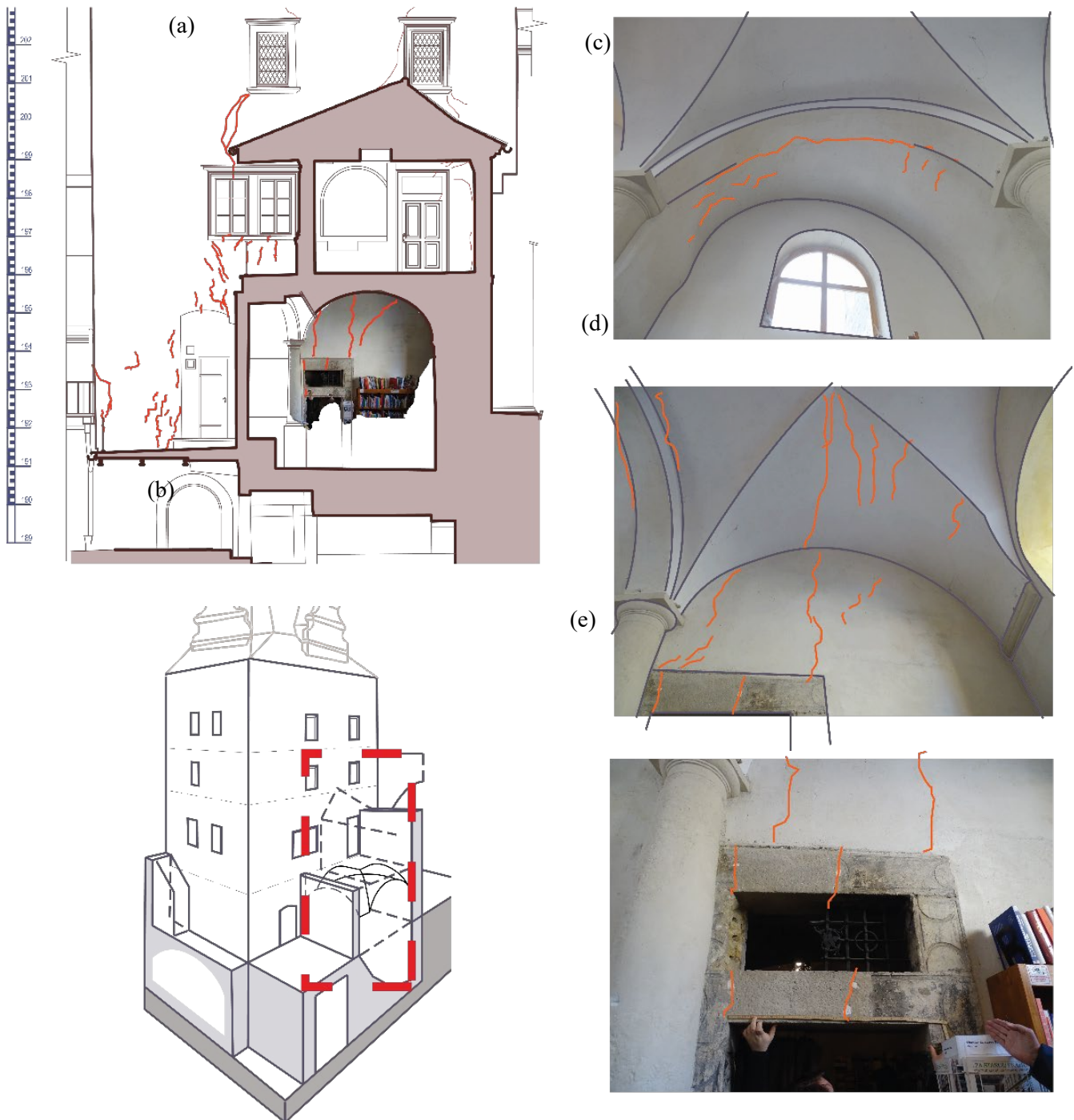


Figure 4.7 Crack mapping – the interior of the intersection between the tower and structure of the house 56.



Figure 4.8 Localization of the crack on the plans – (a) First floor, (b) second floor, (c) third floor.

On the third floor, the timbered partition with a thickness of approximately 350 mm directly above the wall of the 2nd floor is showing cracks long and wide, at the base of which is a beam. These inclined symmetrical cracks, interpreted as shear cracks resulting from the settlement of the fill or the threshold beam beneath the load-bearing wall, were caused by the expansion of the thick plaster, which has detached from the timber structure of the partition (Figure 4.9).



Figure 4.9 Third floor – Wall partition

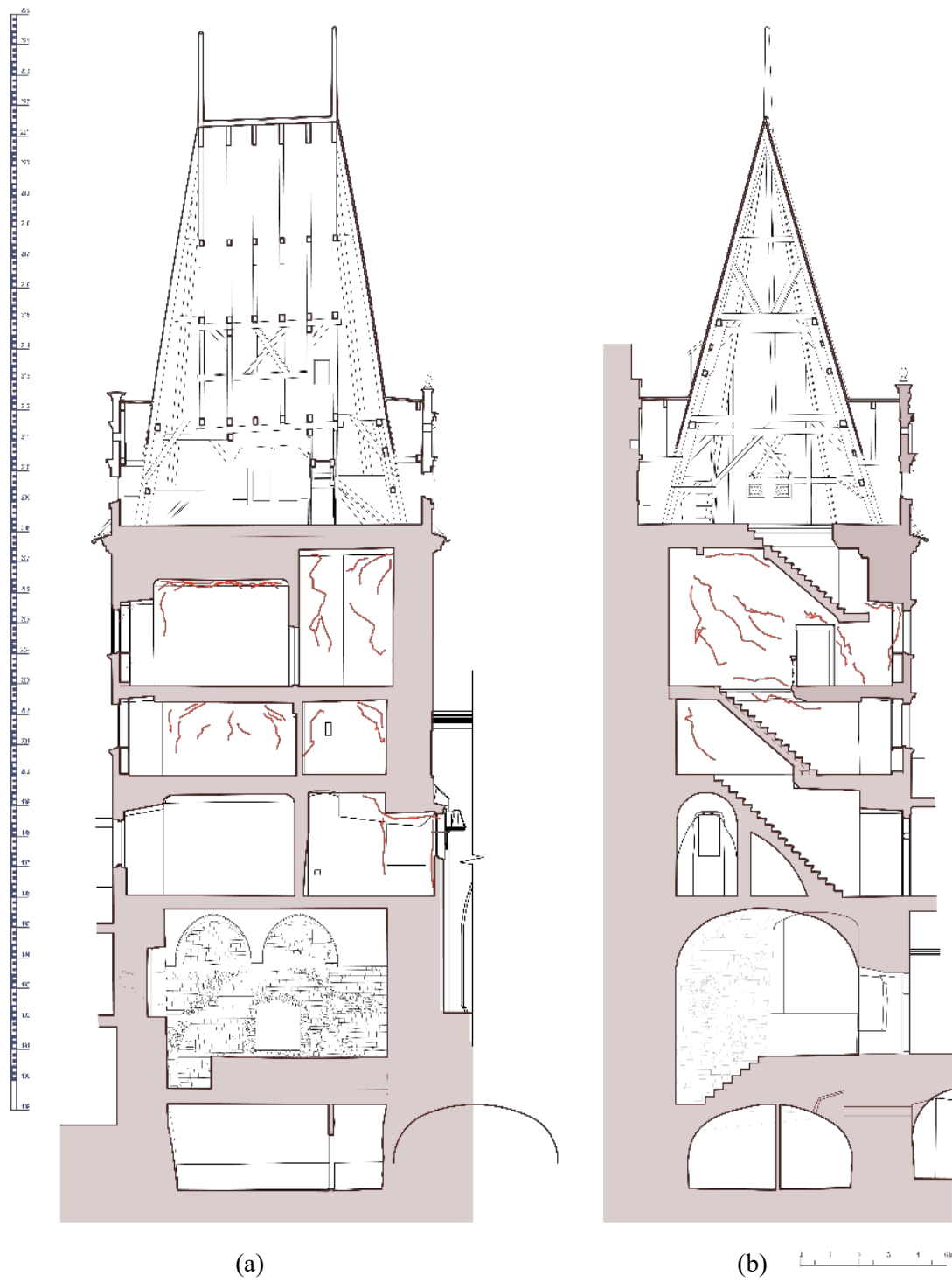


Figure 4.10 Localization of the crack on the sections

4.3.5 Attic, Truss, and Roof

The high gable roof with dormers and massive gable bay windows is one of the most distinctive parts of the building and represents an unchanging element of the left-bank panorama of Prague. It has retained the same form since the end of the 16th century (Veselý, 2011). The current appearance is a result of the work done in the 1960s, particularly concerning the sheet metal elements, roofing composition, and shaping of the dormers. In future roof repairs, the existing roofing should be maximally utilized. It would be appropriate to reduce the area of sheet metal cladding and return to the classical details of the slate composition on the ridge and roof edges. Within the attic space, the Renaissance truss, including the original parts of the formwork, represents the main architectural and historical value. To ensure the longevity of this valuable structure, it is not desirable to make extensive alterations to the truss – recommendation by (Veselý, 2011).

This page is left blank on purpose.

5 GEOMETRY IDEALIZATION AND SYSTEM CHARACTERIZATION

5.1 IDEALIZATION OF BUILDING GEOMETRY AND STRUCTURAL SYSTEM

This section discusses the simplifications made for the creation of geometry for the two Finite Element (FE) models, using Dlubal software. The first model (Figure 5.2) adapted the use of a shell and beam (members) finite element model to reduce the amount of time necessary to both create the simplified geometric model and reduce the analysis time. The second model (Figure 5.2) was created using solid elements for the masonry walls, shell elements for the vaults and wall partitions, and beam elements for the roof and floors. Figure 5.1 illustrates the methodology for modeling for the analysis to be conducted using Dlubal, where first the 2D CAD drawings were studied and prepared to be imported into the Dlubal graphical interface, where both the models were constructed for the structural analysis later on. In addition, the masonry Two different analyses were performed. Firstly, eigenvalue analysis was used to calibrate the building stiffness to obtain agreement between the building's experimental and numerical natural frequencies. This analysis uses both material and geometric linearity. Then a linear Static analysis was performed – see chapter 6.

Regarding the Loading conditions, during the first analysis – the eigenvalue analyses, only the self-weight of the model was used. Portions of the building which were not included in the geometry of the model were included in the model mass by means of the density assignments.



Figure 5.1 Creation of the Finite Elements Model – Methodology

5.1.1 FE Model 1 (M1)

First, the masonry walls were modeled as a continuous homogeneous material where its geometry was constructed using plane surface elements (bi-dimensional elements), and placed at the center of the massive 2-meter walls. Surfaces are defined in the Dlubal manual as the geometry of planar or curved structural components whose surface dimensions are significantly greater than their thicknesses. The stiffness of a surface results from its material and thickness (Dlubal Software GmbH, 2023). The model

simplifies the wall geometry and uses average thickness values, which decrease upward (Figure 5.3). Table 1 and shows the height and thickness of the tower walls.

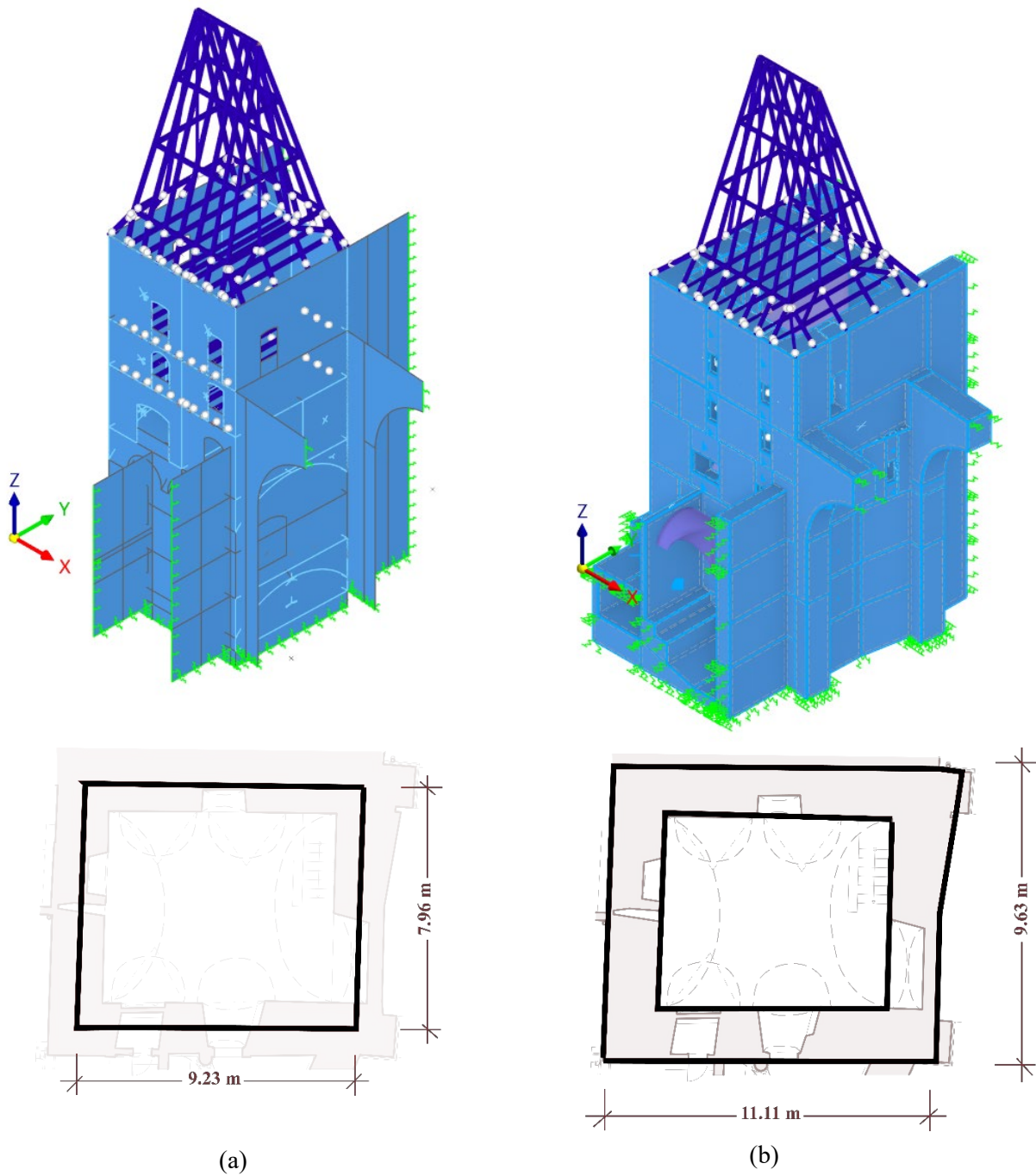
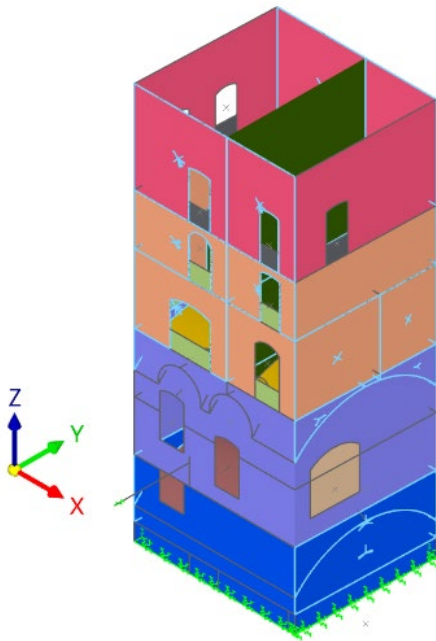


Figure 5.2 Numerical models – (a) Shells model (M1), (b) Detailed solid model (M2)


Table 1 Geometry of the Masonry walls

Floor	Walls Thickness	Walls Height
Third Floor (Pink)	1380	5320
First and Second Floor (yellow)	1700	2930
Ground floor (purple)	1750	6330
Basement - including the foundation (Blue)	2050	3360
Interior partitions	350	-

Figure 5.3 Geometry of the Masonry walls adapted in the first model (M1)

Using Quadrangle surfaces, the geometry of the cross-vaults was based on the CAD documentation and stached to be connected to the wall surface, with a span of 7.93 m, a depth of 9.30 m, and a height (above the spring lines) of 1.90 m. The profile of the four small vaults was unified with a 2.4-m span, then the surfaces of the five elements of the vault intersected, and the geometry of the vault was created (Figure 5.4). It assumed the infill is soil and its density were calculated and added to the vault's density. The wall partition that is loaded above the vault was modeled at the intersection of the vault. These partitions were also modeled using surface elements with thickness of 350 cm. The basement vault is a barrel vault, it has much simpler geometry. It was also constructed using the same Quadrangle surface, with a span of 7.93 m, a depth of 9.30 m, and a height of 1.90 m.

The floors were simplified and modeled using beam elements with spacing of 85 cm in between, as shown in Figure 6.5. Eventually, the model kept the original shape of the roof but simplified it to basic trusses system with three leveled rings that tied it up. Moreover, it was hinged in the connection with the masonry walls.

Regarding the modeling of the windows and doors, the shape of the segmental pediments of each was taken into consideration – since the thickness of the front frame of the windows doesn't exceed 20 cm, while the vaulted niches vary between 1.55 meters on the ground floor and 1.18 meters on the third floor.

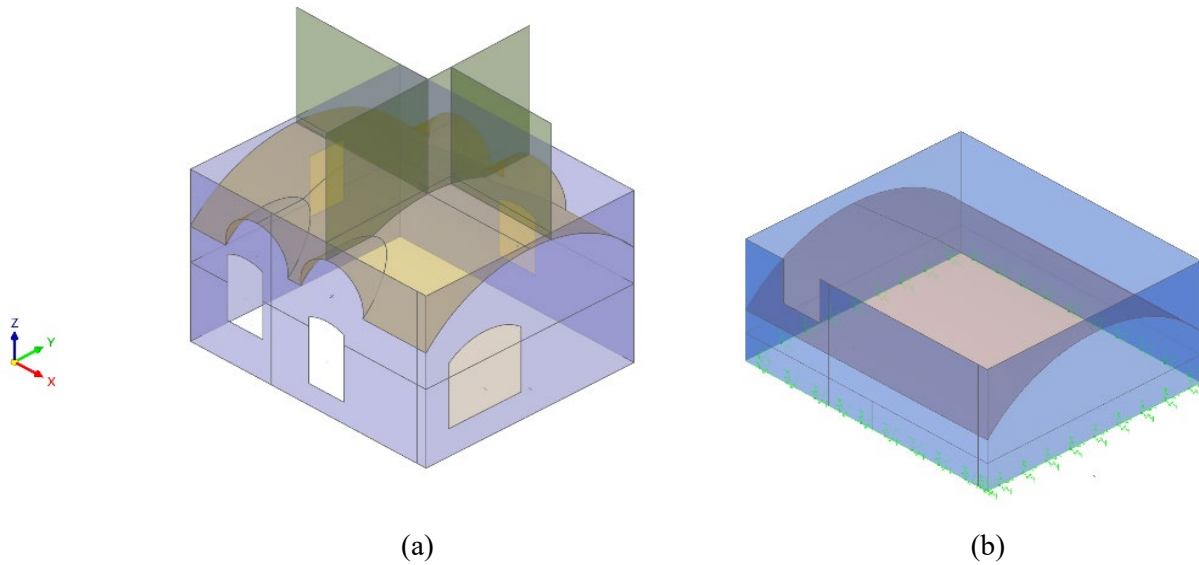


Figure 5.4 Vaults – (a) ground floor vault, (b) basement vault

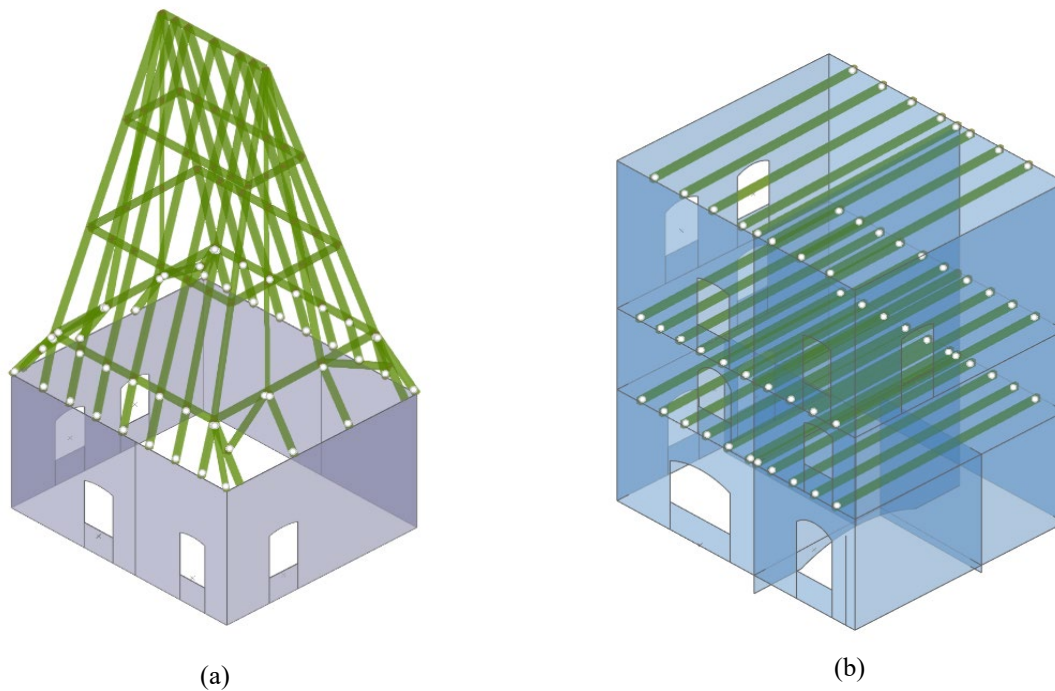


Figure 5.5 Beams elements (a) The roof, (b) Second and third floors.

The boundary conditions were modeled using either (i) a fixed base beam, or (ii) a beam on a flexible base made of translational and rotational spring, simulating the soil-foundation interaction and the adjacent structures to the tower. They were illustrated in Figure 5.7, as follows: (1) The gate pillars were modeled in their correct direction and placed in the center of the massive masonry walls. Half of the gates two arches were modeled as surface elements, and springs were placed at their edges as translational spring constants in the x-direction. (3) The walls of the buildings adjacent to the tower from the west and east were modeled simply as surface elements, placing translation spring constants at the y-directions; the details of the floors and vaults were neglected in this model. (4) The foundation of the tower was assumed to extend 0.5-meter below the basement walls, then fixed with line support. (5) The street is considered active earth (Ground) pressure (Figure 5.6), which, according to European code, occurs when the soil pushes into a structure and moves in the direction of pressure. It's applied as linear loads against the north façade. The size of the horizontal pressure is obtained according to the following relationship:

$$\sigma_x = \sigma_z \cdot k_a - 2c\sqrt{k_a}, \quad \text{Equation 1}$$

where $\sigma_z = \gamma \cdot z + f$ **Equation 2**

and $k_a = \tan^2(45 - \varphi/2) = \frac{1 - \sin \varphi}{1 + \sin \varphi}$. **Equation 3**

Assuming that the angle of shearing resistance (φ) = 90, soil of weight density (γ) = 1, uniform vertical surface load (f)= 2.5 – 5 KN/m², cohesion (c)= 1 or 1.25, is the coefficient of effective horizontal active earth pressure (K_a)= 1, and the distance down the face of the wall (z)= 6.28 m.

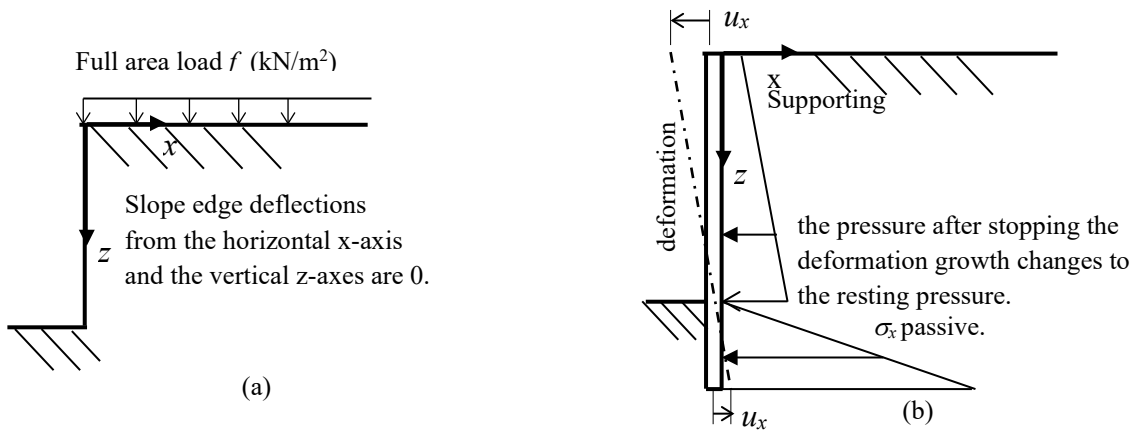


Figure 5.6 Active Earth (Ground) pressure – (a) shape of slope, (b) Types of ground pressures acting on the support wall. (Euro Code 4)

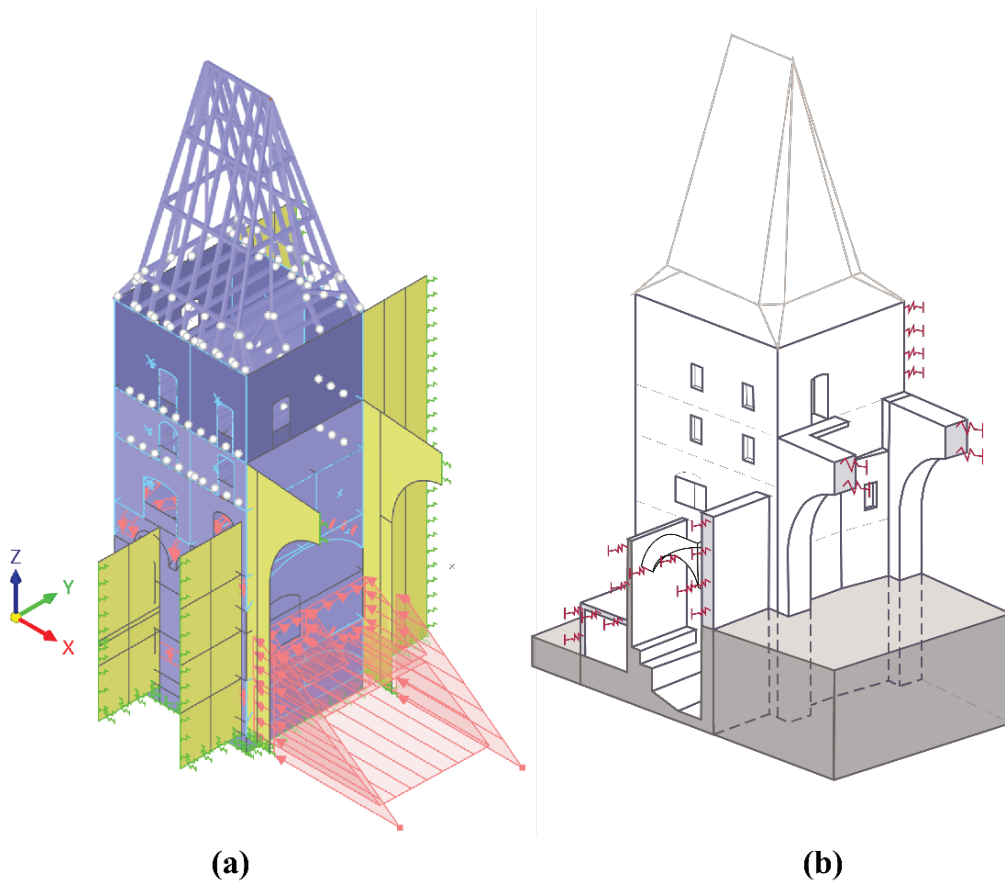


Figure 5.7 Boundary conditions – (a) Finite elements model, (b) sketch demonstrating the reality.

Element types were assigned in accordance with Table 2. Linear shell elements had to be used due to the geometry's complexity in order to obtain a valid mesh for the analysis. The target length – used to control the size of quadrangles-shaped FA mesh – was equal to 200 mm, with the maximum distance between a node and a line being put off by 1 mm. By instructing the software to build the mesh with the same square where it's possible, the resulting mesh consisted of 3554 1D finite elements (member elements) and 135,294 2D Finite elements (surface elements), for a total of around 138,262 degrees of freedom involved in the numerical solution. Figure 5.8 show the mesh of this numerical model.

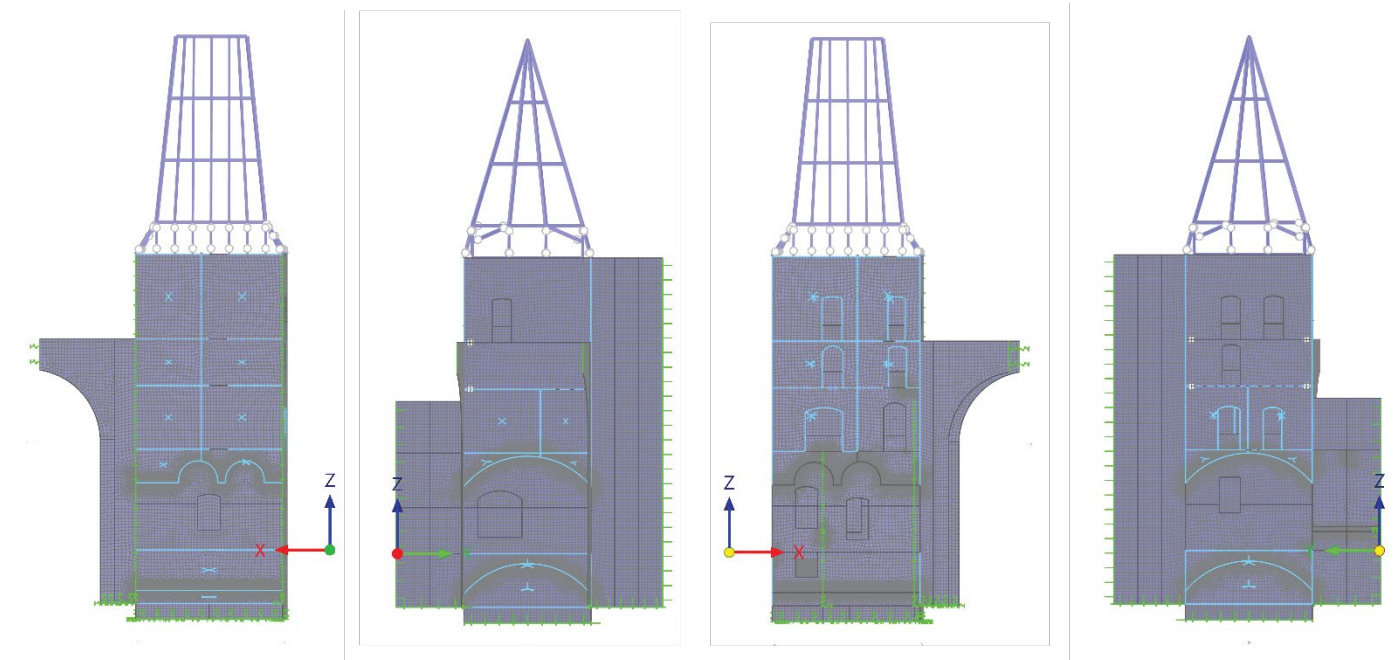


Figure 5.8 Fist numerical model – the Mesh.

Table 2 Model Element and Mesh Parameters

Element types	1D finite elements 2D Finite elements
Mesh seed size	Quadrangles, 200 mm
# Elements	135,294
NDOF	138,262

5.1.2 FE Model 2 (M2)

The geometry of the masonry walls was idealized and constructed using solid elements (Brick elements) that followed the precise outline of the walls (Figure 5.9-a). The solid element type controls the way internal forces and moments are absorbed or which properties are applied to the solid (Dlubal Software GmbH, 2023). The standard model of these solid elements – the type used in our model – is represented by a 3D object with the solid-specific properties of a homogeneous and isotropic material (Dlubal Software GmbH, 2023).

The geometry of the openings and niches on the ground floor were constructed with more precision and detail in comparison with the first models (M1). This was for the purpose of further investigation; as was pointed out in the previous chapter, most of these architecture elements exhibit deficiencies and need to be examined and further monitored. For example, the window segmental pediments were modeled then combined into one solid set with the window exterior frame, taking into consideration the correct thickness of each (Figure 5.9 – b & c).

Similar to the M1, the roof was simplified and modeled using Members (beam) elements, as shown in (Figure 5.9 – d), but more precisely, especially in modeling the slope of the first level of the roof. In accordance with (Dlubal Software GmbH, 2023), by assigning a cross section (that also defines the material), the member gains stiffness. Eventually, the model kept the original shape of the roof but simplified it to basic trusses system with three rings that tied it up on three levels and hinged in the connection with the masonry walls. Also, the floors were simplified and modeled using beam elements, with spacing of 85 cm in between – similar to M1.

Using Quadrangle surfaces, the geometry of the cross-vaults was based on CAD documentation and connected to the solid elements of the ground floor walls. The geometry of the vault is shaped by intersecting four vaults of a 2.4-m span with a bigger barrel vault (Figure 5.9 – e). Its span equals 6.27 m, with a depth of 7.60 m, and a height (above the spring lines) of 1.9 m. The basement barrel vault was also constructed using the same Quadrangle surface, with a span of 5.59 m, a depth of 7.00 m, and a height of 1.90 m (Figure 5.9 – f). The infill above the vault was assumed to be soil and it was added to the density of the vaults - its density was equal to 1300 Kg/m². The wall partition that is loaded above the vault was modeled in the intersection of the vault. These partitions were also modeled using surface elements with a thickness of 350 cm.

The boundary conditions were modeled and illustrated in Figure 5.10 and Figure 5.11, as follows:
(1) The gate pillars were modeled in their correct position using solid elements; the same goes for half of the gate's two arches. Surface Translational Springs were placed perpendicular to the cut surface in the x

direction. (2) The wedge-shaped wall on the north façade was added to the walls of the ground and first floors, increasing the thickness of these walls. (3) The walls of the buildings adjacent to the tower from the west and east were also modeled, placing translation spring at the y-directions; the details of the floors and vaults of the house to the west were neglected in this model, but the cross vault of the bookshop was modeled and simplified using a quadrangle surface. (4) The street is considered active earth (Ground) pressure, as explained earlier in the modeling of the M1. It's applied as linear loads against the north façade.

Element types of the numerical model (M2) were assigned in accordance with Table 3. The target length of the quadrangles-shaped finite elements that were used to control the size of the FE mesh was equal to 300 mm. By instructing the software to build the mesh with the same square where possible, resulting mesh consisted of 2382 1D finite elements (member elements) and 71612 2D Finite elements (surface elements), 436234 3D Finite elements (solid elements), for a total of around 148071 (Nodal elements) – see Figure 5.12.

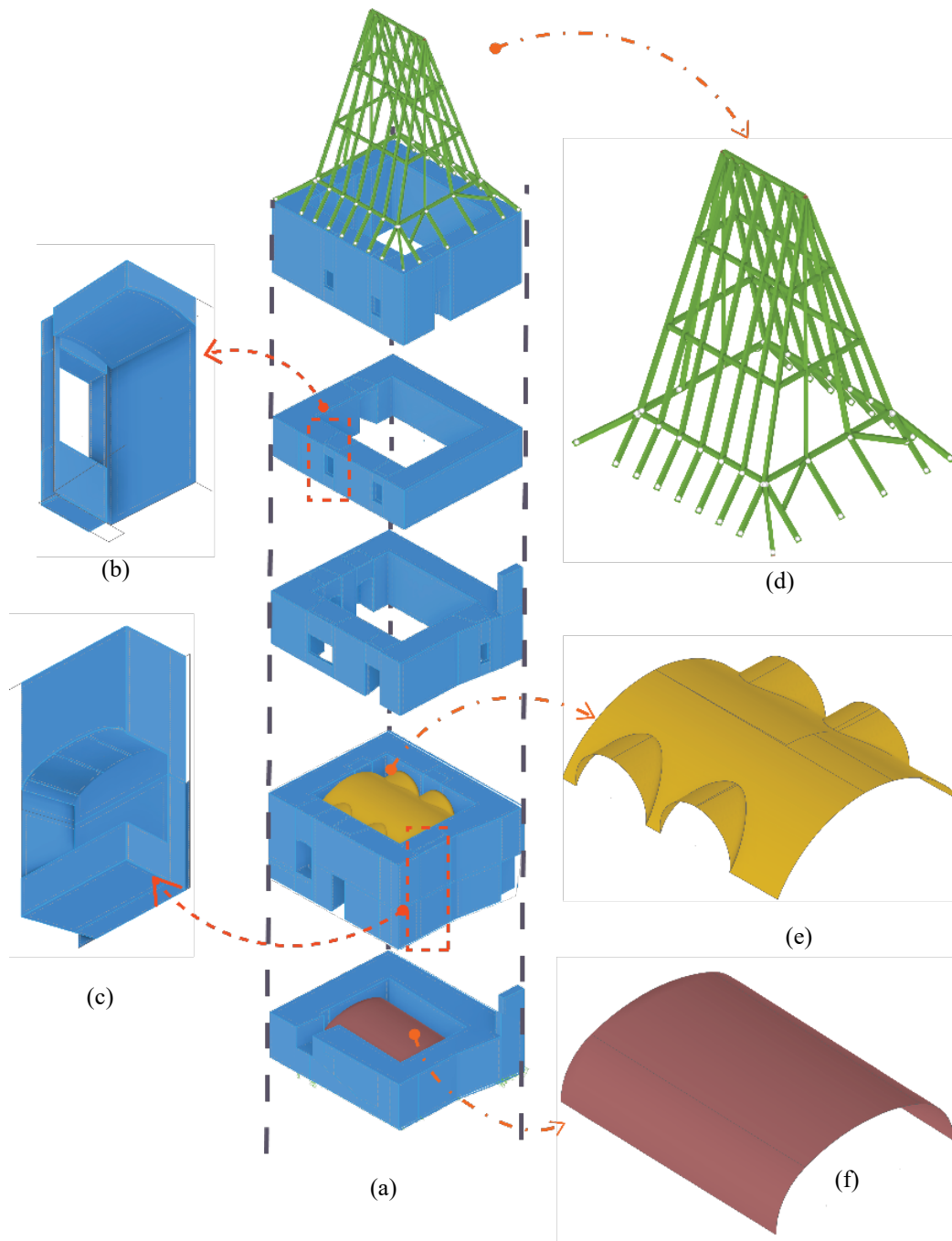


Figure 5.9 Details of Solid numerical model of the tower – (a) Geometry of the walls, (b) Geometry of the windows on the first floor, (c) Niches on the ground floor, (d) Simplified roof, (e) simplified vault on the ground floor, (f) simplified vault of the basement.

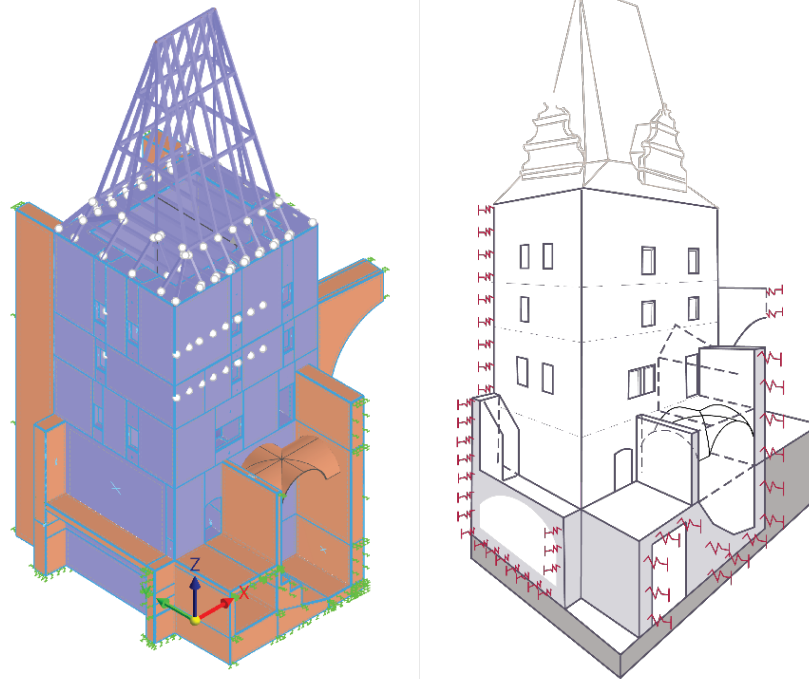


Figure 5.10 Boundary condition – Northeast corner (a) Numerical model, (b) 3D sketch of the tower.

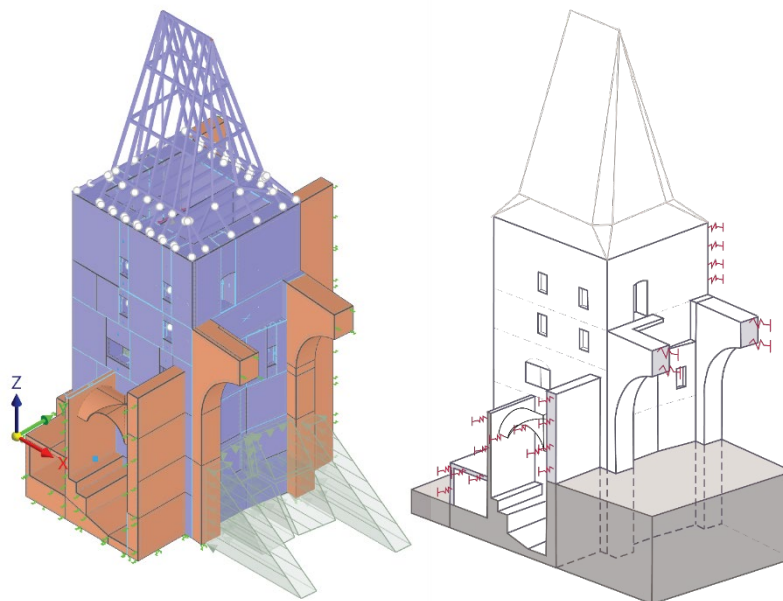


Figure 5.11 Boundary condition – Southeast corner (a) Numerical model, (b) 3D sketch of the tower.

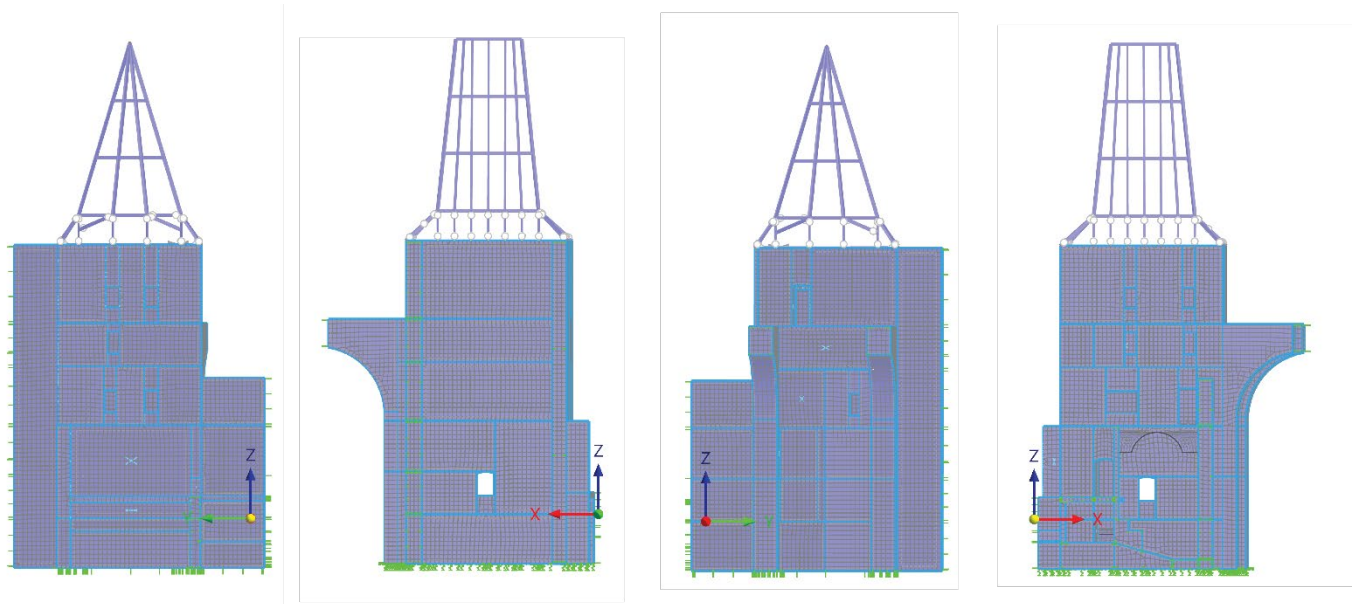


Figure 5.12 Mesh of the M2

Table 3 Model Element and Mesh Parameters (M2)

Element types	1D finite elements 2D Finite elements 3D Finite elements
Mesh seed size	Quadrangles and triangular, 200 mm
# Elements	510,228
NDOF	148,071

5.2 SYSTEM CHARACTERIZATION BASED ON DYNAMIC IDENTIFICATION TEST

Among other investigation techniques, modal characterization (or dynamic identification) has been gaining popularity due to destructiveness for its ability to capture the behavior of the real structure (Faleschinia, et al., 2023). When historical structures are investigated this approach is particularly appealing, avoiding shaking the structure artificially. Operational modal analysis (OMA), also known as output-only or ambient vibration test (AVT) (Alejo, Mendes, Lourenço, & Martínez, 2020), was performed on the Judith Tower aiming to estimating the dynamic properties (frequencies, mode shapes, and damping ratios) and updating a numerical model. OMA technique is able to derive effective information on the dynamic behavior of historical buildings, which in turn is useful to tune reliable and robust numerical models to be employed for structural analysis (Lacanna, Betti, Ripepe, & Bartoli, 2020).

The numerical models were calibrated according to experimental natural frequencies. The overall path that constitutes the vibration-based structural assessment results composed by the following steps: (i) full-scale ambient vibration testing (AVT), usually performed in a output-only framework; (ii) modal identification from ambient vibration response through operational modal analysis (OMA) technique; (iii) parametric finite element (FE) modeling; and (iv) identification of the uncertain mechanical parameters (UMP) of the numerical model (Lacanna, Betti, Ripepe, & Bartoli, 2020). These modal parameters are subsequently used to calibrate the 2D and 3D finite element (FE) models of the Judit Tower. The integration of the results of the dynamic identification with 3D FE model analyses allowed us to gather extensive knowledge of the dynamic behavior of the whole building and to minimize the uncertainties related to the structural parameters.

5.2.1 Experimental campaign

The non-destructive dynamic identification of the modal characteristics of the structure has been carried out by firstly organizing an experimental setup of environmental measurements with several accelerometers placed on two different levels of the Judith tower. The experimental analysis has been performed on the Judith tower on the 8th of June 2023. The data have been acquired during a sunny day with low level of wind. Based on the method of basic dynamic and experimental testing (Ramos, 2007), the test has been elaborated as follows: (1) Each setup was instrumented with five uniaxial piezoelectric accelerometers, with a sensitivity of 10 volt/g and a max range of ± 0.5 g, placed on the corner of the tower. (2) A reference coordinate system O_{xyz} has been introduced (Figure 5.13) in such a way that the X axis is parallel to the eastern façade and direction of the gate. This reference point allowed for correlation among the signals of all setups (Alejo, Mendes, Lourenço, & Martínez, 2020). (3) Before each setup, some signal measurements have been applied on each sensor to check the validity of the obtained signal – Figures 5.14,

5.15 and 5.16). (4) Eight tests of 15 minutes have been recorded, four for each set up. (5) A preliminary check of the quality of the data has been made between each setup to check the measured signals of every sensor to avoid data losses or bad signal quality (Figure 5.17).

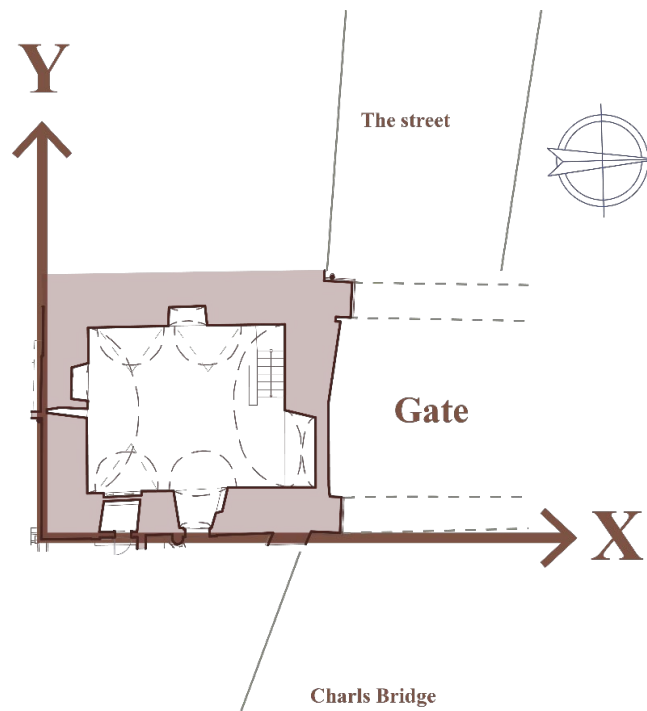


Figure 5.13 The considered reference system with respect to the geographical tower location

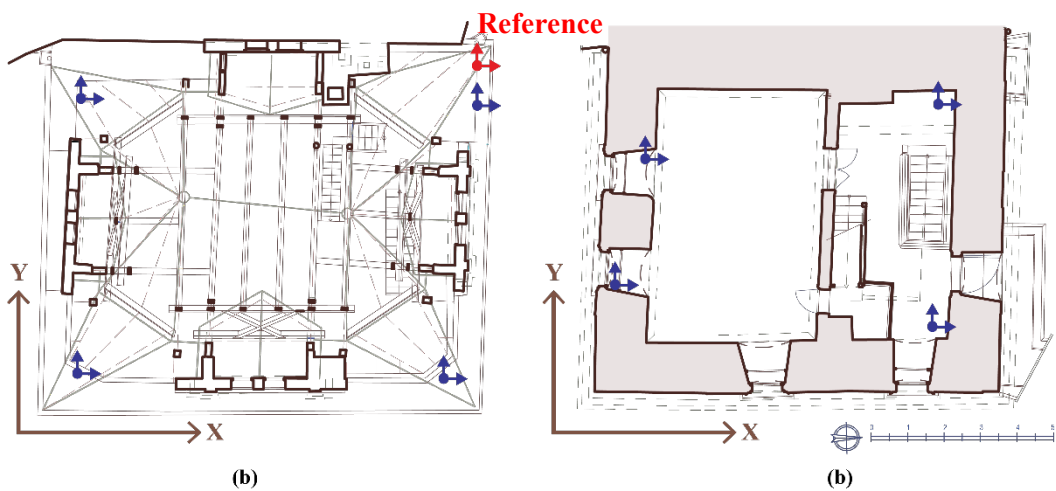


Figure 5.14 Accelerometer placement: (a) First setup at the Roof level, (b) second setup at the Third level



Figure 5.15 First Setup - accelerometer placement



Figure 5.16 Second setup - accelerometer placement

5.2.2 Test results and system characteristics

The extraction of the modal parameters from ambient modes were carried out using the ARTeMIS software. The modes depicted in Figure 5.18 may be classified as following. (1) Bending mode in the North-South (X-direction) direction with a frequency of 2.49 Hz, (2) Bending mode in the East-West (Y-direction) direction with a frequency of 3.15 Hz, (3) the third mode shape is a local bending mode along the diagonal direction with a frequency 3.49 Hz, (4) the fourth was second bending mode with a frequency 5.29 Hz and (5) the fifth was a torsional modes with a frequency of 6.99 Hz.

By analyzing the first and second vibration modes of the experimental test, it is insinuated that the building is stiffer in the y-direction (EW direction) than in the x-direction (NS direction), which indicates that other factors are playing a bigger role in the behavior of the building than its geometry. For sake of clarity, the layout of the building as illustrated (Figure 5.19), the length of the eastern and western walls (parallel in the x direction) is equal to 11.02 meters, which is longer than the northern and Northern walls (Parallel to the y direction), which is equal to 9.70 meters, also, because of the existence of the beams on the floor in the y-direction (EW Direction).

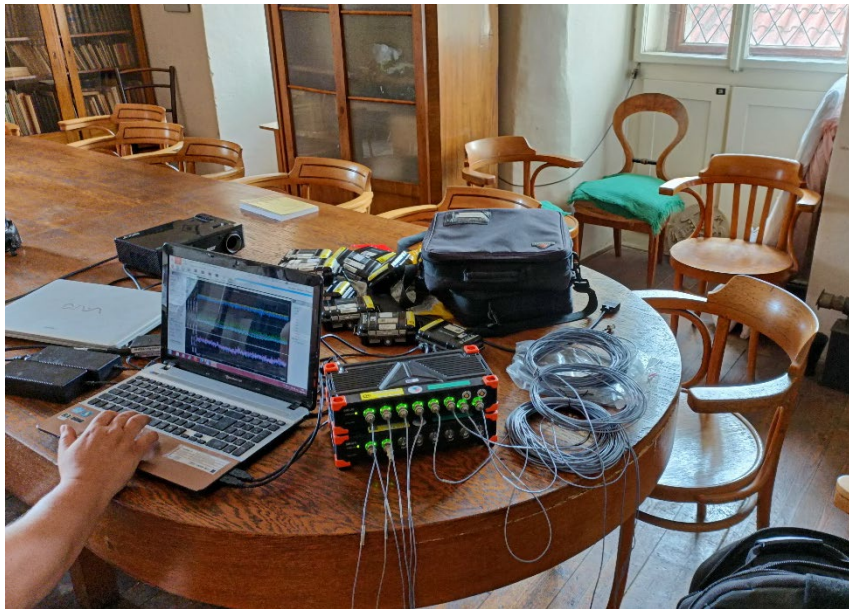


Figure 5.17: Equipment used in the dynamic identification tests: (a) force balance accelerometer; and (b) communication centric multichannel recorder

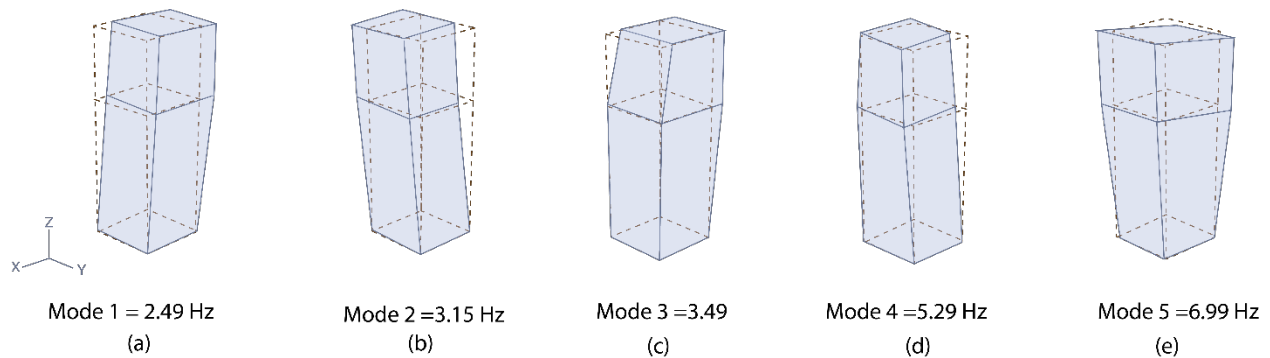


Figure 5.18: Shape modes identified from the dynamic measurement.

Table 4 Experimental frequencies.

Mode	Mode type	f_{exp} Hz
1	Bending mode N-S	2.49
2	Bending mode E-W	3.15
3	Second Bending mode N-S	3.49
4	Second Bending mode E-W	5.29
5	Torsion	6.99

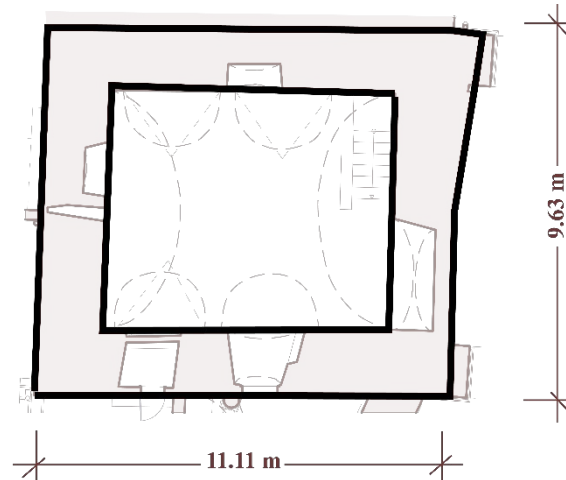


Figure 5.19: Layout of the tower

The third mode indicates that the third floor has a lower stiffness than the others; it vibrates in the x-direction and influences the third mode. This behavior can be the result of the following factors: (a) influenced by its thickness (approximately 370–670 mm less than the other lower levels), (b) the position in relationship with the gate, and/ or (c) its material properties. The fourth mode might be considered a second bending mode, where the building vibrates in the y-direction but also indicates that the northern wall is stiffer than the southern wall – which can be related to wall thickness; the north wall is currently thicker with wedge-shaped additions and is restrained by the gate. The final and fifth (relatively high) mode is torsional mode, where the Eastern and southern walls vibrate together while the Northern and Western walls stay fixed. This mode emphasizes the fact that both the northern and western walls are stiffer than the others, or by the affect other external factors other than the tower geometry.

5.3 MODEL CALIBRATION

A FE models updating was performed based on to the results of an experimental dynamic identification campaign (Faleschinia, et al., 2023), which can be performed by using trial-and-error methods, by simply varying few selected parameters based on expert judgment (Lacanna, Betti , Ripepe, & Bartoli, 2020). The Young's modulus values of the three materials (vaults, masonry walls, and wall partitions) were considered the variables to calibrate (Alejo, Mendes, Lourenço, & Martínez, 2020).

The calibration of the model, in terms of material properties, the masonry walls would have the same material properties. On the other hand, the choice of proper boundary conditions at the base of the structure, however, is still a critical point in the development of sound numerical models able to reproduce

building dynamic response reliably. The contribution of the foundation soil should be ascertained and, if necessary, properly modelled (De Angelis, Ambrosino, Sica, & Lourenco, 2022). Therefore, the foundation was simulated with two different flexible bases made of translational springs; south half and north half. Eventually, they were calibrated and considered on the main factors affecting the vibration modes of the structure.

Both of the numerical models were calibrated manually using Dlubal software, which adapts different methods to solve the eigenvalue problem; the choice is usually dependent on the size of the structural system and is more a question of performance than accuracy (Dlubal Software GmbH, 2023). The method used to calibrate both models is Lanczos, which is an iterative method to determine the lowest eigenvalues and corresponding mode shapes of large models (Dlubal Software GmbH, 2023).

The M1 was calibrated based only on the first and second modes, with a difference of less than 1%. Figure 6.19 shows the experimental and numerical modes. On the other hand, M2 was calibrated based on four modes, with a difference of less than 1%. Unfortunately, calculating the third mode was not achieved in either the two models with a difference of less than 9%.

The calibrated Young’s Modulus of the masonry walls, interior wall and tower’s vaults are showing on Table 4, while the calibrated parameters of the springs used for the boundary conditions showing on Table 7. Regarding the masonry structure type, according to (Lourenco & Gaetani , 2022), based on the calibrated Young’s Modulus, the walls can be categorized under “regular stone masonry with good bonds”, and vaults under the “irregular stone masonry”.

The M2 was modeled in a way that represents the reality more precisely than M1. Moreover, the details from the adjustment building were modeled, including the vaults of the book shop, and the details of the courtyard. These conditions helped calibrate the model in a more accurate way and improved matching the higher experimental modes. Nevertheless, the computational power consuming and time need to calibrate M2 were fourth ($\frac{1}{4}$) what needed for M2.

Table 5 Calibrated Young’s Modulus

Young’s Modulus - E(MPa)					
BC		Tower			
Houses	Gate	Walls		Vaults	
Walls	Pillar	Masonry walls	Int	GF vault	BS vault
2000	1200	2000	690	800	690

Table 6 Values of compressive strength, shear strength, Young's modulus, shear modulus and mass density of masonry - (Lourenco & Gaetani , 2022)

Masonry typology	f_c [MPa] min-max	f_o [MPa] min-max	E [MPa] min-max	G [MPa] min-max	ρ [kN/m ³] min-max
Irregular stone masonry (pebbles, erratic, irregular stones)	1.0-2.0	-	690-1,050	230-350	19
Uncut stone masonry with inhomogeneous thickness of leaves	2.0	-	1,020-1,440	340-480	20
Regular stone masonry with good bonding	2.6-3.8	-	1,500-1,980	500-660	21
Soft stone masonry (tuff, limestone, etc.)	1.4-2.2	-	900-1,260	300-420	13-16
Regular soft stone masonry (tuff, limestone, etc.)	2.0-3.2	0.10-0.19	1,200-1,620	400-500	
Dressed rectangular (ashlar) stone masonry	5.8-8.2	0.18-0.28	2,400-3,300	800-1,100	22
Solid brick masonry with lime mortar	2.6-4.3	0.13-0.27	1,200-1,800	400-600	18
Hollow bricks (voids < 40%) with cement mortar	5.0-8.0	0.20-0.36	3,500-5,600	875-1,400	15

Source: Circolare (2019).

Table 7 Input Parameters of The Boundary Conditions

Stiffness			M1	M2
Boundary condition	Translation (direction)	Spring constant (KN/m ²)	Spring constant (KN/m ²)	Spring constant (KN/m ²)
Foundation /Soil settlement	South Side of the Tower	Cu, x	35000.00	38000.00
		Cu, y	14000.00	16000.00
		Cu, z	50000.00	56000.00
	North Side of the Tower	Cu, x	70000.00	72000.00
		Cu, y	32000.00	34000.00
		Cu, z	100000.00	120000.00
Buildings	West (House)	Cu, y	18000.00	60000.00
	East (House)	Cu, y	10000.00	10000.00
	North (Gate)	Cu, x	80000.00	260000.00
	South (Courtyard)	Cu, x	-	60000.00

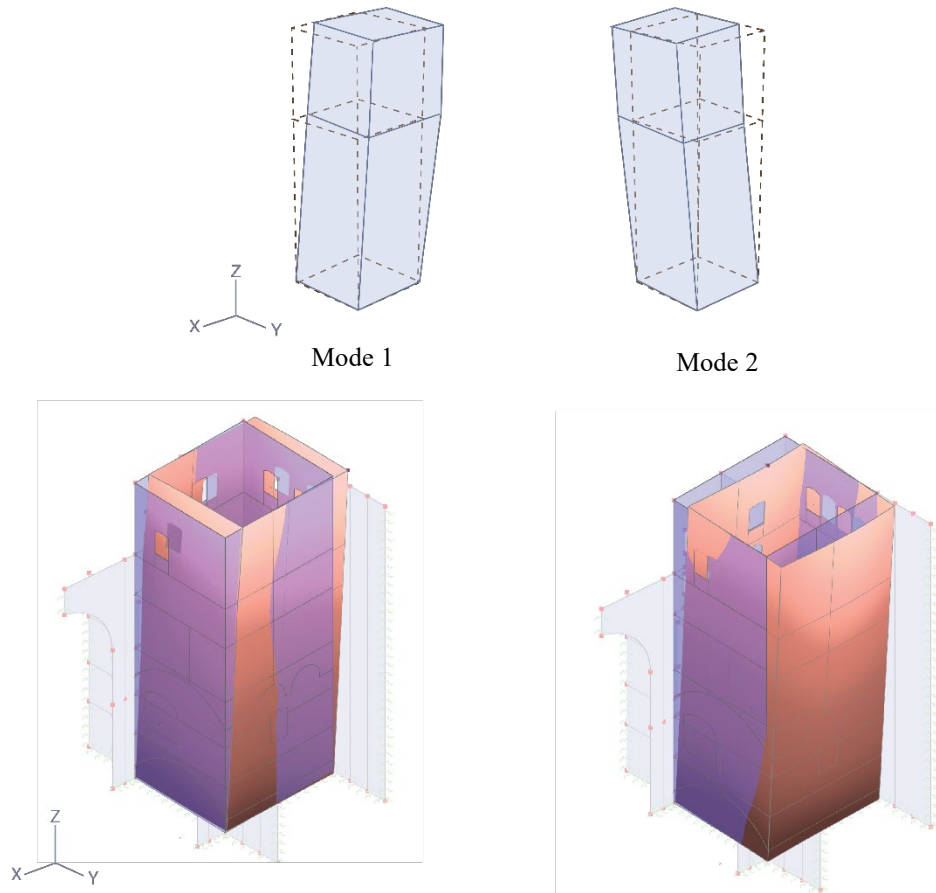


Figure 5.20 Model 1 Updating - Eigenvalues

Table 8 Model 1 Updating - Eigenvalues analysis.

	Mode 1	Mode 2
Experimental	2.49 Hz	3.15 Hz
Numerical	2.49 Hz	3.13 Hz
Difference %	0.0%	0.67%

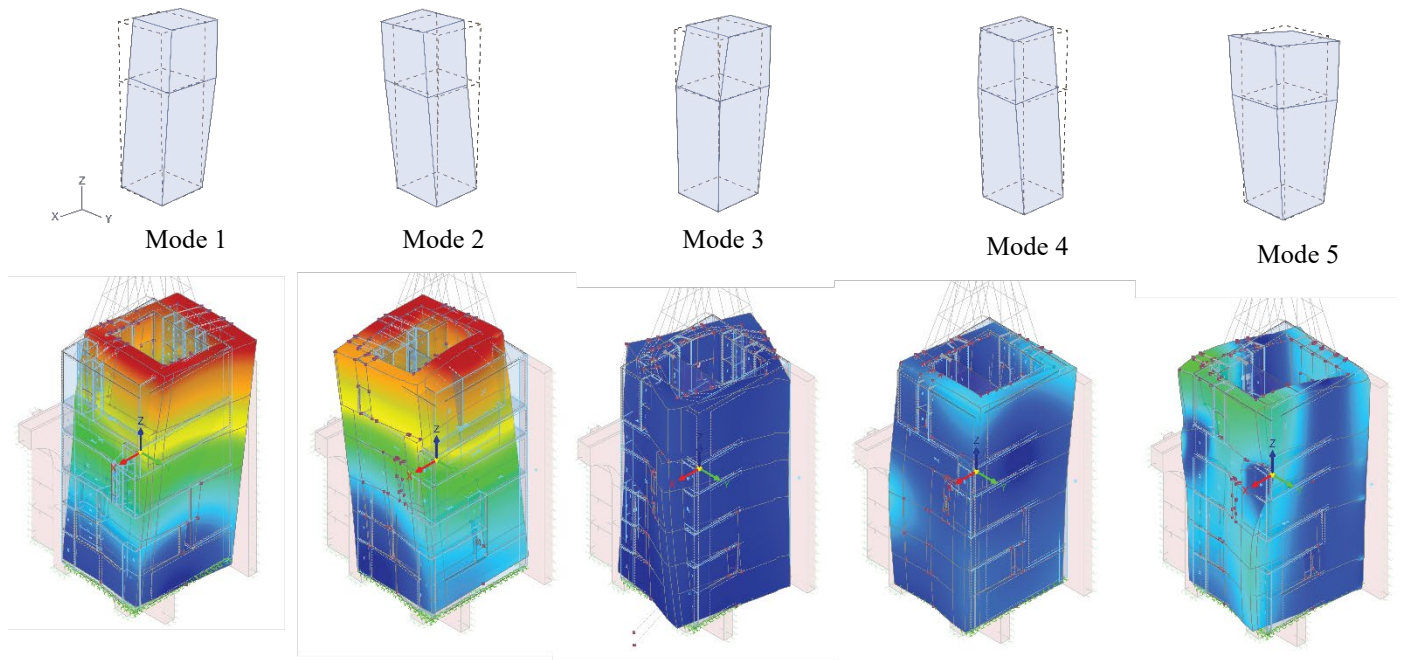


Figure 5.21 Model 2 calibration – Eigenvalues analysis

Table 9 Model 2 calibration – Eigenvalues analysis

	Mode 1	Mode 2	Mode 3	Mode 4	Mode 5
Experimental	2.49 Hz	3.15 Hz	3.49 Hz	5.29 Hz	6.99 Hz
Numerical	2.487 Hz	3.167 Hz	3.80 Hz	5.21 Hz	6.962 Hz
Difference %	0.12%	0.54%	8.80%	1.50%	0.40%

This page is left blank on purpose.

6 LINEAR ANALYSIS

This section discusses the results of the 3D geometrically linear static analysis of Judith Tower. The system, as explained before, is loaded with the infill material above the vaults and with the active pressure of the street to the North of the tower. The floors were simplified and modeled as beams on both models, which ties the West and East walls together. The result will be demonstrated in the following section with a comparison between both models.

6.1.1 Displacement

In both models, the tower shows greater deformation in the (-x) direction than in the (+y) direction (Figure 6.1). The first model shows that the highest displacement of 10.9 mm is at the top of the southeast corner, whereas the second model shows that the highest displacement of 11.6 mm at the ground floor level (6.33 meters height). The accurate distribution of the mass of the walls and the relationship between the walls and vaults in the second model might have contributed to shaping the deformation in M2. The presence of the gate to the north of the tower and the decrease in the thickness of the third floor's walls contributed to the deformation shape observed in the top north corner in both models (Figure 6.2).

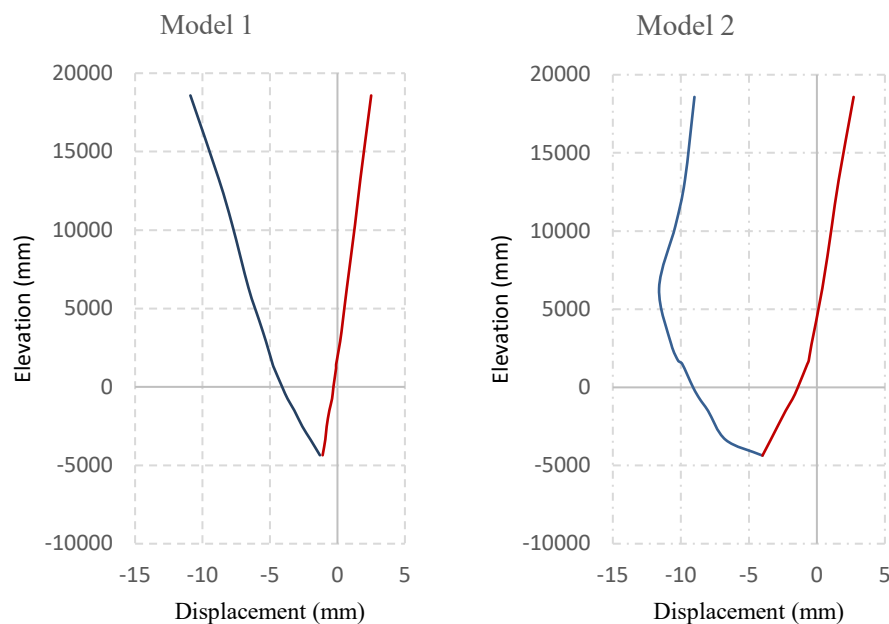


Figure 6.1 Displacement – Southeastern Corner of the Tower

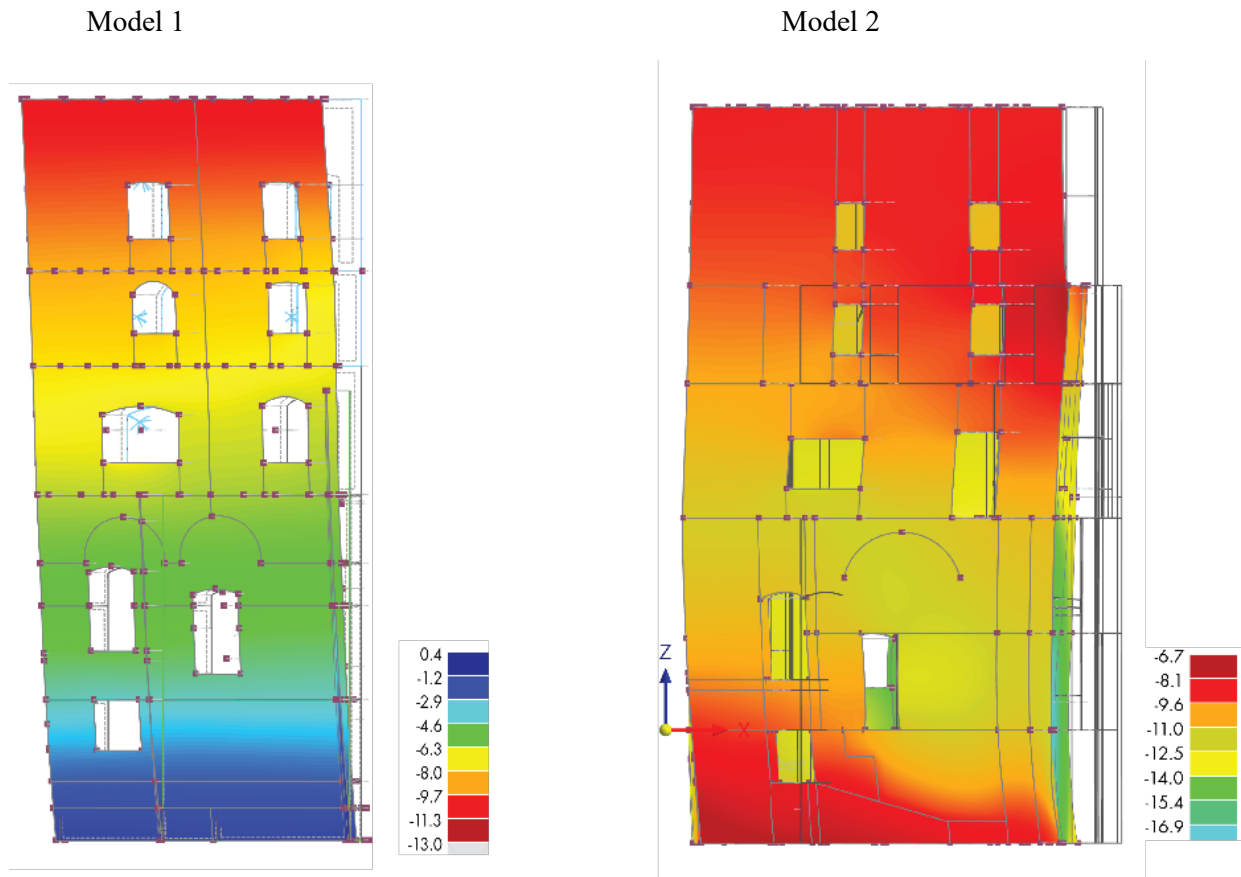


Figure 6.2 Global Displacement – X direction U_x (mm)

6.1.2 Stresses

The stresses were investigated in the eastern façade, which shows the most damage. Figures 6.3 and 6.4 show the distribution of stresses in both models, including the compressive stresses σ_x and shear stresses τ_{xz} along with the principal shear stresses τ_{max} . It should be noted that the tension stress experienced is relatively low compared to the compression stress. As a conservative assumption, masonry should not have any tensile stresses. However, in the numerical model, tensile stresses are observed. They are approximately below 1.5 MPa, and it is possible that the masonry may actually resist these stresses.

The concentration of the stresses is shown in Figures 6.3 and 6.4, appeared mainly in the weakest elements, above and under the opening, and in the intersection between the tower and the adjacent structures. The latter have contributed greatly distribution of to the shear stresses along the structure. Moreover, the compression and shear stresses distribution's angle are results of the soil settlement. Figures 6.6 and 6.7 illustrate and compare between the result from numerical model and the visual inspection (crack maps).

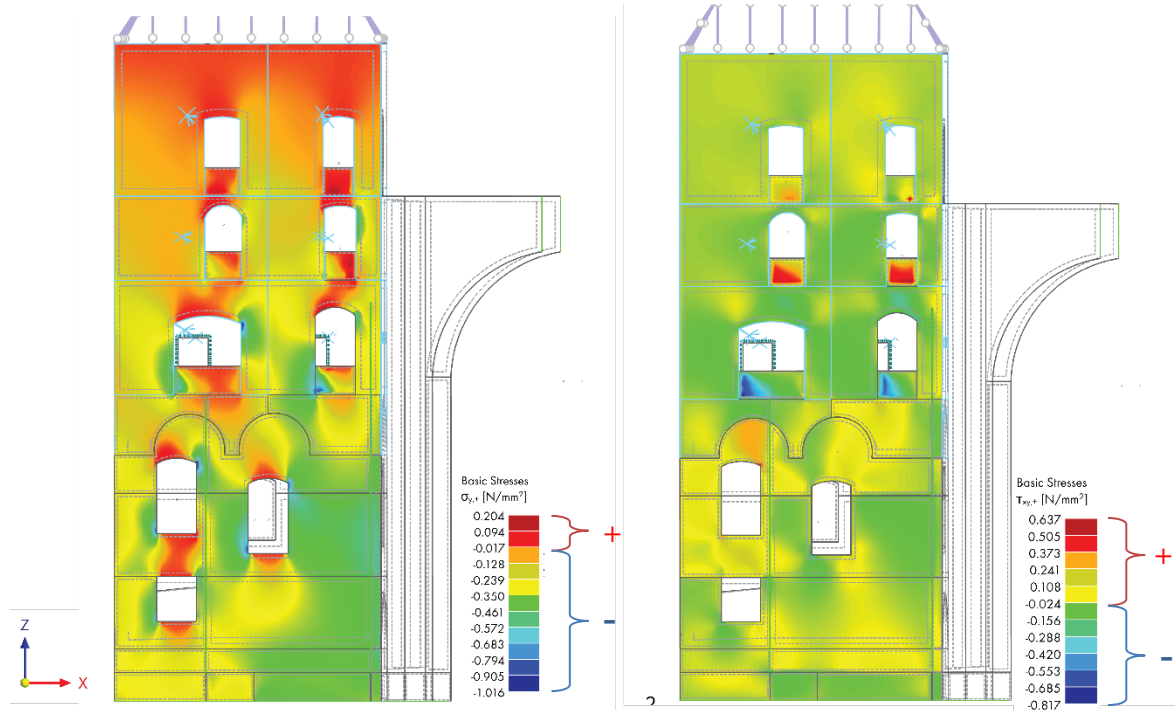


Figure 6.3 Eastern Façade – M1, (a) compressive [basic] stress σ_x , (b) Tension stress τ_{xy}

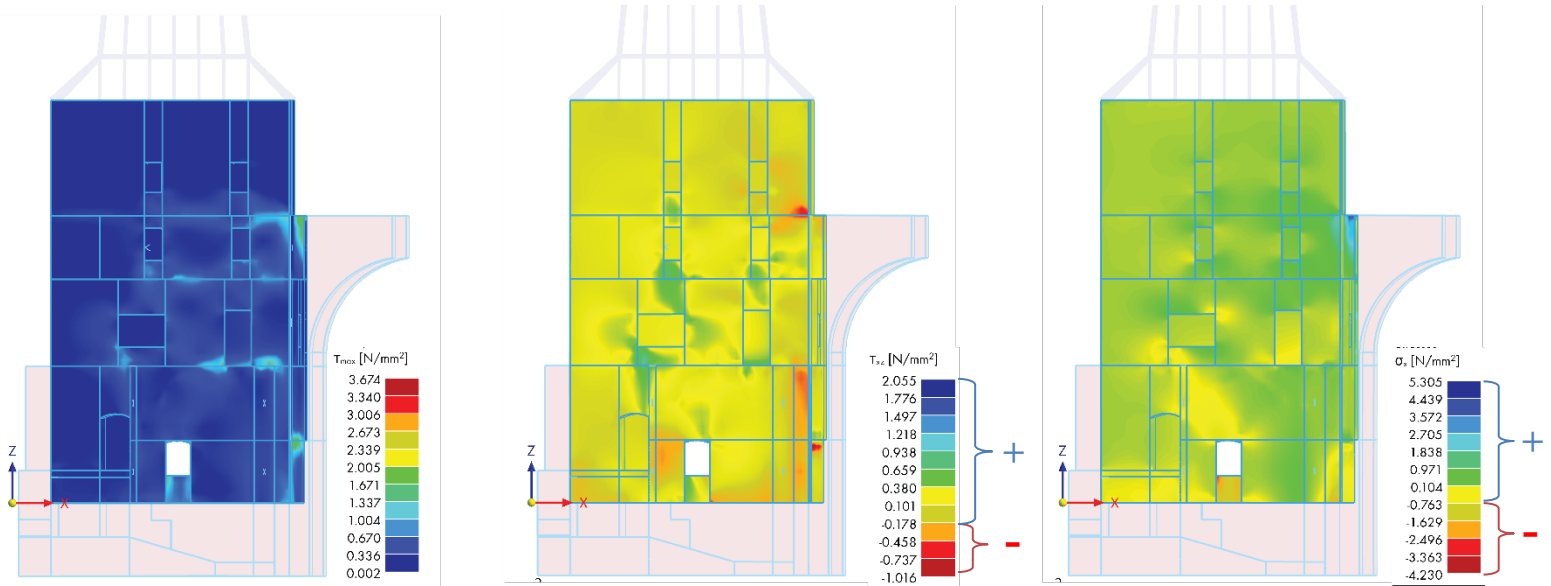


Figure 6.4 Eastern Façade – M2, (a) compressive stress σ_x , (b) Tension stress τ_{xy} , (c) Shear stress τ_{max}

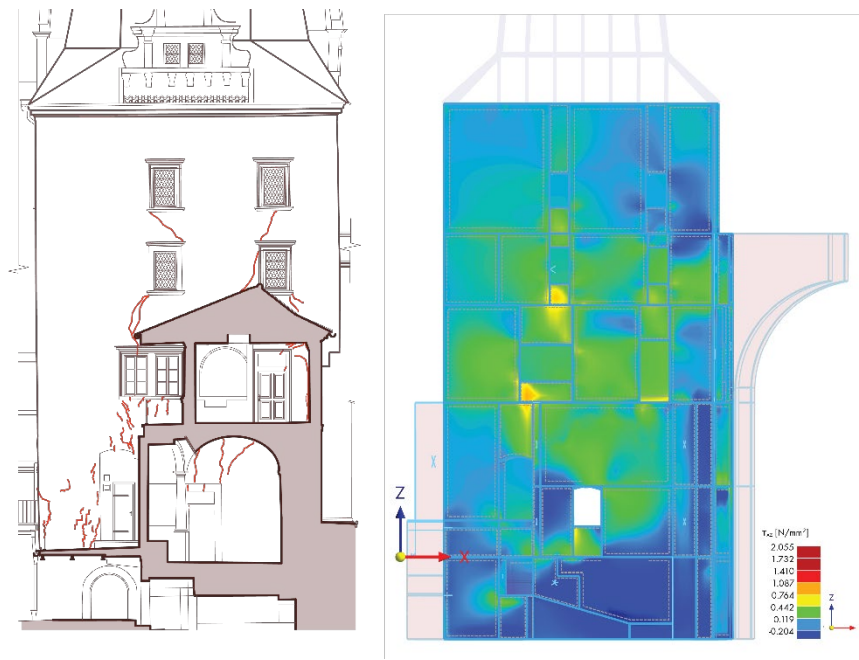


Figure 6.5 Eastern Façade: Comparison between (a) the Visual inspection, and (b) the shear stress distribution in M2

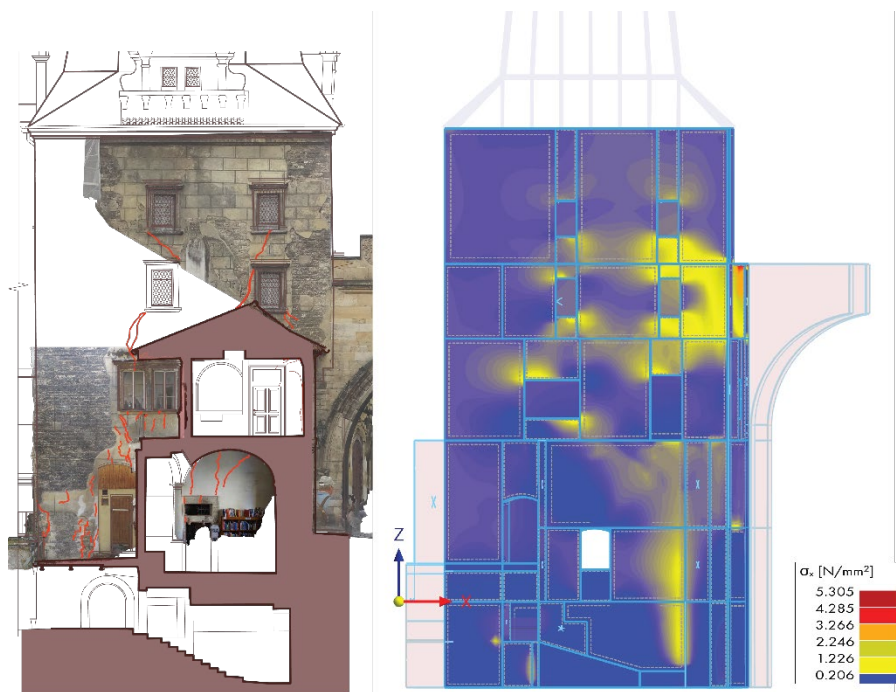


Figure 6.6 Eastern Façade: Comparison between (a) the photogrammetric documentation, and (b) the compressive stress distribution in M2

Additionally, the continuation and propagation of these stresses through the thickness of the walls have been studied. As expected, these shear stresses have been distributed into the pediment of the openings in the eastern façade, then to the interior of the structure. The original theory established by (Vesely, 2011) indicated that these cracks started during the restoration of the 16th century. However, the result of the numerical model shows that the propagation of these cracks can be caused by current boundary conditions, specifically the soil settlement and foundation movement (Figure 6.7).

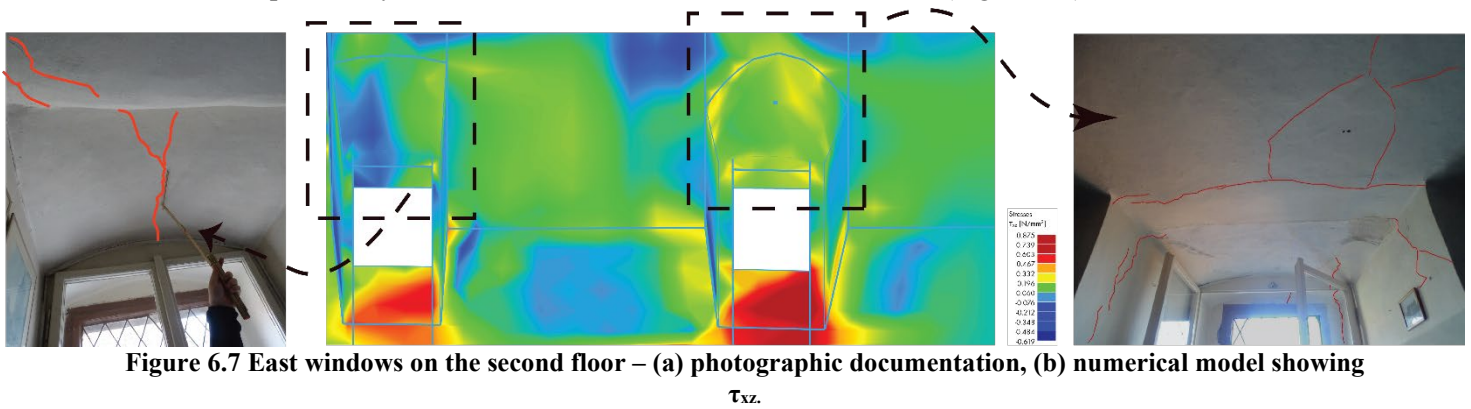


Figure 6.7 East windows on the second floor – (a) photographic documentation, (b) numerical model showing τ_{xz} .

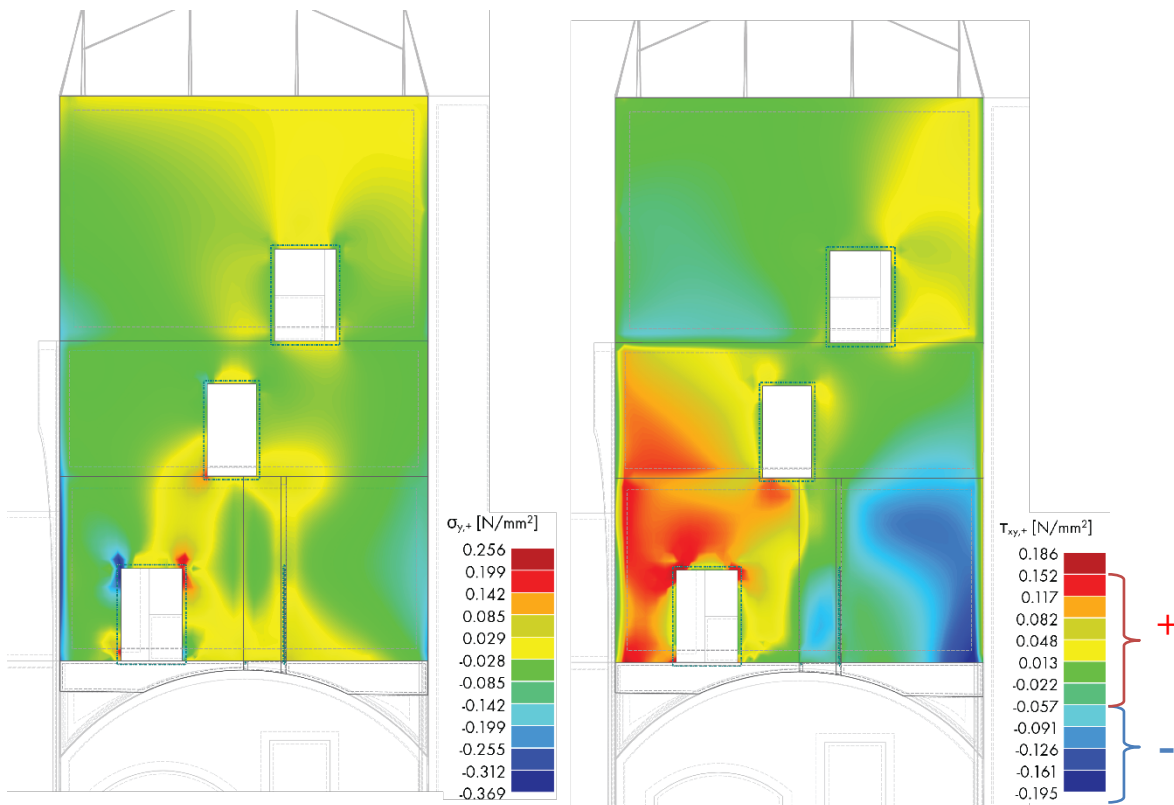


Figure 6.8 Interior wall partition, (a) Compressive stress σ_y , (b) Shear stress τ_{xy} .

Furthermore, linear analysis was performed on interior wall partitions (Figure 6.8). It shows cracks long and wide. These are inclined symmetrically, interpreted as shear cracks resulting from the settlement of the fill or the threshold beam beneath the load-bearing wall. The numerical models showed compressive and shear stresses concentration, which matches the previously described deficiencies (Figure 6.9).

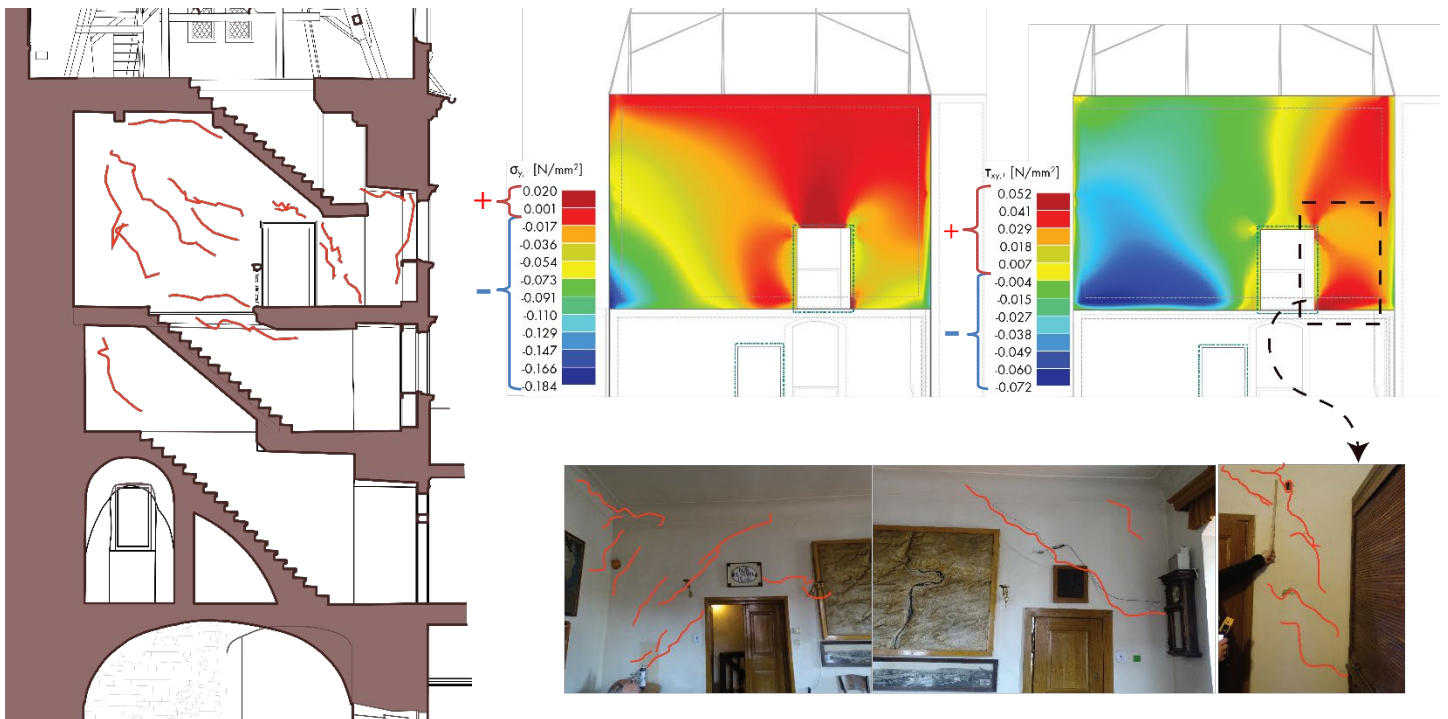


Figure 6.9 Interior wall partition on the third floor; (a) Compressive stress σ_y , (b) Shear stress τ_{xz} , (c) photographic documentation with crack mapping

6.1.3 Vault

By examining the local deformation of the vault in the numerical model, the analysis shows that the vault exhibits displacement of 18.6 mm in the (-x) direction and 17.4 mm in the (+y) direction, influenced by the global deformation of the tower (Figure 6.10). However, the vault also suffers from compressive stress from the weight of wall partitions, and shear stress caused probably from global behavior of the structure (Figure 6.11).

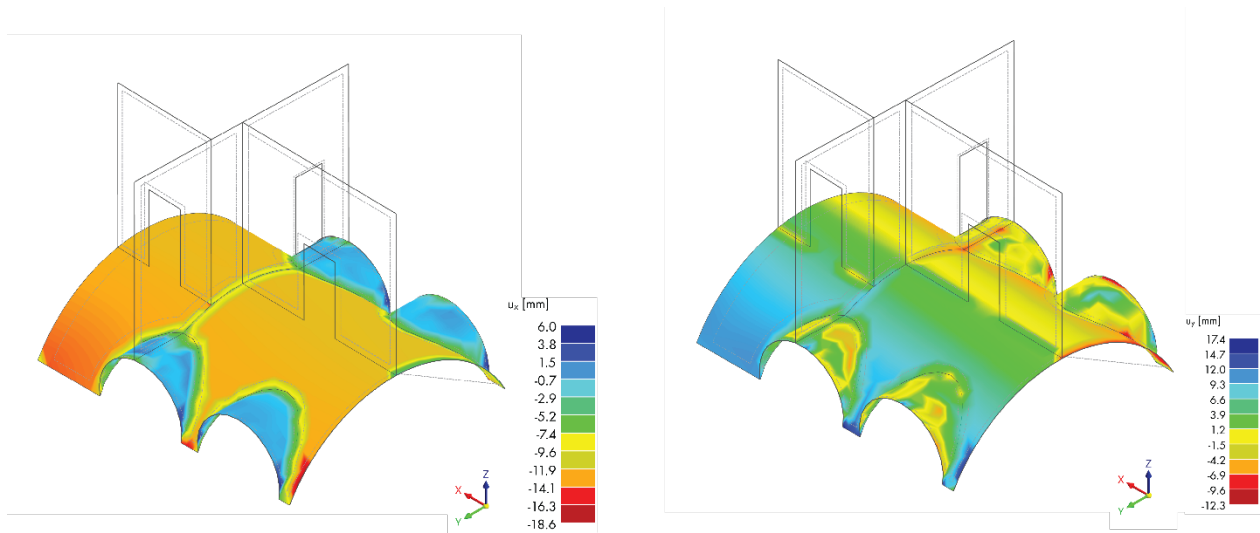


Figure 6.10 Local deformation of the cross vaults; (a) Displacement on the x-direction, (b) Displacement on the y-direction

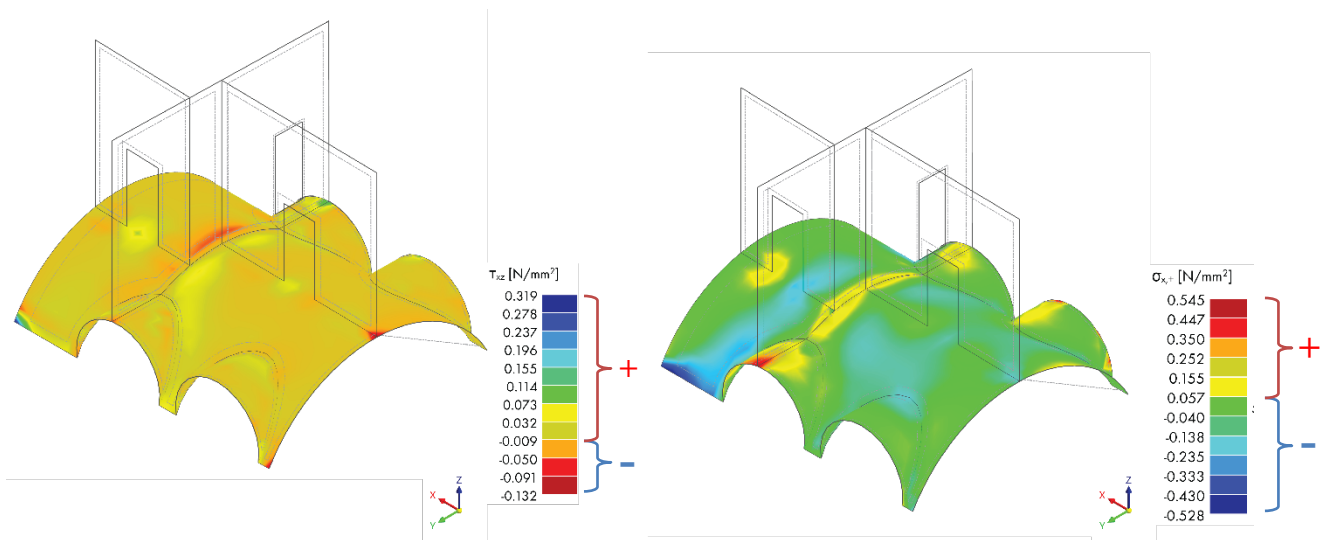


Figure 6.11 Stresses on the cross vaults: (a) Shear stress τ_{xz} , (b) Compressive stress σ_y .

This page is left blank on purpose.

7 CONCLUSION AND RECOMMENDATIONS

7.1 CONCLUSIONS

In order to execute the static assessment and diagnosis of the Judit and perform an initial static analysis, a series of documentary and in-situ activities were performed.

7.1.1 Historical survey

The historical survey aimed at understanding the constructive sequence and current morphology of the building. It also identifies the major construction stages and major restoration activities for the different regions of events that the building went through, which was the starting point for identifying the building system and materials. The information obtained from the historical survey helped planning the first campaign. Some archival documents of the construction work were clearly helpful in identifying parts of the structural system that were built into the model later on.

7.1.2 Visual inspection and damage survey

A thorough visual inspection of the masonry pathologies was conducted on both the three exterior façades and the interior of the tower. After identifying the types of damage in the building, localizing mapping of these damages occurred over, mainly, the CAD drawings and orthophotos. Also, extensive Excel sheets for the inspection of the interior masonry were prepared, illustrating and localizing the different damages with detailed information for each, with intervention recommendations and limitations. No imminent concerns were discovered in the in-situ inspection, but further investigation and timely maintenance and repair are warranted on some issues, and some recommendations are made to that end. Before then, A geometrical survey of the building was accomplished via validation of the existing drawing, by taking few measurements manually and laser meter.

By examining the crack pattern on the drawing of the eastern façade, it can be traced that the directions of the cracks correspond to tensile stresses resulting from the redistribution of loads in the wall during the creation of openings and reconstructing of the vault after it collapsed. The impetus that caused the formation of cracks could have been the Baroque renovation or, more likely, the installation of a large opening on the ground floor (current toilet). The structure might be susceptible to soil and foundation settlement, which could contribute to the progression of shear stresses and cause cracks on the façade.

7.1.3 Material and system characterization

The non-destructive testing campaign helped elucidate the quality and type of materials used throughout the building, as well as the presence of degradation mechanisms. Operational Modal Analysis (OMA) was performed on the tower. These conclusions provided a basis for the material properties adopted in the numerical analysis. Moreover, it contributed to understanding many aspects of tower's behaviour, and insinuated that the building is stiffer in the y-direction (EW direction) than in the x-direction (NS direction). These results helped in concluding that soil and foundation settlement is a direct effect on the dynamic behavior of the tower.

7.1.4 Structure idealization and numerical model creation

Together, these activities were necessitated for the creation of a finite element model which was used to perform a static assessment of the building in its current condition. Two FA-models of the tower were created. The first model adapted the use of a shell (2D-finite elements) and beams (1D- finite elements), while the second element generated with more details by using the solid (brick or 3D-finite elements) for the massive exterior walls, shells elements for the vaults and interior partitions, and beam element for the roof and wood beams. The building was modelled in 6 basic units, whose simplified geometry was constructed based on the AutoCAD drawings in the Dlubal software environment. The resulting mesh of the first had approximately 135,294 elements, for a total of around 138,262 degrees of freedom involved in the numerical solution, while the second model had approximately 510,228 elements, and total 148,071 degrees of freedom. The elastic modulus of the masonry was manually updated by calibrating the numerical model natural frequencies to within 1% of the experimental natural frequencies.

7.1.5 Preliminary static analysis

A preliminary static assessment was performed on the tower by means of a linear analysis on the calibrated numerical models. It indicated that the most vulnerable regions of the building where shear stresses are concentrated and appeared in a form of shear cracks on the eastern façade and interior walls partitions. However, the assessment indicated that soil and foundation settlement have effectively caused the damages and deficiencies that the tower exhibited. This might be caused by the presence of the other buildings, but also it started with the renaissance restoration of tower, which practically, was dragged on throughout the rest of the 16th century.

7.2 RECOMMENDATIONS:

7.2.1 Material damages and pathologies

It is important to point out that stone structures' present different problems due to the different types of stones used. For future interventions, an analysis of the physical properties, i.e., durability tests of the elements, should be carried out. It is recommended to perform some basic tests like freeze-thaw cycles, and salt crystallization cycles. Atmosphere reproduction tests should be executed as well including contaminated atmospheres, salt spray, and acid rain. Other durability tests including UV rays, crumbling, and combined tests also recommended. Other durability tests including UV rays, crumbling, and combined tests are also recommended.

However, certain general stages of intervention can be established with several considerations, e.g. intervention should be as minimal as possible, must respect the antiquity of the constructive elements, and differentiate between existing buildings that are still in good condition and degraded areas. For the case of the tower, it is recommended:

- a) Replacement of the affected part with a compatible material, protection of the element.
- b) The density of the mortar to be used must be less or equal to that of the original stone, this avoids incorporating tensions in the stones.
- c) Fungicide for the elimination of mold, fungi, and spores on the affected surfaces.
- d) Transparent consolidated: Mineralizing consolidated based on ethyl silicate. It should not affect the mortar; it should not alter the color of the stone.
- e) Abrasive methods that deteriorate the surface and increase porosity should be avoided at all costs.
- f) If it is necessary to clean with chemical products, these must be acid-free, have a medium alkalinity and not contain solvents.
- g) Cleaning with water can be done at a certain pressure, hot water is effective but high temperatures can cause reactions in the salts of the material. Special care must be taken.
- h) Water-repellent products that allow the material to "breathe" should be used. Never use products that do not allow the passage of water vapor.

Recommendations for each pathology identified in the damage survey are given in Annex C

7.2.2 Future inspection and diagnosis

In order to address some of the most significant uncertainties in the current work, the following inspection and diagnosis tasks are recommended:

- a) Foundations: More investigation on the foundation is highly recommended, both on geometrical and material level. Important points to be considered during the inspection of the foundation: (i) what is the contact point or areas (in plan), (ii) how deep the foundation is, (iii) what is under the foundation. Be able to answer these questions, several tests are recommended, e.g., test pits, drilling and cone penetration test (CPT).
- b) Soil settlement: Investigate the ground deformation, and main reason for the settlement. It could be three main reasons: (i) insufficient shear strength, (ii) Reduction in pore volume (consolidation, compaction, etc.), and (iii) Reduction in the grain volume (creep). Other factors and soil-foundation compliance can be investigated including: (a) Presence of low rigidity soil, (b) water sensitivities soils, (c) proximity of new high load construction, (d) shrinkage and swellings. The inspection of the pathology related to settlement requires carrying out in situ and laboratory tests in order to assess the strength and deformability parameters of the involved formation and water conditions of the ground. Moreover, it also recommended the calculate the geological parameters of the soil, including the friction angle, effective/undrained cohesion, and deformation Modulus (to be used for displacement computation).
- c) Floor infill and structure: More understanding of the infill above the vaults – both vault of the basement and cross vaults of the ground floor – is necessary to further detailed analysis of some parts of the building. It assumed here in the analysis that the infill is soil. But some historical photos show that pottery pots were at some parts of the building. This assumption changes the mass load on the vaults, which changes the behavior of the vaults.
- d) Modal properties of towers: According to the preliminary visual inspection, the four towers were constructed of 3-leave (Rubble infill, brick and Opuka) walls. It assumed here in the analysis that all the masonry walls have the same stiffness. Therefore, it is recommended to conduct More NDT including Sonic test and Dynamic identification test to calibrate their stiffness.
- e) Crack Monitoring: Long-term structural health monitoring (SHM) systems should be designed in order to fully capture the behavior of a structure in time, the development of the soil settlement. Health monitoring is also essential for damage identification and damage localization scope. It can be achieved through the continuous collection of vibration data (in

- case of vibrations-based systems), as well as static data, e.g., strains, cracks opening, displacements, tilts (in case of mixed static-vibrations-based systems).
- f) Roof: Full geometrical and visual inspection of the roof system should be carried out. Including investigation of health of the wood system, its joining and connection.
 - g) Roof-wall connection efficiency: Given the current condition of the roof, further inspection with high safety measures is needed, more investigation of the connection between the roof and masonry walls is significantly important.

7.2.3 Recommendations for future numerical analysis

a) Building foundations: The current model assumes that the foundation is extended 0.5 meters below the wall base with a uniform cross-section. Based on the further tests recommended in the previous section, an updated idealization should be made that more accurately represents reality.

b) Detailed partial models (using solid elements) for the most vulnerable parts of the buildings: Detailed partial models are recommended to study the most vulnerable regions of the building. It is suggested to model a middle unit ground floor with cross vaults to better understand the behavior of the south walls under the out-of-plane or under increased vertical loading from the first floor. The detailed model should be constructed using solid elements in order to better represent the loading of the infill and provide a more realistic connection between the vault shells and the walls.

c) Nonlinear analysis: investigate the nonlinear behavior of the structure and calculate the material properties. It can be derived from the linear properties based on literature recommendations for the types of masonry observed in the inspection and NDT the projected tower update. It is also recommended that other software with academic algorithm research be used, (for instance Diana or Atina., etc.)

This page is left blank on purpose.

8 REFERENCES

- Bilgin, H., & Ramadani, F. (2021). Numerical Study to Assess the Structural Behavior of the Bajrakli Mosque (Western Kosovo). *Hindawi Advances in Civil Engineering*, 17.
- Lacanna, G., Betti, M., Ripepe, M., & Bartoli, G. (2020). Dynamic Identification as a Tool to Constrain Numerical Models for Structural Analysis of Historical Buildings.
- Agisoft. (2023). <https://www.agisoft.com/>.
- Alejo, L., Mendes, N., Lourenço, P., & Martínez, G. (2020). Protecting the Historic Buildings of Mexico: The Barrel Vault of San Agustín Church in Morelia. *American Society of Civil Engineers*.
- Angelillo, M., Lourenco, P., & Milani, G. (2014). Masonry behaviour and modelling.
- Brně, T. K. (2008). *Dendrochronologické datování vzorků dřeva ze stropních konstrukcí provedl* .
- De Angelis,, A., Ambrosino, A., Sica, S., & Lourenco, P. (2022). Soil contribution on the structural identification of a historical masonry bell-tower: Simplified vs advanced numerical models. *Geotechnical Engineering for the Preservation of Monuments and Historic Sites III – Lancellotta, Viggiani, Flora, de Silva & Mele (Eds)*.
- Diaferio, M., Foti, D., La Scala, A., & Sabbà, M. F. (2021). Selection Criteria of Experimental Setup for Historical Structures. *IEEE*.
- Diaferio, M., Foti, D., Giannoccaro, N. I., & Ivorra, S. (2017). MODEL UPDATING BASED ON THE DYNAMIC IDENTIFICATION OF A BAROQUE BELL TOWER. *M. Diaferio, et al., Int. J. of Safety and Security Eng*, 7(4), 519-531.
- Dimitrios, L., Sarhosis, V., Adamopoulos, E., & Drougkas, A. (2021). An innovative image processing-based framework for the numerical modelling of cracked masonry structures. *ELSEVIER - Automation in Construction*, 15.
- Dlubal Software GmbH. (2023). *RFEM 6 online manual* . Retrieved 2023, from <https://www.dlubal.com/en/downloads-and-information/documents/online-manuals/rfem-6/000040>
- Dragoun, Z. (2002). , *Praha 885–1310, Praha 2002*.
- Faleschinia, F., Toskaa, K., Andreosea, F., Gobbia, G., Fltrin, G., Zanini, M., . . . Ricciardi, G. (2023). Modal characterization and NDTs of a historical church in Noto.
- Heyman, J. (1997). The Stone Skeleton. (*Structural Engineering of Masonry Architecture*) Cambridge University Press: Cambridge,.
- ICCOMOS Monuments and sites XV. (2008). Illustrated Glossary on Stone Deterioration Patterns. *ICCOMOS Monuments and sites XV*, 1-83.

- Jan Veselý. (2007). *Prostory Informačního centra klubu Za starou Prahu a jejich stavebně-historická dokumentace Za starou Prahu, Věstník Klubu Za starou Prahu XXXVII (VIII)*.
- Klein, A., & Grabner, M. (2015). Analysis of Construction Timber in Rural Austria: Wooden Log Walls.
- Kolar, T., Dobrovolny, P., Szabo, P., Mikita, T., Kyncl, T., Kyncl, J., . . . Rybnicek, M. (2021). Wood species utilization for timber constructions in the Czech lands over the period 1400–1900. 8.
- Kržan, M., & Bosiljkov, V. (2023). Compression and In-plane Seismic Behaviour of Ashlar Three-leaf Stone Masonry walls. *INTERNATIONAL JOURNAL OF ARCHITECTURAL HERITAGE*, 17(NO. 6), 829-845.
- Latifi, R., Hadzima-Nyarko, M., Radu, D., & Rouhi, R. (2023). A Brief Overview on Crack Patterns, Repair and Strengthening of Historical Masonry Structures. *Materials*.
- Lourenco, P., & Gaetani, A. (2022). Recommended properties for advanced numerical analysis. In P. B. Lourenco, & A. Gaetani, *Finite Elements Analysis for Building Assessment* (p. 266).
- Loverdos, D., Sarhosis, V., Adamopoulos, E., & Drougkas, A. (2021). An innovative image processing-based framework for the numerical modelling of cracked masonry structures. *Elsevier - Automation in Construction*, 15.
- Palacký, F. (1941). , *Starí letopisové čeští – viz Jaroslav Charvát (ed.), Dílo Františka Palackého. Svazek druhý, Praha 1941, Praha*.
- Pallarés, F., Betti, M., Bartoli, G., & Pallarés, L. (2022). Structural health monitoring (SHM) and Nondestructive testing (NDT) of slender masonry structures: A practical review.
- Průkryl, R., Průkrylova, J., Racek, M., Weishauptova, Z., & Kreislova, K. (2017). Decay mechanism of indoor porous opuka stone: a case study from the main altar located in the St. Vitus Cathedral, Prague, (Czech Republic). *Environ Earth Sci*, 15.
- Prikryl, R., Lokajcekb, T., Svobodov, J., & Weishauptovab, Z. (2003). Experimental weathering of marlstone from Predn Kopanina (Czech Republic)—historical building stone of Prague. *Elsevier Ltd.*, 9.
- Ramos, L. F. (2007). *Damage identification on masonry structures based on vibration signatures*. [DoctoralThesis]. <http://repositorium.sdum.uminho.pt>.
- Ruzicka, P. (n.d.). *Model of Half-timbered wall with different typed of infill*. Centrum stavitelského dědictví NTM, Plasy.
- Schiitznerovd-Havelkow, D. V. (1979). The Thoundsanf year olf building stone of Romanesque Prague. *Bulletin of the International Association of Engineering Geology*, 9.
- Václav Vladivoj Tomek. (1974). *Základy místopisu Pražského III., Praha 1872, s. 63. – Pokračovatelé Kosmovi, Praha 1974, s. 158*.

- Veselý, J. (2011). Menší malostranská mostecká věž Karlova mostu v Praze, při čp. 56/1 zvaná „Juditina věž“.
- Za Satarou Praha. (2018). Juditina věž je víc než „nějaký barák“. *vĚSTNÍK KLUBU ZA STAROU PRAHU*.
- Zahradník, P. (2005.). *Dějiny Karlova mostu (nepublikovaný rukopis, archiv NPÚ GnŘ), praha.*

This page is left blank on purpose.

9 ANNEX A



LEGENDS & SYMBOLS:

Camera Position



Crack



Thesis title:

**Static assessment of
Judit tower
in Prague**

PROJECT TITLE:

Juditina věž

LOCATION:

Pargue, Cezch

PREPARED BY:

ing. arch. Jan Vesely

REDRAW BY:

Arch. Safa Joudeh

SUPERVISOR:

Prof. Pter Fajman

PROJ. NO.

SAHC-02

DATE:

July 2023

SHEET CONTENTS:

**Ground Floor Plan
Camera Location
Crack mapping**

DWG. NO.

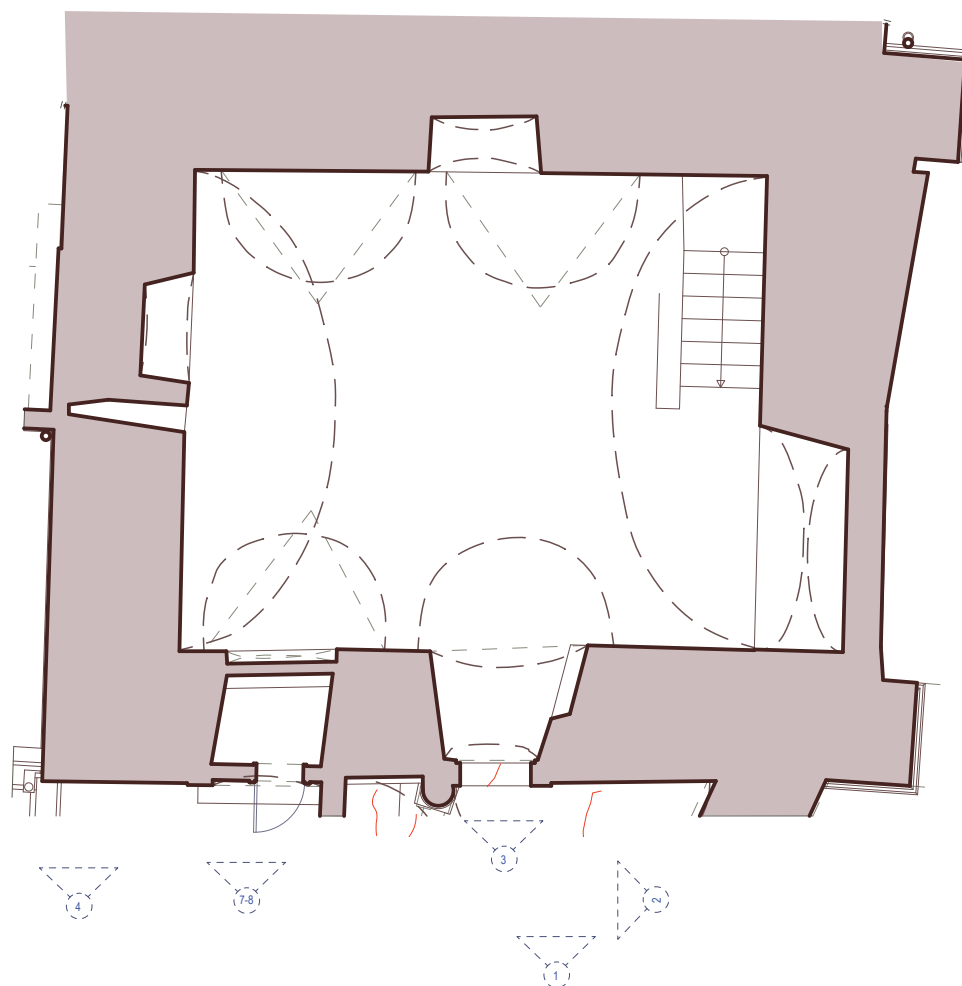
A100

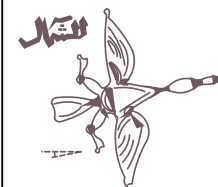
SCALE:

1:50

REV. NO.

2





LEGENDS & SYMBOLS:

Camera Position

Crack



Thesis title:

**Static assessment of
Judit tower
in Prague**

PROJECT TITLE:

Juditina věž

LOCATION:

Pargue, Czech

PREPARED BY:

ing. arch. Jan Vesely

REDRAW BY:

Arch. Safa Joudeh

SUPERVISOR:

Prof. Pter Fajman

PROJ. NO.

SAHC-02

DATE:

July 2023

SHEET CONTENTS:

**First Floor Plan
Camera Location
Crack mapping**

DWG. NO.

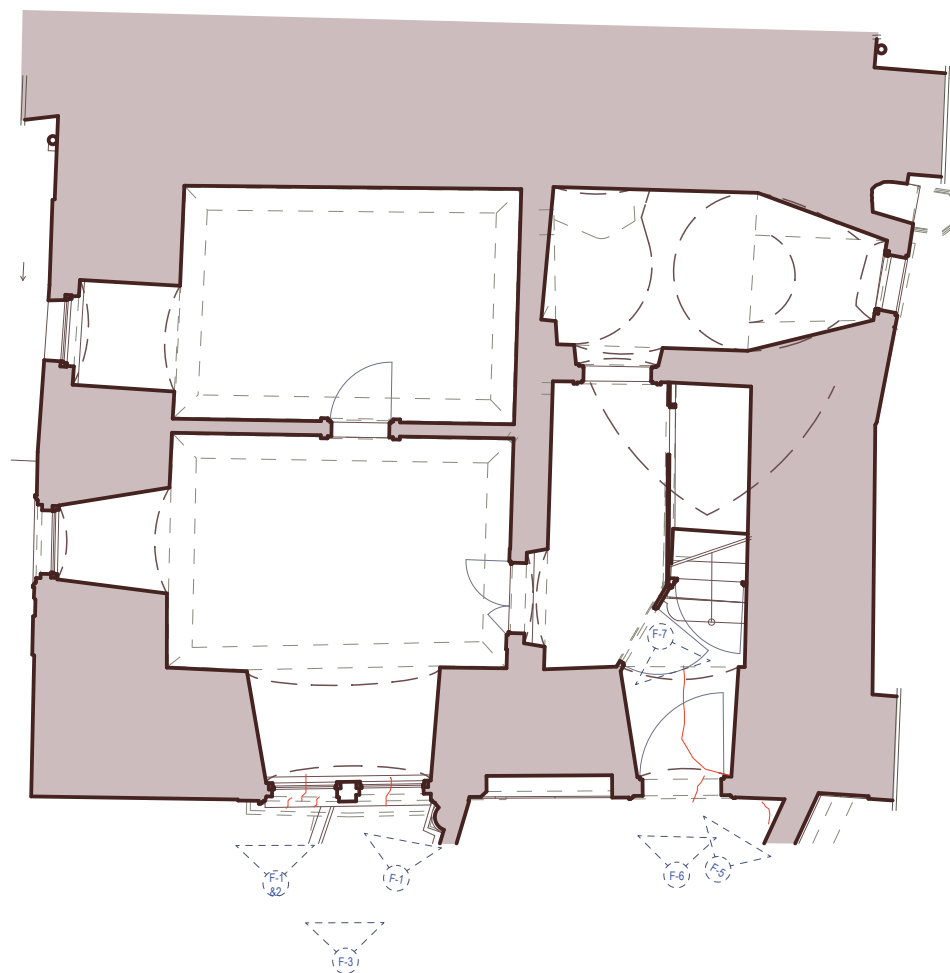
A101

SCALE:

1:50

REV. NO.

2





LEGENDS & SYMBOLS:

Camera Position

Crack



Thesis title:

**Static assessment of
Judit tower
in Prague**

PROJECT TITLE:

Juditina věž

LOCATION:

Pargue, Czech

PREPARED BY:

ing. arch. Jan Vesely

REDRAW BY:

Arch. Safa Joudeh

SUPERVISOR:

Prof. Pter Fajman

PROJ. NO.

SAHC-02

DATE:

July 2023

SHEET CONTENTS:

**Second Floor Plan
Camera Location
Crack mapping**

DWG. NO.

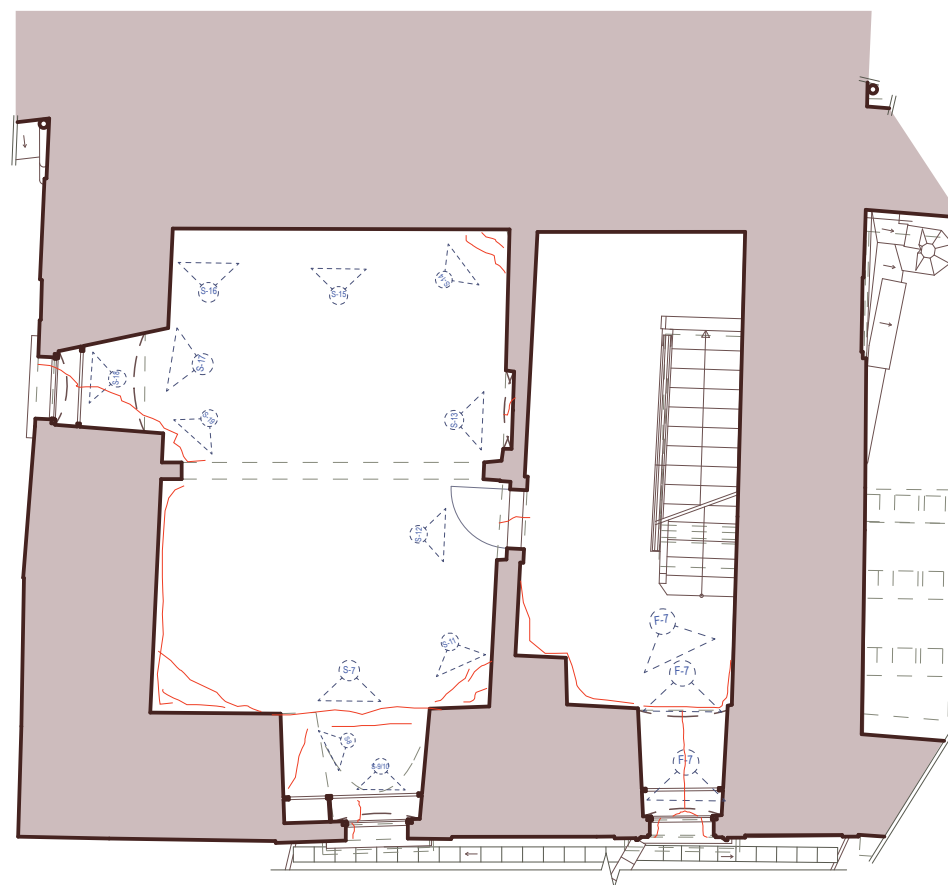
A102

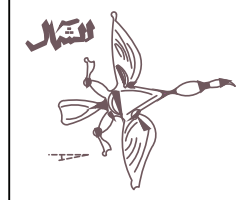
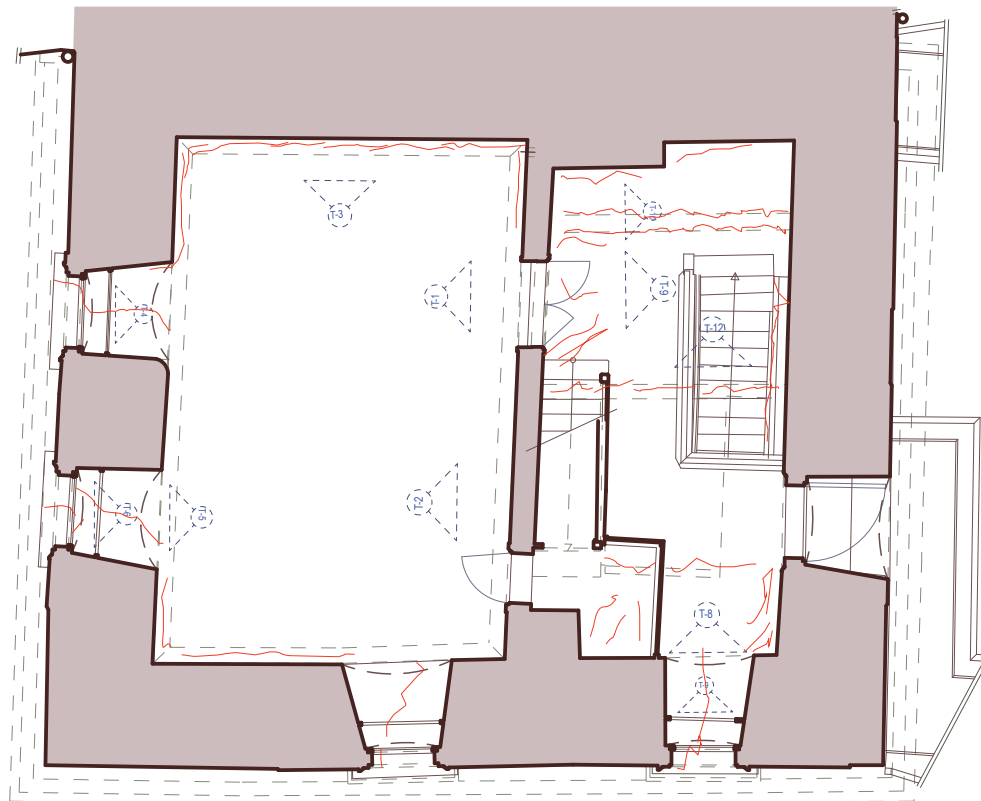
SCALE:

1:50

REV. NO.

2





LEGENDS & SYMBOLS:

Camera Position

Crack



Thesis title:
Static assessment of Judit tower in Prague

PROJECT TITLE:
Juditina věž

LOCATION:
Pargue, Cezch

PREPARED BY:
ing. arch. Jan Vesely

REDRAW BY:
Arch. Safa Joudeh

SUPERVISOR:
Prof. Pter Fajman

PROJ. NO.	DATE:
SAHC-02	July 2023

SHEET CONTENTS:
Third Floor Plan
Camera Location
Crack mapping

DWG. NO.
A103

SCALE:	REV. NO.
1:50	2



LEGENDS & SYMBOLS:

Camera Position

Crack



Thesis title:

**Static assessment of
Judit tower
in Prague**

PROJECT TITLE:

Juditina věž

LOCATION:

Pargue, Cezch

PREPARED BY:

ing. arch. Jan Vesely

REDRAW BY:

Arch. Safa Joudeh

SUPERVISOR:

Prof. Pter Fajman

PROJ. NO.

SAHC-02

DATE:

July 2023

SHEET CONTENTS:

Roof Floor Plan

Camera Location

Crack mapping

DWG. NO.

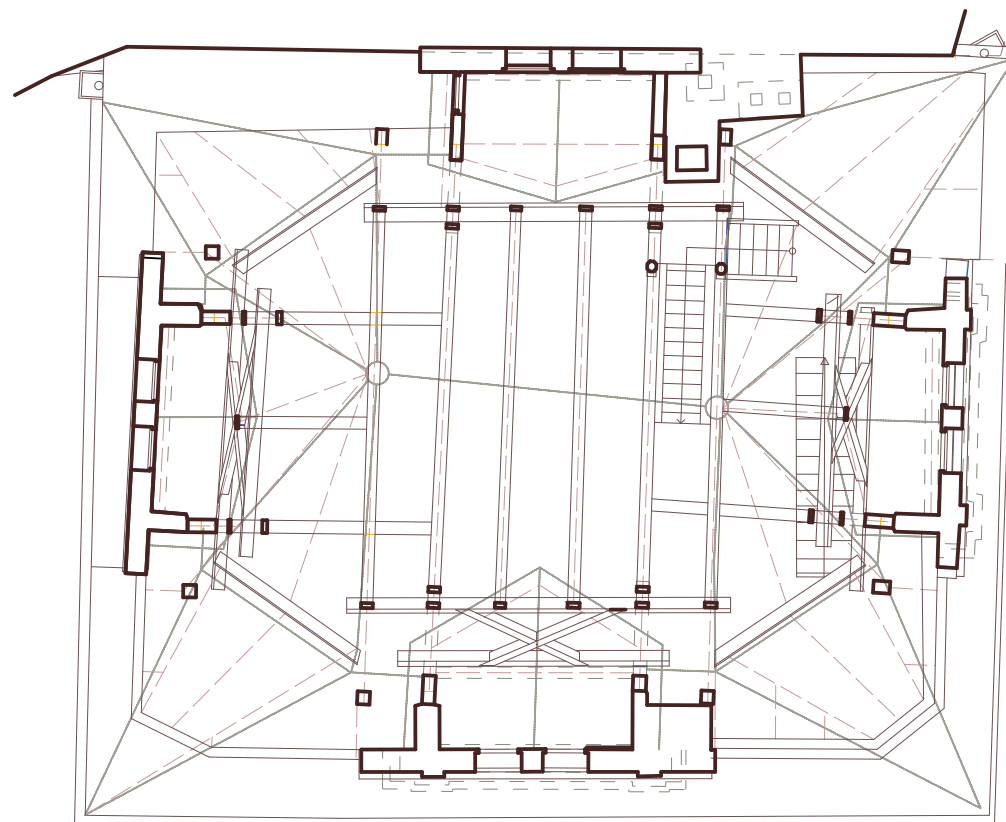
A104

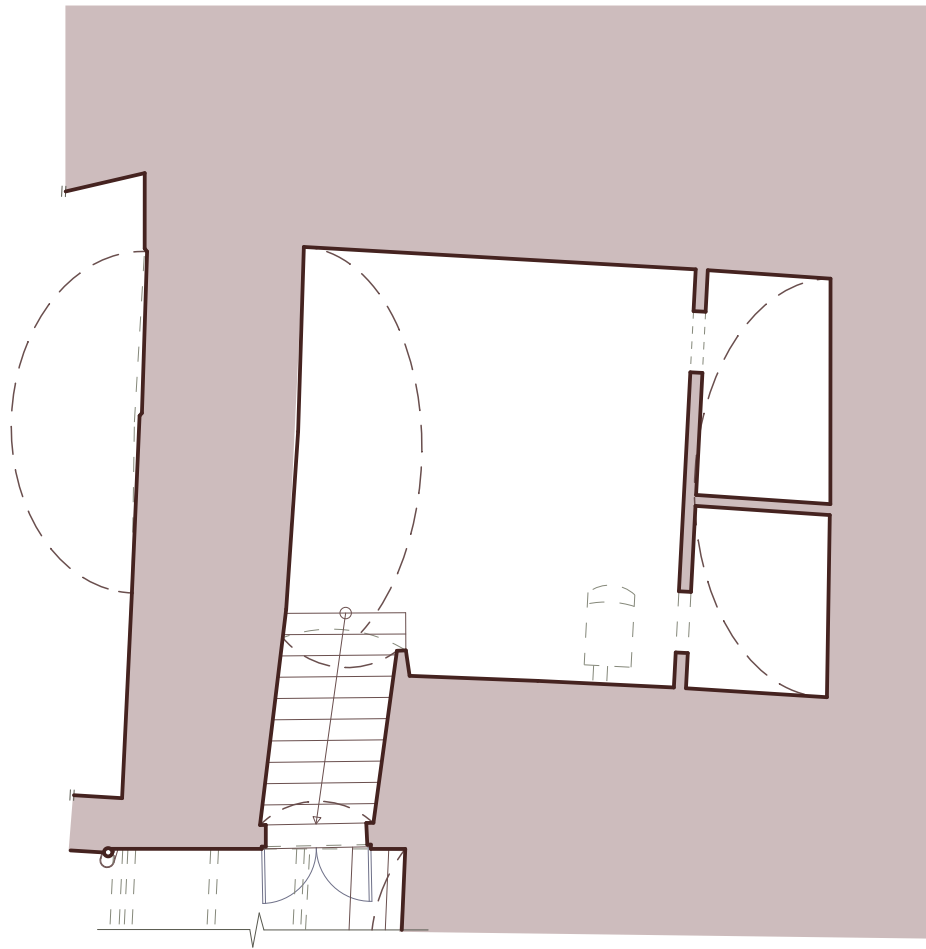
SCALE:

1:50

REV. NO.

2





LEGENDS & SYMBOLS:

Camera Position 

Crack 



Thesis title:
**Static assessment of
Judit tower
in Prague**

PROJECT TITLE:
Juditina věž

LOCATION:
Pargue, Cezch

PREPARED BY:
ing. arch. Jan Vesely

REDRAW BY:
Arch. Safa Joudeh

SUPERVISOR:
Prof. Pter Fajman

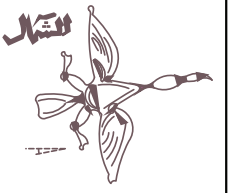
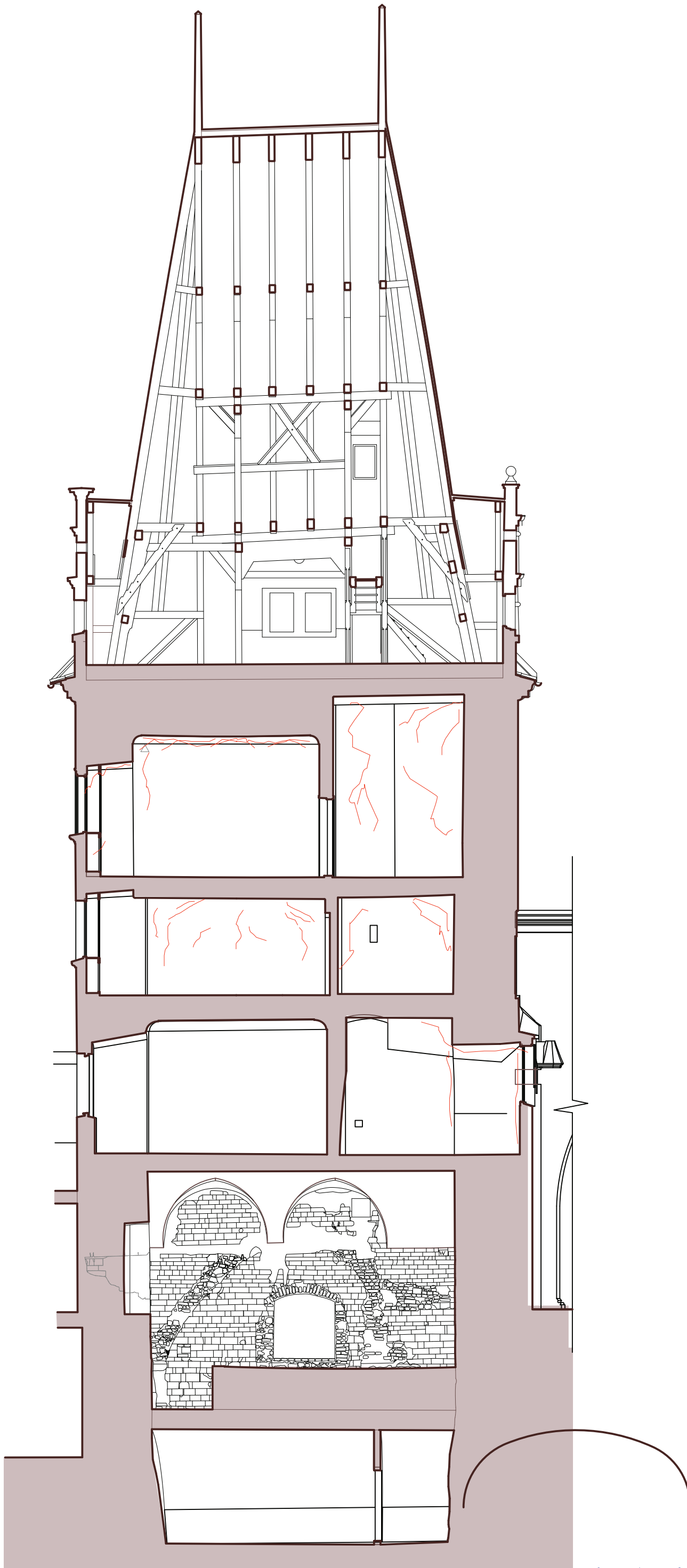
PROJ. NO. SAHC-02	DATE: July 2023
-----------------------------	---------------------------

SHEET CONTENTS:
Basement Floor Plan
Camera Location
Crack mapping

DWG. NO.
A105

SCALE: 1:50	REV. NO. 2
-----------------------	----------------------

225
224
223
222
221
220
219
218
217
216
215
214
213
212
211
210
209
208
207
206
205
204
203
202
201
200
199
198
197
196
195
194
193
192
191
190
189



LEGENDS & SYMBOLS:

- Camera Position
- Crack



Thesis title:
**Static assessment of
Juditina věž
in Prague**

PROJECT TITLE:
Juditina věž

LOCATION:
Prague, Czech

PREPARED BY:
ing. arch. Jan Veselý

REDRAW BY:
Arch. Safa Joudeh

SUPERVISOR:
Prof. Pter Fajman

PROJ. NO. DATE:
SAHC-02 July 2023

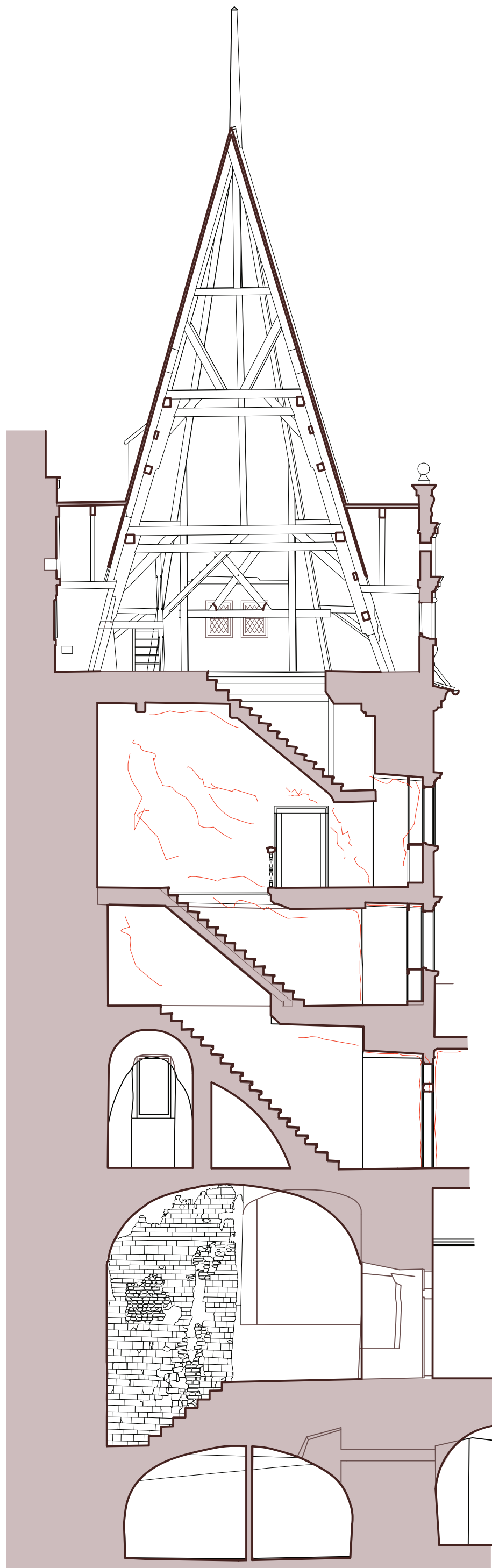
SHEET CONTENTS:
Section A
Camera Location
Crack mapping

DWG. NO.
A200

SCALE: REV. NO.
1:50 2

0 1 2 3 4 5 M

225
224
223
222
221
220
219
218
217
216
215
214
213
212
211
210
209
208
207
206
205
204
203
202
201
200
199
198
197
196
195
194
193
192
191
190
189



LEGENDS & SYMBOLS:

- Camera Position
- Crack



Thesis title:
**Static assessment of
Judit tower
in Prague**

PROJECT TITLE:
Juditina věž

LOCATION:
Prague, Czech

PREPARED BY:
ing. arch. Jan Veselý

REDRAW BY:
Arch. Safa Joudeh

SUPERVISOR:
Prof. Pter Fajman

PROJ. NO. DATE:
SAHC-02 July 2023

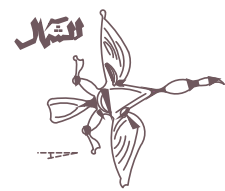
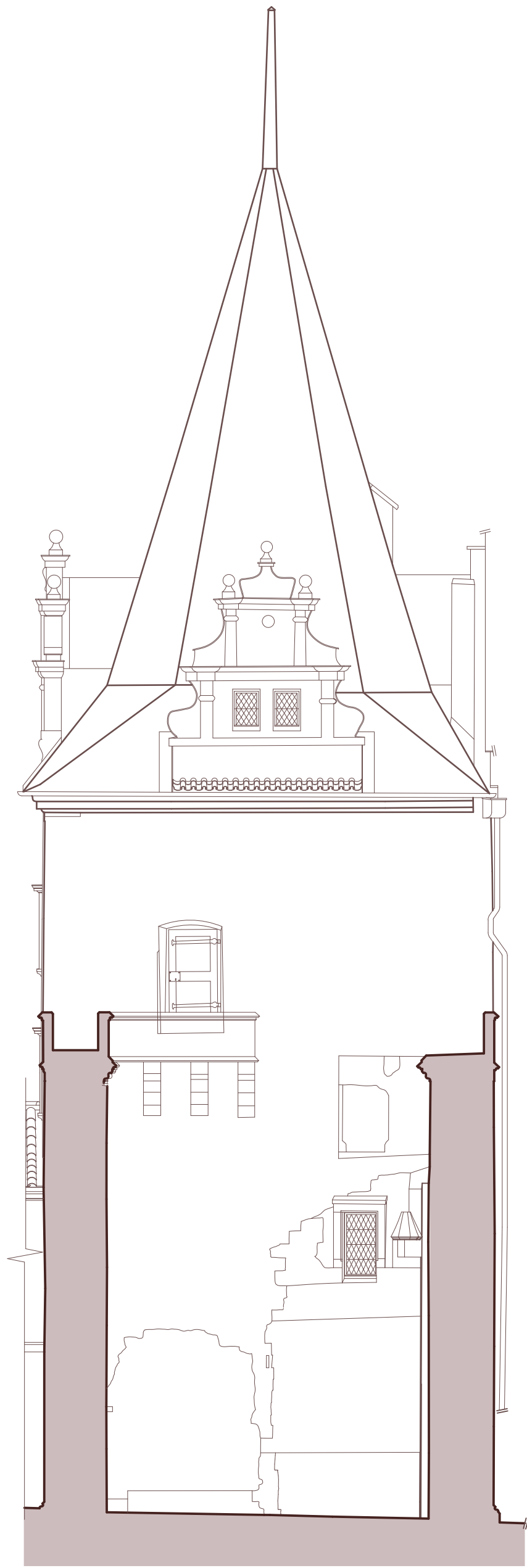
SHEET CONTENTS:
Section B
Camera Location
Crack mapping

DWG. NO.
A201

SCALE: REV. NO.
1:50 2



225
224
223
222
221
220
219
218
217
216
215
214
213
212
211
210
209
208
207
206
205
204
203
202
201
200
199
198
197
196
195
194
193
192
191
190
189



LEGENDS & SYMBOLS:

- Camera Position
- Crack



Thesis title:
**Static assessment of
Judit tower
in Prague**

PROJECT TITLE:
Juditina věž

LOCATION:
Prague, Czech

PREPARED BY:
ing. arch. Jan Veselý

REDRAW BY:
Arch. Safa Joudeh

SUPERVISOR:
Prof. Pter Fajman

PROJ. NO. DATE:
SAHC-02 July 2023

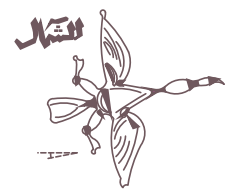
SHEET CONTENTS:
**North Elevation
Camera Location
Crack mapping**

DWG. NO.
A202

SCALE: REV. NO.
1:50 2



225
224
223
222
221
220
219
218
217
216
215
214
213
212
211
210
209
208
207
206
205
204
203
202
201
200
199
198
197
196
195
194
193
192
191
190
189



LEGENDS & SYMBOLS:

- Camera Position
- Crack



Thesis title:
Static assessment of Judit tower in Prague

PROJECT TITLE:
Juditina věž

LOCATION:
Prague, Czech

PREPARED BY:
ing. arch. Jan Veselý

REDRAW BY:
Arch. Safa Joudeh

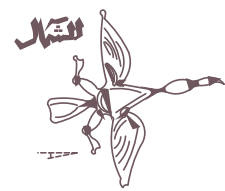
SUPERVISOR:
Prof. Pter Fajman

PROJ. NO. DATE:
SAHC-02 July 2023

SHEET CONTENTS:
**East Elevation
Camera Location
Crack mapping**

DWG. NO.
A203

SCALE: REV. NO.
1:50 2

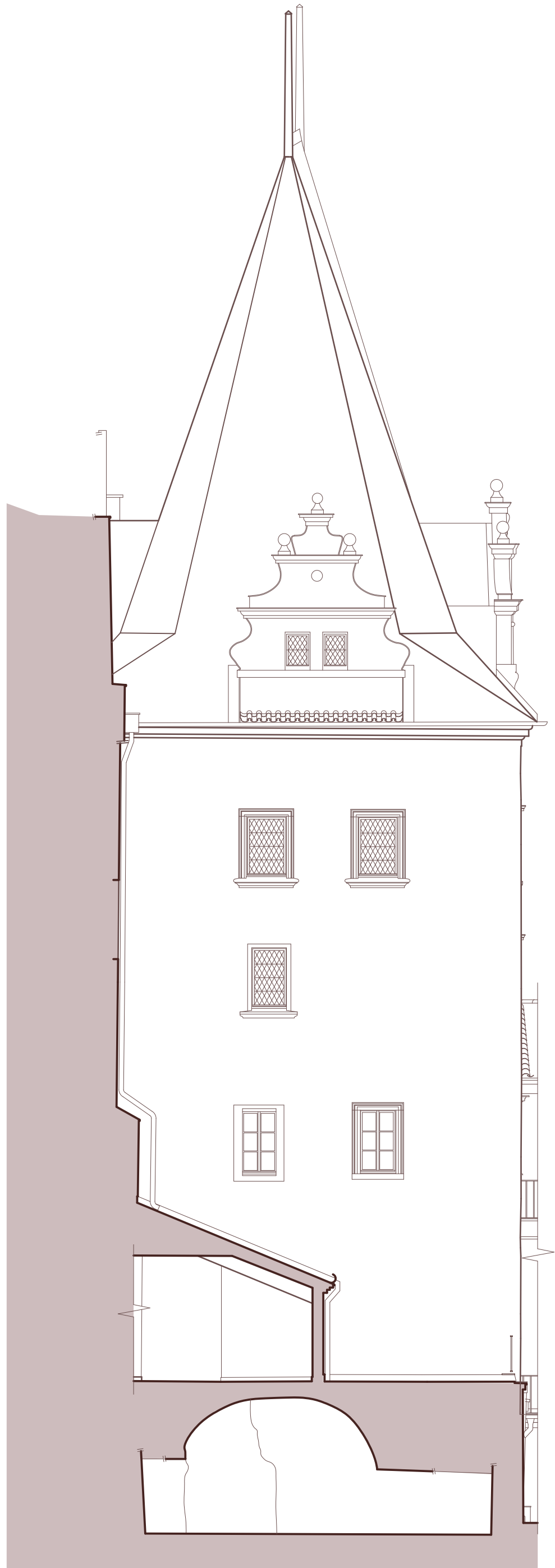


LEGENDS & SYMBOLS:

Camera Position



Crack



Thesis title:
**Static assessment of
Juditina věž
in Prague**

PROJECT TITLE:
Juditina věž

LOCATION:
Prague, Czech

PREPARED BY:
ing. arch. Jan Veselý

REDRAW BY:
Arch. Safa Joudeh

SUPERVISOR:
Prof. Pter Fajman

PROJ. NO. DATE:
SAHC-02 July 2023

SHEET CONTENTS:
**South Elevation
Camera Location
Crack mapping**

DWG. NO.
A204

SCALE: REV. NO.
1:50 2



10 ANNEX B

DAMAGE SURVEY - DATA SHEET

PROJECT NAME: Static Assessment of Judit Tower In Prague
 ADDRESS/ COORDINATES: Mostecká 56/1, 118 00 Malá Strana
 ELEMENT TO BE ANALYZED: East Façade
 MATERIAL: Kopaninská opuk Marl Stone
 UNIT OF MEASURE: Meters

ORIGINALITY YES NO UNKNOWN
 DATE (dd/mm/yyyy): 28/05/2023
 REFERENCE PLANE: A100 & A203

DEGREE OF DAMAGE	
X	

CODE: Z1-WALLS

LOCALIZATION	DAMAGE LOCALIZATION	RELEVANT IMAGES
Plan Ground Floor 	Crack Mapping East Façade - Ground Floor level 	Image number: G-1 Code: MD-01-2
Section East Elevation - crack mapping 	Crack mapping East South corner 	Image number: G-2 Code: MD-01-3
		Image number: G-3 Damage Code: MD-01-1
		Image number: G-3-1 & G-3-2 Damage Code: MD-01-1
		Image number: G-4 Damage Code: MD-02-2
		Image number: G-5 Damage Code: MD-03-1
		Image number: G-6 Damage Code: MD-02-2
		Image number: G-7 Damage Code: MD-01-1
		Image number: G-8 Damage Code: MD-01-3

PHOTO	Cod.	DAMAGE	DEFINITION	INTERVENTION PROPOSAL
G-1	MD-01-2	Hair crack	Minor crack with width dimension < 0.1 mm	Craftsmanship consists of sealing the cracks by hand with acrylic-based stone mortar or lime, as appropriate.
G-2	MD-01-3	Splitting	Fracturing of a stone along planes of weakness such as microcracks or clay/silt layers, in cases where the structural elements are orientated vertically. For instance, a column may split into several parts along bedding planes if the load above it is too high.	Once the cause of the pathology has been identified and eradicated, the element is reinforced with compatible materials. Structure consolidation: tie rods, metal inserts, stapling and consolidation of foundations.
G-3	MD-01-1	Fracture	Crack that crosses completely the stone piece	In the case of cracks without settlement, or with minimal settlement. Sealing of the open joint with lime mortar, consolidation of the stones on top. In cases of major damage (once the cause of the problem has been identified and eradicated) the crack is repaired with hidden staples and subsequent sealing
G-4	MD-02-2	Deformations due to generalized movements	Differential settlement, presence of cracks at 45° with emphasis on spans (weak points)	Study of soils, reinforcement of existing foundations (increase of the section, or restitution). Insertion of foundation elements up to the bearing soil, e.g. micropiles. Crack stitching, replacement and reinforcement with compatible material.
G-5	MD-03-1	Impact damage	Mechanical damage due to the impact of a projectile (bullet, shrapnel) or of a hard tool.	replacement of the affected piece with a compatible material, protection of the element. In case of using mortar, its density must be less or equal to that of the original stone, this avoids incorporating tensions in the stones.
G-6	MD-02-2	Deformations due to generalized movements	Differential settlement, presence of cracks at 45° with emphasis on spans (weak points)	Study of soils, reinforcement of existing foundations (increase of the section, or restitution). Insertion of foundation elements up to the bearing soil, e.g. micropiles. Crack stitching, replacement and reinforcement with compatible material.
G-7	MD-01-1	Fracture	Crack that crosses completely the stone piece	In the case of cracks without settlement, or with minimal settlement. Sealing of the open joint with lime mortar, consolidation of the stones on top. In cases of major damage (once the cause of the problem has been identified and eradicated) the crack is repaired with hidden staples and subsequent sealing
G-8	MD-01-3	Splitting	Fracturing of a stone along planes of weakness such as microcracks or clay/silt layers, in cases where the structural elements are orientated vertically. For instance, a column may split into several parts along bedding planes if the load above it is too high.	Once the cause of the pathology has been identified and eradicated, the element is reinforced with compatible materials. Structure consolidation: tie rods, metal inserts, stapling and consolidation of foundations.

DAMAGE SURVEY - DATA SHEET

PROJECT NAME: Static Assessment of Judit Tower In Prague
 ADDRESS/ COORDINATES: Mostecká 56/1, 118 00 Malá Strana
 ELEMENT TO BE ANALYZED: East Façade
 MATERIAL: Kopaninská opuk Marl Stone
 UNIT OF MEASURE: Meters

ORIGINALITY YES NO UNKNOWN
 DATE (dd/mm/yyyy): 26/05/2023
 REFERENCE PLANE: A101 & A203

DEGREE OF DAMAGE	
X	

CODE: Z1-WALLS

LOCALIZATION	DAMAGE LOCALIZATION	RELEVANT IMAGES	
Plan First Floor	Crack Mapping East Sectional Façade - First Floor level - Photogrammetric Documentation	Image number: F-1 Damage Code MD-01-2	Image number: F-2 Damage Code MD-01-2
Section East Elevation -	Crack Mapping East Sectional Façade - First Floor level	Image number: F-3 Damage Code MD-01-1 MD-01-3	Image number: F-3-1 Damage Code MD-01-1
		Image number: F-3-2 Damage Code MD-01-1	Image number: F-4 Damage Code MD-01-3
		Image number: F-5 Damage Code MD-01-2	Image number: F-5-1 Damage Code MD-01-2
		Image number: F-6 Damage Code MD-01-1	

PHOTO	Cod.	DAMAGE	DEFINITION	INTERVENTION PROPOSAL
F-1	MD-01-2	Hair crack	Minor crack with width dimension < 0.1 mm	Craftsmanship consists of sealing the cracks by hand with acrylic-based stone mortar or lime, as appropriate.
F-2	MD-01-2	Hair crack	Minor crack with width dimension < 0.1 mm	Craftsmanship consists of sealing the cracks by hand with acrylic-based stone mortar or lime, as appropriate.
F-3	MD-01-1	Fracture	Crack that crosses completely the stone piece	In the case of cracks without settlement, or with minimal settlement. Sealing of the open joint with lime mortar, consolidation of the stones on top. In cases of major damage (once the cause of the problem has been identified and eradicated) the crack is repaired with hidden staples and subsequent sealing
F-4	MD-01-3	Splitting	Fracturing of a stone along planes of weakness such as microcracks or clay/silt layers, in cases where the structural elements are orientated vertically. For instance, a column may split into several parts along bedding planes if the load above it is too high.	Once the cause of the pathology has been identified and eradicated, the element is reinforced with compatible materials. Structure consolidation: tie rods, metal inserts, stapling and consolidation of foundations.
F-5	MD-01-2	Hair crack	Minor crack with width dimension < 0.1 mm	Craftsmanship consists of sealing the cracks by hand with acrylic-based stone mortar or lime, as appropriate.
F-6	MD-01-1	Fracture	Crack that crosses completely the stone piece	In the case of cracks without settlement, or with minimal settlement. Sealing of the open joint with lime mortar, consolidation of the stones on top. In cases of major damage (once the cause of the problem has been identified and eradicated) the crack is repaired with hidden staples and subsequent sealing

DAMAGE SURVEY - DATA SHEET

PROJECT NAME: Static Assessment of Judit Tower In Prague
 ADDRESS/ COORDINATES: Mostecká 56/1, 118 00 Malá Strana
 ELEMENT TO BE ANALYZED: East Façade
 MATERIAL: Kopaninská opuk Marl Stone
 UNIT OF MEASURE: Meters

ORIGINALITY YES NO UNKNOWN
 DATE (dd/mm/yyyy): 26/05/2023
 REFERENCE PLANE: A101, A102 & A201

DEGREE OF DAMAGE	
X	

CODE: Z1-WALLS

LOCALIZATION	DAMAGE LOCALIZATION	RELEVANT IMAGES	
Plan First Floor - Room A	Crack mapping & Camera positions Second Floor Plan	Image number: F-8 Damage Code: MD-01-2	Image number: F-9 Damage Code: MD-02-2
SECTION FLOOR Section A-A	Localization - Plan Second Floor - Room A	Image number: S-1 Damage Code: MD-02-2	Image number: S-2 Damage Code: MD-01-1
		Image number: S-3 Damage Code: MD-02-2	Image number: S-4 Damage Code: MD-01-2
		Image number: S-5 Damage Code: MD-01-2	Image number: S-6 Damage Code: MD-01-2

PHOTO	Cod.	DAMAGE	DEFINITION	INTERVENTION PROPOSAL
F-8	MD-01-2	Hair crack	Minor crack with width dimension < 0.1 mm	Craftsmanship consists of sealing the cracks by hand with acrylic-based stone mortar or lime, as appropriate.
F-9	MD-02-2	Deformations due to generalized movements	Differential settlement, presence of cracks at 45° with emphasis on spans (weak points)	Study of soils, reinforcement of existing foundations (increase of the section, or restitution). Insertion of foundation elements up to the bearing soil, e.g. micropiles. Crack stitching, replacement and reinforcement with compatible material.
S-1	MD-02-2	Deformations due to	Differential settlement, presence of cracks at 45° with emphasis on spans (weak points)	Study of soils, reinforcement of existing foundations (increase of the section, or restitution). Insertion of foundation elements up to the bearing soil, e.g. micropiles. Crack stitching, replacement and reinforcement with compatible material.
S-4	MD-01-2	Hair crack	Minor crack with width dimension < 0.1 mm	Craftsmanship consists of sealing the cracks by hand with acrylic-based stone mortar or lime, as appropriate.
S-5	MD-01-2	Hair crack	Minor crack with width dimension < 0.1 mm	Craftsmanship consists of sealing the cracks by hand with acrylic-based stone mortar or lime, as appropriate.
S-6	MD-01-2	Hair crack	Minor crack with width dimension < 0.1 mm	Craftsmanship consists of sealing the cracks by hand with acrylic-based stone mortar or lime, as appropriate.

DAMAGE SURVEY - DATA SHEET

PROJECT NAME: Static Assessment of Judit Tower In Prague
 ADDRESS/ COORDINATES: Mostecká 56/1, 118 00 Malá Strana
 ELEMENT TO BE ANALYZED: East Façade
 MATERIAL: Kopaninská opuk Marl Stone
 UNIT OF MEASURE: Meters

ORIGINALITY YES NO UNKNOWN
 DATE (dd/mm/yyyy): 26/05/2023
 REFERENCE PLANE: A102 & A200

DEGREE OF DAMAGE	
X	

CODE: Z1-WALLS

LOCALIZATION	DAMAGE LOCALIZATION	RELEVANT IMAGES
Plan First Floor 	Crack Mapping East Sectional Façade - First Floor level 	Image number: S-7 Damage Code MD-01-2
Section East Elevation - 	Image number: S-17 Damage Code MD-01-2 	Image number: S-8 Damage Code MD-01-2
	Image number: S-18 Damage Code MD-01-2 	Image number: S-9 Damage Code MD-01-2
	Image number: S-19 Damage Code MD-01-2 	Image number: S-10 Damage Code MD-01-1
		Image number: S-11 Damage Code MD-01-2
		Image number: S-12 Damage Code MD-01-2
		Image number: S-13 Damage Code MD-01-2
		Image number: S-14 Damage Code MD-01-2
		Image number: S-15 Damage Code MD-01-2
		Image number: S-16 Damage Code MD-01-2
		Image number: S-17 Damage Code MD-01-2

PHOTO	Cod.	DAMAGE	DEFINITION	INTERVENTION PROPOSAL
S-7	MD-01-2	Hair crack	Minor crack with width dimension < 0.1 mm	Craftsmanship consists of sealing the cracks by hand with acrylic-based stone mortar or lime, as appropriate.
S-8	MD-01-2	Hair crack	Minor crack with width dimension < 0.1 mm	Craftsmanship consists of sealing the cracks by hand with acrylic-based stone mortar or lime, as appropriate.
S-9	MD-01-2	Hair crack	Minor crack with width dimension < 0.1 mm	Craftsmanship consists of sealing the cracks by hand with acrylic-based stone mortar or lime, as appropriate.
S-10	MD-01-1	Fracture	Crack that crosses completely the stone piece	In the case of cracks without settlement, or with minimal settlement. Sealing of the open joint with lime mortar, consolidation of the stones on top. In cases of major damage (once the cause of the problem has been identified and eradicated) the crack is repaired with hidden staples and subsequent sealing
S-11	MD-01-2	Hair crack	Minor crack with width dimension < 0.1 mm	Craftsmanship consists of sealing the cracks by hand with acrylic-based stone mortar or lime, as appropriate.
S-12	MD-01-2	Hair crack	Minor crack with width dimension < 0.1 mm	Craftsmanship consists of sealing the cracks by hand with acrylic-based stone mortar or lime, as appropriate.
S-13	MD-01-2	Hair crack	Minor crack with width dimension < 0.1 mm	Craftsmanship consists of sealing the cracks by hand with acrylic-based stone mortar or lime, as appropriate.
S-14	MD-01-2	Hair crack	Minor crack with width dimension < 0.1 mm	Craftsmanship consists of sealing the cracks by hand with acrylic-based stone mortar or lime, as appropriate.
S-15	MD-01-2	Hair crack	Minor crack with width dimension < 0.1 mm	Craftsmanship consists of sealing the cracks by hand with acrylic-based stone mortar or lime, as appropriate.
S-16	MD-01-2	Hair crack	Minor crack with width dimension < 0.1 mm	Craftsmanship consists of sealing the cracks by hand with acrylic-based stone mortar or lime, as appropriate.
S-17	MD-01-2	Hair crack	Minor crack with width dimension < 0.1 mm	Craftsmanship consists of sealing the cracks by hand with acrylic-based stone mortar or lime, as appropriate.
S-18	MD-01-2	Hair crack	Minor crack with width dimension < 0.1 mm	Craftsmanship consists of sealing the cracks by hand with acrylic-based stone mortar or lime, as appropriate.
S-19	MD-01-2	Hair crack	Minor crack with width dimension < 0.1 mm	Craftsmanship consists of sealing the cracks by hand with acrylic-based stone mortar or lime, as appropriate.

DAMAGE SURVEY - DATA SHEET

PROJECT NAME: Static Assessment of Judit Tower In Prague
 ADDRESS/ COORDINATES: Mostecká 56/1, 118 00 Malá Strana
 ELEMENT TO BE ANALYZED: East Façade
 MATERIAL: Kopianinská opuk Marl Stone
 UNIT OF MEASURE: Meters

ORIGINALITY YES NO UNKNOWN
 DATE (dd/mm/yyyy): 26/05/2023
 REFERENCE PLANE: A103 & A201

DEGREE OF DAMAGE	
X	

CODE: Z1-WALLS

LOCALIZATION	DAMAGE LOCALIZATION	ROOM A - RELEVANT IMAGES	
Plan 3rd Floor	Crack mapping 3rd Floor Plan	Image number: T-1 Damage Code: MD-01-2	Image number: T-2 Damage Code: MD-02-2
Section East Elevation -	Camera Positons 3rd Floor Plan	Image number: T-3 Damage Code: MD-01-2	Image number: T-4 Damage Code: MD-01-1
		Image number: T-5 Damage Code: MD-01-1	Image number: T-6 Damage Code: MD-01-2
		Image number: T-7 Damage Code: MD-02-2	Image number: T-8 Damage Code: MD-02-2
		Image number: T-9 Damage Code: MD-01-3	Image number: T-10 Damage Code: MD-01-3
		Image number: T-11 Damage Code: MD-01-2	Image number: T-12 Damage Code: MD-01-2

PHOTO	Cod.	DAMAGE	DEFINITION	INTERVENTION PROPOSAL
T-1	MD-01-2	Hair crack	Minor crack with width dimension < 0.1 mm	Craftsmanship consists of sealing the cracks by hand with acrylic-based stone mortar or lime, as appropriate.
T-2	MD-02-2	Deformations due to generalized movements	Differential settlement, presence of cracks at 45° with emphasis on spans (weak points)	Study of soils, reinforcement of existing foundations (increase of the section, or restitution). Insertion of foundation elements up to the bearing soil, e.g. micropiles. Crack stitching, replacement and reinforcement with compatible material.
T-3	MD-01-2	Hair crack	Minor crack with width dimension < 0.1 mm	Craftsmanship consists of sealing the cracks by hand with acrylic-based stone mortar or lime, as appropriate.
T-4	MD-01-1	Fracture	Crack that crosses completely the stone piece	In the case of cracks without settlement, or with minimal settlement. Sealing of the open joint with lime mortar, consolidation of the stones on top. In cases of major damage (once the cause of the problem has been identified and eradicated) the crack is repaired with hidden staples and subsequent sealing.
T-5	MD-02-2	Deformations due to generalized movements	Differential settlement, presence of cracks at 45° with emphasis on spans (weak points)	Study of soils, reinforcement of existing foundations (increase of the section, or restitution). Insertion of foundation elements up to the bearing soil, e.g. micropiles. Crack stitching, replacement and reinforcement with compatible material.
T-6	MD-01-2	Hair crack	Minor crack with width dimension < 0.1 mm	Craftsmanship consists of sealing the cracks by hand with acrylic-based stone mortar or lime, as appropriate.
T-7	MD-02-2	Deformations due to generalized movements	Differential settlement, presence of cracks at 45° with emphasis on spans (weak points)	Study of soils, reinforcement of existing foundations (increase of the section, or restitution). Insertion of foundation elements up to the bearing soil, e.g. micropiles. Crack stitching, replacement and reinforcement with compatible material.
T-8	MD-02-2	Deformations due to generalized movements	Differential settlement, presence of cracks at 45° with emphasis on spans (weak points)	Study of soils, reinforcement of existing foundations (increase of the section, or restitution). Insertion of foundation elements up to the bearing soil, e.g. micropiles. Crack stitching, replacement and reinforcement with compatible material.
T-9	MD-01-3	Splitting	Fracturing of a stone along planes of weakness such as microcracks or clay/silt layers, in cases where the structural elements are orientated vertically. For instance, a column may split into several parts along bedding planes if the load above it is too high.	Once the cause of the pathology has been identified and eradicated, the element is reinforced with compatible materials. Structure consolidation: tie rods, metal inserts, stapling and consolidation of foundations.
T-10	MD-01-3	Splitting	Fracturing of a stone along planes of weakness such as microcracks or clay/silt layers, in cases where the structural elements are orientated vertically. For instance, a column may split into several parts along bedding planes if the load above it is too high.	Once the cause of the pathology has been identified and eradicated, the element is reinforced with compatible materials. Structure consolidation: tie rods, metal inserts, stapling and consolidation of foundations.
T-11	MD-01-2	Hair crack	Minor crack with width dimension < 0.1 mm	Craftsmanship consists of sealing the cracks by hand with acrylic-based stone mortar or lime, as appropriate.
T-12	MD-01-2	Hair crack	Minor crack with width dimension < 0.1 mm	Craftsmanship consists of sealing the cracks by hand with acrylic-based stone mortar or lime, as appropriate.

DAMAGE SURVEY - DATA SHEET

PROJECT NAME: Static Assessment of Judit Tower In Prague
 ADDRESS/ COORDINATES: Mostecká 56/1, 118 00 Malá Strana
 ELEMENT TO BE ANALYZED: East Façade
 MATERIAL: Kopaninská opuk Marl Stone
 UNIT OF MEASURE: Meters

ORIGINALITY YES NO UNKNOWN
 DATE (dd/mm/yyyy): 26/05/2023
 REFERENCE PLANE: A103 & A201

DEGREE OF DAMAGE	
	X

CODE: Z1-WALLS

LOCALIZATION	DAMAGE LOCALIZATION	ROOM A - RELEVANT IMAGES
Plan First Floor	Crack mapping 3rd Floor Plan	Image number: NF-1 Damage Code: MD-03-2
Section East Elevation -		Image number: NF-2 Damage Code: MD-03-2
		Image number: NF-3 Damage Code: MD-01-3

PHOTO	Cod.	DAMAGE	DEFINITION	INTERVENTION PROPOSAL
NF-1	MD-03-2	Cut	Loss of material due to the action of an edge tool. It can have the appearance of an excavated cavity, an incision, a missing edge, etc...Tool marks can be considered as special kinds of cuts but should not be considered as damage features	Mortar application, by trowel or other, for the reconstruction of the original profile. It is molded and carved in situ, you can choose between industrial mortars or on the contrary formulated in a specific way by the restoration workshop. The density must be less or equal to that of the original stone, this avoids incorporating tensions in the stones.
NF-2	MD-03-2	Cut	Loss of material due to the action of an edge tool. It can have the appearance of an excavated cavity, an incision, a missing edge, etc...Tool marks can be considered as special kinds of cuts but should not be considered as damage features	Mortar application, by trowel or other, for the reconstruction of the original profile. It is molded and carved in situ, you can choose between industrial mortars or on the contrary formulated in a specific way by the restoration workshop. The density must be less or equal to that of the original stone, this avoids incorporating tensions in the stones.
NF-3	MD-01-3	Splitting	Fracturing of a stone along planes of weakness such as microcracks or clay/silt layers, in cases where the structural elements are orientated vertically. For instance, a column may split into several parts along bedding planes if the load above it is too high.	Once the cause of the pathology has been identified and eradicated, the element is reinforced with compatible materials. Structure consolidation: tie rods, metal inserts, stapling and consolidation of foundations.

11 ANNEX C

Code	STONE DAMAGE	DEFINITION	INTERVENTION	ICOMOS (REFERENCE PHOTO)
1 MD-01-1	Fracture	Crack that crosses completely the stone piece	In the case of cracks without settlement, or with minimal settlement. Sealing of the open joint with lime mortar, consolidation of the stones on top. In cases of major damage (once the cause of the problem has been identified and eradicated) the crack is repaired with hidden staples and subsequent sealing	
2 MD-01-2	Hair crack	Minor crack with width dimension < 0.1 mm	Craftsmanship consists of sealing the cracks by hand with acrylic-based stone mortar or lime, as appropriate.	
3 MD-01-3	Splitting	Fracturing of a stone along planes of weakness such as microcracks or clay/silt layers, in cases where the structural elements are orientated vertically. For instance, a column may split into several parts along bedding planes if the load above it is too high.	Once the cause of the pathology has been identified and eradicated, the element is reinforced with compatible materials. Structure consolidation: tie rods, metal inserts, stapling and consolidation of foundations.	
4 MD-02-1	Mechanical deformation	Change in shape without losing integrity, leading to bending, buckling or twisting of a stone block.	The objective is to recover volumes or shapes of the element, therefore the reconstitution is carried out by means of mortars (with density and resistance lower or equal to those of the original stone to avoid tensions on it), natural carved stones or artificial molded reproductions.	
5 MD-02-2	Deformations due to generalized movements	Differential settlement, presence of cracks at 45° with emphasis on spans (weak points)	Study of soils, reinforcement of existing foundations (increase of the section, or restitution). Insertion of foundation elements up to the bearing soil, e.g. micropiles. Crack stitching, replacement and reinforcement with compatible material.	
7 MD-03-1	Impact damage	Mechanical damage due to the impact of a projectile (bullet, shrapnel) or of a hard tool.	replacement of the affected piece with a compatible material, protection of the element. In case of using mortar, its density must be less or equal to that of the original stone, this avoids incorporating tensions in the stones.	
8 MD-03-2	Cut	Loss of material due to the action of an edge tool. It can have the appearance of an excavated cavity, an incision, a missing edge, etc...Tool marks can be considered as special kinds of cuts but should not be considered as damage features	Mortar application, by trowel or other, for the reconstruction of the original profile. It is molded and carved in situ, you can choose between industrial mortars or on the contrary formulated in a specific way by the restoration workshop. The density must be less or equal to that of the original stone, this avoids incorporating tensions in the stones.	
9 MD-04	Missing Part	Empty space, obviously located in the place of some formerly existing stone part. Protruding and particularly exposed parts of sculptures (nose, fingers) are typical locations for material loss resulting in missing parts.	Reconstruction of the missing piece with suitable materials that do not generate stresses to the original material or generate pathologies of chemical or biological origin.	
10 PD-01-1	Moisture due to condensation	Occurs when the air inside the building comes into contact with the colder surfaces of the walls, the air lowers the temperature and causes condensation, it is a common phenomenon in facade walls, it appears inside the building in the form of surface stain and is usually located in corners, corners and behind large objects, i.e. in poorly ventilated areas.	A thorough study of the temperature gradients and constructive links must be made, once the origin of the lesion has been identified, the actions to be carried out will be focused on avoiding that the dew point temperature is reached at any point. This can be addressed by increasing the general temperature inside the section of the element; a decrease in the dew point temperature, or by dissipating the water vapor that crosses the enclosure. In case of hygroscopic condensation, the crystallized hygroscopic salts must be removed by cleaning the surface and applying dressings of a drying product.	
11 PD-02-1	Differential erosion	Result of selective lichen attack on calcitic rocks. Differential erosion is synonymous with relief, i.e. the formation of irregularities on the surface of the stone.	It is important to avoid moisture, since the presence of water is the constant in almost all forms of erosion, in this sense, the right thing to do is to take measures to prevent water from stagnating on the surface through additional works on the facades, if this is not possible, water-repellent coatings should be applied, generally based on siloxanes without altering the breathability, and respecting the natural appearance of the bases as much as possible.	
12 PD-02-2	filtration	water seepage through the cover generates dark spots	If it is due to the porosity of the material, the solution is to apply a waterproofing finish that allows the enclosure to breathe, normally based on siloxanes, in order to maintain the originality of the elements. On the other hand, it is possible to seal joints, increase the slope of roofs, and replace affected or missing parts.	
13 CD-01-1	Crumbling	Detachment of single grains or aggregates of grains. Crumbling: Detachment of aggregates of grains from the substrate. These aggregates are generally limited in size (less than 2 cm). This size depends on the nature of the stone and its environment.	The deterioration processes must be interrupted, in general the process is based on the manual cleaning of the material in order not to generate strong abrasions in the rock, it is advisable to make samplings of the dirt to determine its nature and to eradicate them in an effective way. Within this work is included the pre-consolidation, this should be done when there are pieces of great historical value where the cleaning itself can generate destruction of the element, desalination in which salts are extracted with the application on the surface of the stone of an additional absorbent material, a consolidation will be executed with the objective of increasing the cohesion of the components of the superficial zone of the stone.	
14 CD-01-2	Roughening	Selective loss of small particles from an originally smooth stone surface. The substrate is still sound. Roughening can appear either progressively in case of long term deterioration process (for instance in case of granular disintegration), or instantaneously in case of inappropriate reactions, such as aggressive cleaning	The deterioration processes must be interrupted, in general the process is based on the manual cleaning of the material in order not to generate strong abrasions in the rock, it is advisable to make samplings of the dirt to determine its nature and to eradicate them in an effective way. Within this work is included the pre-consolidation, this should be done when there are pieces of great historical value where the cleaning itself can generate destruction of the element, desalination in which salts are extracted with the application on the surface of the stone of an additional absorbent material, a consolidation will be executed with the objective of increasing the cohesion of the components of the superficial zone of the stone.	

15	CD-01-3	Rounding	Preferential erosion of originally angular stone edges leading to a distinctly rounded profile. Rounding can especially be observed on stones which preferably deteriorate through granular disintegration, or when environmental conditions favor granular disintegration.	The deterioration processes must be interrupted, in general the process is based on the manual cleaning of the material in order not to generate strong abrasions in the rock, it is advisable to make samplings of the dirt to determine its nature and to eradicate them in an effective way, Within this work is included the pre-consolidation, this should be done when there are pieces of great historical value where the cleaning itself can generate destruction of the element, desalination in which salts are extracted with the application on the surface of the stone of an additional absorbent material, a consolidation will be executed with the objective of increasing the cohesion of the components of the superficial zone of the stone.	
16	CD-01-4	Discolouration	Change of the color of the stone in one or three of the color parameters: hue, value and chroma. Frequently produced by salts, by the corrosion of metals by micro-organisms. Some typical yellow, orange, brown and black discolouration patterns are due to the presence of carotenoids and melanins produced by fungi and cyanobacteria. Darkened areas due to moistening may have different shapes and extension according to their origin: pipe leakage, rising damp,hygroscopic behaviour due to the presence of salts, condensation	The deterioration processes must be interrupted, in general the process is based on the manual cleaning of the material in order not to generate strong abrasions in the rock, it is advisable to make samplings of the dirt to determine its nature and to eradicate them in an effective way, Within this work is included the pre-consolidation, this should be done when there are pieces of great historical value where the cleaning itself can generate destruction of the element, desalination in which salts are extracted with the application on the surface of the stone of an additional absorbent material, a consolidation will be executed with the objective of increasing the cohesion of the components of the superficial zone of the stone.	
17	CD-01-4-1	Moist Area	on a sandstone rubble built wall as a result of a concentrated discharge of rain water from a broken down pipe.	The deterioration processes must be interrupted, in general the process is based on the manual cleaning of the material in order not to generate strong abrasions in the rock, it is advisable to make samplings of the dirt to determine its nature and to eradicate them in an effective way, Within this work is included the pre-consolidation, this should be done when there are pieces of great historical value where the cleaning itself can generate destruction of the element, desalination in which salts are extracted with the application on the surface of the stone of an additional absorbent material, a consolidation will be executed with the objective of increasing the cohesion of the components of the superficial zone of the stone.	
18	CD-01-4-2	Patina	Chromatic modification of the material, generally resulting from natural or artificial ageing and not involving in most cases visible surface deterioration.	The deterioration processes must be interrupted, in general the process is based on the manual cleaning of the material in order not to generate strong abrasions in the rock, it is advisable to make samplings of the dirt to determine its nature and to eradicate them in an effective way, Within this work is included the pre-consolidation, this should be done when there are pieces of great historical value where the cleaning itself can generate destruction of the element, desalination in which salts are extracted with the application on the surface of the stone of an additional absorbent material, a consolidation will be executed with the objective of increasing the cohesion of the components of the superficial zone of the stone.	
19	CD-01-4-3	Encrustation	Compact, hard, mineral outer layer adhering to the stone. Surface morphology and colour are usually different from those of the stone.	The deterioration processes must be interrupted, in general the process is based on the manual cleaning of the material in order not to generate strong abrasions in the rock, it is advisable to make samplings of the dirt to determine its nature and to eradicate them in an effective way, Within this work is included the pre-consolidation, this should be done when there are pieces of great historical value where the cleaning itself can generate destruction of the element, desalination in which salts are extracted with the application on the surface of the stone of an additional absorbent material, a consolidation will be executed with the objective of increasing the cohesion of the components of the superficial zone of the stone.	
20	CD-01-05	Efflorescence	Generally whitish, powdery or whisker-like crystals on the surface. Efflorescences are generally poorly cohesive and commonly made of soluble salt crystals	The deterioration processes must be interrupted, in general the process is based on the manual cleaning of the material in order not to generate strong abrasions in the rock, it is advisable to make samplings of the dirt to determine its nature and to eradicate them in an effective way, Within this work is included the pre-consolidation, this should be done when there are pieces of great historical value where the cleaning itself can generate destruction of the element, desalination in which salts are extracted with the application on the surface of the stone of an additional absorbent material, a consolidation will be executed with the objective of increasing the cohesion of the components of the superficial zone of the stone.	
21	CD-01-06	Crust	A crust is frequently dark coloured (black crust) but light colours can also be found. Crusts may have an homogeneous thickness, and thus replicate the stone surface, or have irregular thickness and disturb the reading of the stone surface details.	The deterioration processes must be interrupted, in general the process is based on the manual cleaning of the material in order not to generate strong abrasions in the rock, it is advisable to make samplings of the dirt to determine its nature and to eradicate them in an effective way, Within this work is included the pre-consolidation, this should be done when there are pieces of great historical value where the cleaning itself can generate destruction of the element, desalination in which salts are extracted with the application on the surface of the stone of an additional absorbent material, a consolidation will be executed with the objective of increasing the cohesion of the components of the superficial zone of the stone.	

22	CD-01-7	Pitting	point-like millimetric or submillimetric shallow cavities. The pits generally have a cylindrical or conical shape and are not interconnected. Pitting is due to partial or selective deterioration. Pitting can be biogenically or chemically induced, especially on carbonate stones. Pitting may also result from a harsh or inadapted abrasive cleaning method.	The deterioration processes must be interrupted, in general the process is based on the manual cleaning of the material in order not to generate strong abrasions in the rock, it is advisable to make samplings of the dirt to determine its nature and to eradicate them in an effective way, Within this work is included the pre-consolidation, this should be done when there are pieces of great historical value where the cleaning itself can generate destruction of the element, desalination in which salts are extracted with the application on the surface of the stone of an additional absorbent material, a consolidation will be executed with the objective of increasing the cohesion of the components of the superficial zone of the stone.	
23	BD-01-1	Algae	Algae are microscopic vegetal organisms without stem or leaves which can be seen outdoors and indoors. Algae form green, red, brown, or black veil like zones and can be found mainly in situations where the substrate remains moistened for long periods of time. Depending on the environmental conditions and substrate type, algae may form solid layers or smooth films.	Use of biocidal products with a broad disinfectant spectrum and low solubilization in water, which should not react with the products used for consolidation and cleaning of the stone. The most commonly used biocides are benzalkonium chloride, ammonia (ammonium salts), formaldehyde and sodium hypochlorite.	
24	BD-01-2	Lichen	Vegetal organism forming rounded millimetric to centimetric crusty or bushy patches. Lichen is a common feature of outdoor stone and is generally best developed under clean air conditions, but growth may be facilitated by certain pollutant such as nitrogen oxides derived primarily from vehicle pollution or agriculture. Former lichen growth may be detected by typical pitting structures (see this term) or lobate or mosaic patterns and even depressions	Use of biocidal products with a broad disinfectant spectrum and low solubilization in water, which should not react with the products used for consolidation and cleaning of the stone. The most commonly used biocides are benzalkonium chloride, ammonia (ammonium salts), formaldehyde and sodium hypochlorite.	
25	BD-01-3	Moss	Vegetal organism forming small, soft and green cushions of centimetric size. Mosses often grow on stone surface open cavities, cracks, and in any place permanently or frequently wet (masonry joints), and usually shady	Use of biocidal products with a broad disinfectant spectrum and low solubilization in water, which should not react with the products used for consolidation and cleaning of the stone. The most commonly used biocides are benzalkonium chloride, ammonia (ammonium salts), formaldehyde and sodium hypochlorite.	
26	BD-01-4	Plants	Vegetal living being, having, when complete, root, stem, and leaves, though consisting sometimes only of a single leafy expansion	Use of biocidal products with a broad disinfectant spectrum and low solubilization in water, which should not react with the products used for consolidation and cleaning of the stone. The most commonly used biocides are benzalkonium chloride, ammonia (ammonium salts), formaldehyde and sodium hypochlorite.	
27	AD-01-01	Perforation	A single or series of surface punctures, holes or gaps, made by a sharp tool or created by an animal. The size is generally of millimetric to centimetric scale. Perforations are deeper than wide, and penetrate into the body of the stone.	Care, repair and maintenance.	